Reconstruction of Paleoclimatic History of the northern Indian Ocean using isotopic and geochemical proxies

A THESIS

Submitted for the Award of Ph.D. degree of

MOHANLAL SUKHADIA UNIVERSITY

In the

Faculty of Science

by

Chandana K. R

Under the Supervision of

Dr. Ravi Bhushan
PHYSICAL RESEARCH LABORATORY,
AHMEDABAD

DEPARTMENT OF GEOLOGY
MOHANLAL SUKHADIA UNIVERSITY, UDAIPUR

2018

D E C L A R A T I O N

I, Ms. **Chandana K. R**, S/o Mr. K. G Ramamurthy, resident of I-113, PRL residences, Navrangpura, Ahmedabad – 380009, hereby declare that the research work incorporated in the present thesis entitled **"Reconstruction of Paleoclimatic History of the northern Indian Ocean using isotopic and geochemical proxies"** is my own work and is original. This work (in part or in full) has not been submitted to any University for the award of a Degree or a Diploma. I have properly acknowledged the material collected from secondary sources wherever required.

I solely own the responsibility for the originality of the entire content.

Date: (Chandana K. R)

C E R T I F I C A T E

I feel great pleasure in certifying that the thesis entitled "**Reconstruction of Paleoclimatic History of the northern Indian Ocean using isotopic and geochemical proxies**" embodies a record of the results of investigations carried out by **Chandana K. R** under my guidance.

She has completed the following requirements as per Ph.D. regulations of the University

(a) Course work as per the university rules

(b) Residential requirements of the university

(c) Presented her work in the departmental committee

(d) Published/accepted minimum of one research paper in a referred research journal.

I am satisfied with the analysis of data, interpretation of results and conclusions drawn.

I recommend the submission of thesis.

Date:

Name and designation of supervisor
Ravi Bhushan,
Scientist-SG

Countersigned by

Head of the Department

Acknowledgement

At this stage of my career, I am short of words to express my feelings for the many persons who have shaped my life, work and personality. I would like to thank all of them for their help and cooperation.

First of all, I would like to express my sincere gratitude to my guide Dr. Ravi Bhushan. His supportive and humble nature is one of the many nice things I appreciate in him. He introduced me to the field of isotope geochemistry and mass spectrometry. Whenever I was in the slightest of the doubts, a discussion with him was enough to get to the right working direction. He patiently taught me the shades of paleoclimatology. Working with him has always been a pleasure, whether on a cruise or during scientific discussions. I acknowledge him for his consistent support and guidance and for providing me ample freedom to work. I thank him from the bottom of my heart for all he has done for me. In the same breath, I express my sincere gratitude to Prof. Devesh Sinha who introduced me to the science of micropaleontology and oceanography. His erudite discourses on various topics were always a treat to hear.

I owe special thanks to Prof. M. M. Sarin for his constant support and valuable inputs during my thesis work. I am indebted to Drs. A.J.T.Jull and Rajesh Agnihotri and Mr. Ravi Sawlani for carrying out supporting measurements during the course of this study.

I am enormously thankful to the PRL Director and the Dean for providing me support and facilities throughout the thesis work. I thank the members of the Academic Committee for reviewing my work from time to time and providing their constructive inputs. My sincere thanks to Profs. Sunil Kumar Singh, K. P. Subramanian, J. Banerji, D. Banerjee, P. Venkatakrishnan, Drs. N. Rastogi, R. D. Deshpande, M. G. Yadava, L. K. Sahu, D. Chakraborty, N. M. Ashok, K. K. Marhas, Amit Basu, V. K. Rai, D. Ray, J. Pabari and Bhas Bhapat for their informative lectures during the course work. I acknowledge Profs. R. Ramesh, J. S Ray, R. Ramachandran, Drs. R Rengarajan, S. Kumar, A. D. Shukla, A. Singh and Mr. Sudheer for their valuable comments and encouragement during division seminar.

I would like to thank all members of the Chemistry Lab for their help, encouragement and support during my thesis work. I thank my labmates Anil, Atinder, Subha, Damodar, Mahesh, Romi, Harsh Raj, Rahul Khichi, Naman, Nisha, Shivam, Ankur, Chinmay, Upasana, Satish and Ravikant for their help and support. I would also thank my ex lab-mates Abhishek, Priyanka, Prabhuti, Wriju, Sanjukta, Akshay, Batuk, Rupali, Nitesh, Balaji, Preksha, Sneha and Jivesh for being part of Chemistry Lab. I thank my seniors Satinder, Srinivas, Vineet, Prashant, Neeraj, Jayati for their valuable suggestions. I duly acknowledge help provided by Jaldhi, Ramsha, Trupti, Payal, Pravin, Ravi Bhai and Rashmit.

I accord my thanks to all GSDN members for their help and support during this work. I am grateful to all the staff-members of Library, Computer Centre, Canteen, Workshop, Administration, Dispensary and Maintenance section of PRL for their assistance and cooperation.

I would like to thank Department of Space (DOS) for the scholarship and support for the research. Thanks are due to MoES, Government of India for financial and logistic supports provided to GEOTRACES (India) programme. My thesis is part of this programme. I thank NCAOR and NORINCO for resourceful help during the ocean expeditions. I thank the captains, crew and scientific members of Saga Kanya cruise No. 311/312 and 324 and Sagar Manjusha 13/24. I thank Lathika, Racheal, Murugananthan, Naveen for their support during on board sampling.

I take an opportunity to express gratitude to all my friends at PRL. I would like to thank my batchmates of JRF12: Jinia, Deepak, Dipti, Venkatesh, Bivin, Ashim, Rahul, Apurv, Lalit, Newton, Pankaj. My special thanks to Anirban, Manu, Abhaya, Kiran, Rupa, Niharika, Abdur, Dipika, Manab, Harsh, Ashish, Kuldeep, Rukmini, Navpreet, Aarthy, Neeraj, Jayakrishna, Avdhesh, Abhishek Attreya, Srinivas, Gaurav, Rahul, Dimpy bhabhi for my stay at hostel. And I would like to specially thank Shraddha, Ikshu and Sneha Yadav for their love and support.

Lastly, but most importantly I thank my parents, my sisters, niece, nephew and Debrup for their love, care, affection and support during this work. It was

their confidence that inspired me the most to complete this work, and hence, I take this opportunity to dedicate this thesis to them.

ABSTRACT

The prime focus of the present study is to understand paleo processes operating near the equatorial Indian Ocean deciphered through the temporal distributions and associated variations of geochemical parameters. The study encompasses the mechanism responsible for variation in monsoon, productivity and behaviour of redox sensitive elements as a function of surface ocean processes for the late Quaternary period (~25000 to 2000 yr BP) on millennial timescale using multi-proxy approach on AMS radiocarbon dated sediment core. The study suggests high productivity prevailed at central equatorial Indian Ocean (off Sri Lanka) during LGM as deciphered from increased OC and $CaCO_3$ but a simultaneous depleted $\delta^{15}N$ is attributed to incomplete utilisation of upwelled nutrients due to strengthened NE monsoonal winds triggered by southward migration of Intertropical Convergence Zone (ITCZ). Thus, the depleted $\delta^{15}N$ values along with high OC signifies a link between enhanced productivity and partial nutrient utilization and ITCZ migration. On the basis of behaviour and distribution of redox sensitive elements, the study demonstrates prevalence of anoxic bottom water conditions during LGM. Where high OC, low C/N ratio and enriched $\delta^{13}C$ suggests availability of more labile organic matter for decomposition under sulfate reducing bacteria that resulted in depleted $\delta^{34}S$. Thus, the depleted $\delta^{34}S$ values along with high OC and redox sensitive elements signifies a link between enhanced productivity and better preservation under anoxic conditions. Early Holocene (11-8 ka BP) shows high OC with depleted $\delta^{13}C$ implying enhanced terrestrial supply as a result of intense monsoonal activity during this time coinciding with solar insolation maximum of the Northern Hemisphere. With the onset of Holocene (mid-late), increase in BSi, decrease in OC and $CaCO_3$, low redox sensitive elements with enriched $\delta^{15}N$ and $\delta^{34}S$ suggests shift in productivity pattern with complete nutrient utilisation and oxic conditions at sediment water interface. The equatorial Indian Ocean witnessed productivity shifts (calcareous or siliceous) as function of nutrient utilisation modulated by micro-nutrient availability caused by monsoonal variations which in turn was closely linked with ITCZ.

CONTENTS

LIST OF FIGURES

LIST OF TABLES

CHAPTER 1

INTRODUCTION

1.1 Introduction

A large-scale sea breeze originating due to significant difference between the temperatures on land and ocean is termed as Monsoon. The term 'Monsoon' has been coined from Arabic word 'Mausam', which means season. It was first witnessed by Arab sailors navigating through the Arabian Sea, who observed a persistent wind reversal every year during the same time. Monsoon is generally associated with dry or wet weather. The northern Indian Ocean differs from other global oceans due to its unique topographical setting and noticeable behavioural pattern with changes in the strong monsoonal winds over the ocean. The northern Indian Ocean being separated by Indian subcontinent compared to the other oceans comprises of two basins i.e., the Arabian Sea and the Bay of Bengal. The strong differential land-ocean thermal contrast leads to seasonal wind reversal, and regulates the monsoonal circulation that influences weather pattern between 30°N and 30°S over the Indian, Asian and African landmasses (Schott and McCreary, 2001). The initiation of the Indian Monsoon system with its peak intensity around 5 Ma (Molnar et al., 1993) has been attributed to the upliftment of the Tibetan Plateau during the late Miocene (10–8 Ma) (Niitsuma and Naidu, 2001). The Arabian Sea records and the windblown dust in the loess plateau of China suggested the commencement of Indian Summer Monsoon (ISM) occurred at ~8 Ma.

During Northern Hemisphere summer (June to September), the Indian subcontinent and surrounding landmass receives excessive heat due to the influence of direct sun rays over the equator. This leads to the development of low pressure over the continent of about 994 mb. Subsequently, a high-pressure cell of about 1020 mb develops over the adjoining sea allowing the south-westerly (SW) monsoonal winds that travels from ocean towards the land (Tomczak and Godfrey, 2003). Another high pressure about 1026 mb is developed southeast coast of Madagascar causing the SE trade winds to rush towards the low-pressure region and becoming SW winds after crossing the equator. These warm moisture-laden winds from ocean causes intense precipitation over India and adjoining areas during the months of June to September. The word monsoon in India usually

refers to SW monsoon or the Indian Summer Monsoon (ISM) as most of the precipitation is during summer.

During Northern Hemisphere winter (November to February), the landmass gets cooled up quickly due to less solar radiation and increased albedo due to snow cover over the Asia, resulting in high pressure over landmass. Subsequently, a low pressure is generated over the Indian Ocean due to direct heating by sun rays. Due to this pressure difference the cold and dry NE monsoonal winds rushes towards the equator by picking up moisture from the Bay of Bengal and causing precipitation over the SE India, Sri Lanka, Malaysia and Indonesia.

ISM is also associated with the migration of the ITCZ- a narrow latitudinal zone of low pressure of wind convergence near equator (Chao and Chen, 2001; Gadgil, 2003). During boreal summer, ITCZ shifts north of the equator and the winds blow across the equator to reach ITCZ, inducing strong SW monsoon winds. During boreal winter, strong NE monsoon winds are generated due to the shift of ITCZ south of equator (Fig. 1.1). Thus, the ISM is responsible for heat and moisture transport from tropical to higher latitude regions across the equator (Clemens et al., 2003).

The surface and the coastal currents in the northern Indian Ocean reverse their direction in response to wind reversals (Fig. 1.1). During summer monsoon, a branch of Somali current (SC) at 4° turns offshore and supplies the summer monsoon current (SMC) flowing eastward. Additionally, the SMC also receives water from southward flowing West Indian Coastal Current (WICC) (Tiwari et al., 2006a). After crossing Sri Lanka coast, SMC current forms an anticlockwise eddy termed as Sri Lanka Dome (SLD) (Vinayachandran and Yamagata, 1998). The eddy current splits into two with one arm flowing southward along the eastern coast of Sri Lanka and again merging with SMC flowing eastward, while the other arm flows northward along the East Indian coast as EICC (de Vos et al., 2014) (Fig. 1.1B).

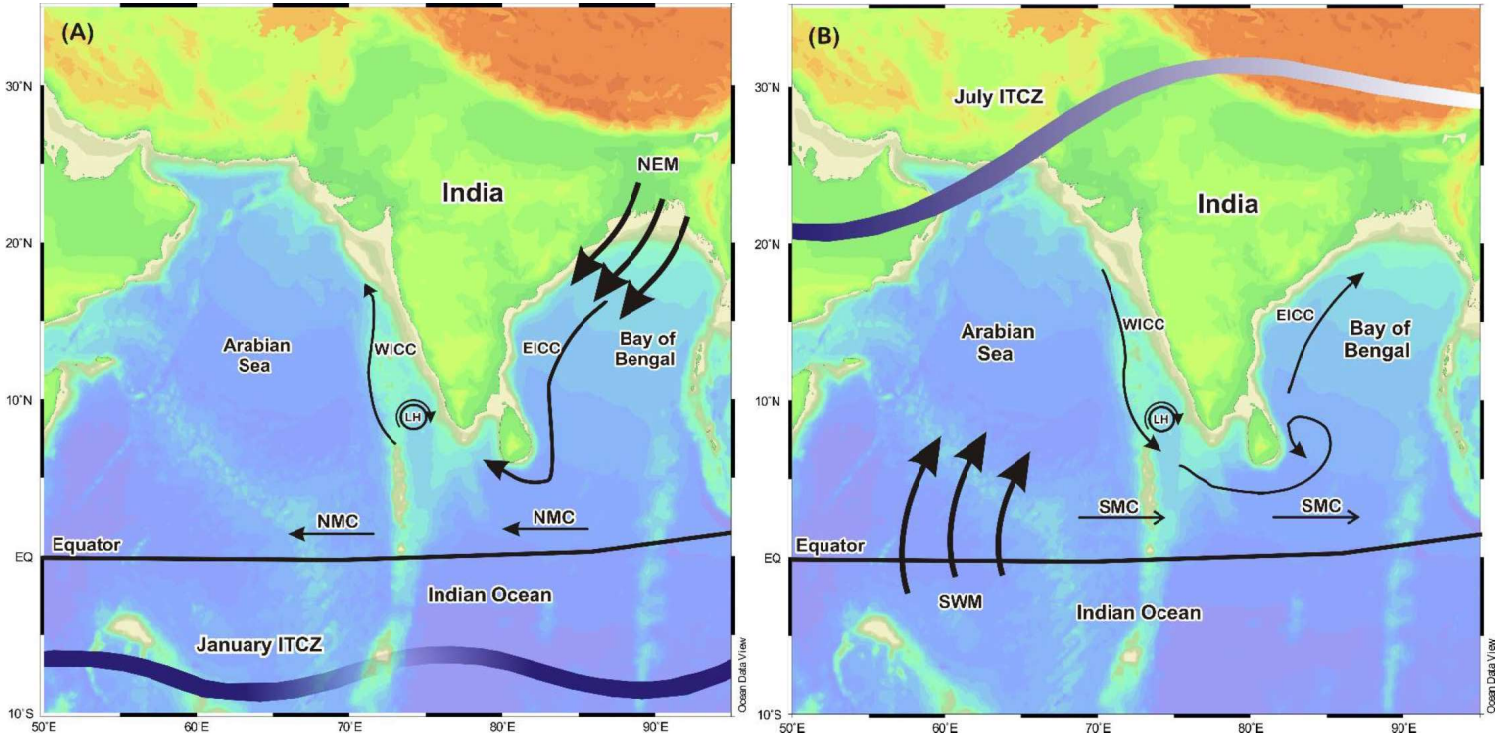

Figure 1.1: Migration of Intertropical Convergence Zone (ITCZ), wind pattern and surface circulation pattern in the northern Indian Ocean during winter monsoon (A) and summer monsoon (B) (Modified after Schott and McCreary Jr, 2001). WICC - West Indian Coastal Current; EICC - East Indian Coastal Current; NMC - Northeast Monsoon current; SMC - Summer Monsoon Current; LH - Lakshadweep High.

Thus, the SMC along with the WICC flows from west to east transporting highly saline water from the Arabian Sea to the Bay of Bengal (Schott et al., 1994). But reversal of currents occurs during winter monsoon. The EICC along the eastern Indian coast flows southward and merges with NMC flowing from east to west transporting low salinity water from the Bay of Bengal to the Arabian Sea. After crossing Sri Lanka coast, the currents flow around the clockwise Lakshadweep eddy and northward along the western Indian coastline as the West Indian Coastal Current (WICC) (Schott et al., 1994; de Vos et al., 2014) (Fig. 1.1A). Thus, these currents play a crucial role in nutrient distribution and chlorophyll concentrations in the equatorial regions (Vinayachandran et al., 2004; Vidya et al., 2013).

Due to the seasonal reversal of wind pattern and current directions, both the basin the Arabian Sea and the Bay of Bengal show distinctive characteristics properties both biologically and geochemically. Upwelling i.e. the replacement of surface waters from subsurface intermediate waters is one such major feature of summer monsoonal circulation in the Arabian Sea and has been observed noticeably near Somalia and Oman margins. The upwelling causes intense biological and physical changes in the regions with ~4 ºC lowering of sea surface temperature (SST) but enhancing nutrient levels leading to high surface biological productivity. High productivity is also observed during NE monsoon but unlike summer monsoon, it results due to convective mixing of the surface waters causing mixed layer deepening that enhances nutrient levels triggering high productivity accompanied by high sea surface salinity due to evaporation (Madhupratap et al., 1996). In Bay of Bengal the vertical mixing is constrain. Only the southwest region witness upwelling with weaker strength compared to Arabian Sea (Vinayachandran and Mathew, 2003). But, high river discharge by Ganges and Brahmaputra forms a freshwater lens over Bay of Bengal surface layer which restricts upwelling or vertical mixing leading to high SST with low salinity and less biological productivity (Kumar, 2006).

Occurrence of seasonal hypoxia with low oxygen concentrations from the water depth 250–1250 m in the Arabian Sea is another remarkable feature observed in Northern Indian Ocean (Naqvi et al., 2000). Such hypoxia arises due

to upwelling which results in intense biological productivity that demands enhanced oxidant supply to support bacterial respiration for oxidation of organic matter supplied by high overhead productivity. Even though, the Arabian sea witnesses higher biological productivity compared to Bay of Bengal but the sinking fluxes to the sediment in the Arabian sea is low compared to the Bay of Bengal (Nair et al., 1989; Ittekkot et al., 1991). This is due to the fact that more sinking of organic carbon in the Bay of Bengal is associated with high clay mineral compared to the Arabian Sea.

1.2 Late Quaternary variation of ISM in Northern Indian Ocean

ISM is an important phenomenon of Asian monsoon system resulting in >70 % rainfall on the Indian subcontinent (Warrier and Shankar, 2009) with huge impacts on socio-economic status of India (Roy and Collins, 2015). The ISM has been found to be associated with other modes of climate variability and most significant teleconnections linked to ISM variability are El Nino Southern Oscillation (Maity and Kumar, 2006), Total Solar Irradiance (Agnihotri et al., 2002) Indian Ocean Dipole (Abram et al., 2009), North Atlantic osicllation (NAO) (Menzel et al., 2014) and ITCZ (Saraswat et al., 2013). Abrupt variations in ISM with extreme drought and flood events in last few decades is the major impediment that reinvigorated various paleoclimatologists to understand the ISM fluctuations since Last Glacial Maxima (LGM) till present (Agnihotri et al., 2003; Singh et al., 2006; Tiwari et al., 2006b) to develop understanding for the present global climatic perturbations and modelling the future changes. Therefore, various paleoclimatic archives such as marine sediments (Bhushan et al., 2001; Saraswat et al., 2012; 2013; Banerji et al., 2017), lake sediments (Juyal et al., 2009; Dixit et al., 2014; Prasad et al., 2014), peats (Sukumar et al., 1993; Hong et al., 2003; Rühland et al., 2006), speleothems (Sinha et al., 2005; Yadava and Ramesh, 2005; Fleitmann et al., 2007) and corals (Ahmad et al., 2011) at varying temporal resolution have been investigated for the reconstruction of ISM during the late Quaternary. Though, there have been extensive studies on late Quaternary ISM reconstruction from marine and terrestrial records but understanding the response of both the basins towards ISM variability needs to be expound which in turn will

provide a platform to comprehend the ISM variability since late Quaternary period in the intermixing zone of the Arabian Sea and the Bay of Bengal.

1.2.1 Glacial-Interglacial (25-10 ka) records of ISM

Both the Arabian Sea and the Bay of Bengal in the northern Indian Ocean respond differently with influence of ISM. The reconstruction of ISM based on oxygen isotopes of foraminifera of various sediment cores from the northern Indian Ocean during LGM suggests ISM weakening resulted in warmer sea surface temperature (SST) for Arabian Sea due to reduced upwelling, while enhanced salinity for the Bay of Bengal caused by declining continental influx (Prell et al., 1980).

The Arabian Sea is a highly productive region strongly linked with monsoon system and accompanied by shift in ITCZ. The sediment trap study from the Arabian Sea shed light on enhanced biological productivity during ISM (Prahl et al., 2000; Wakeham et al., 2002). The primary productivity for the Arabian Sea has varied as a function of change in monsoon intensity on Milankovitch and Holocene time scales. The reconstructed paleo-productivity for the past 135 ka from the northern and eastern Arabian Sea suggests large variation in productivity during glacial-interglacial periods. Intensification of ISM during interglacial period with increased wind velocities caused strengthened upwelling resulting into high productivity at the northern Arabian Sea. But during glacial periods, the intensified NE monsoon led to mixed layer deepening causing high productivity in the eastern Arabian Sea (Ivanova et al., 2003). Similar observations of enhanced productivity during LGM from the eastern Arabian Sea has been described as a result of nutrients shoaling due to enhanced convective mixing led by intensified NE monsoon (Ishfaq et al., 2013). On the contrary, reduced overhead productivity witnessed during glacial interglacial transition following which enhanced productivity occurred during Holocene as evidenced by the geochemical proxies for the sediment core retrieved from the eastern Arabian Sea (Agnihotri et al., 2003).

The large scale differential heating of landmass and Indian Ocean along with complex dynamics of ocean atmosphere system of Indian Ocean controls the atmospheric circulation associated with ISM (Kessarkar et al., 2013). The

reconstructed upwelling history and monsoon circulation from the western Arabian Sea based on pollen and upwelling foraminifera suggested stronger ISM during interglacial period (Prell and Campo, 1986). This is in agreement with the investigation on reconstruction of SST derived from Mg/Ca in combination with calcification temperature of the planktonic foraminiferal species for the last 20 ka from the western Arabian Sea made by Saher et al., (2007). The study claimed improved ISM with weakening of NE monsoon winds during interglacial periods while weak ISM with enhanced cooling by NE monsoon winds during LGM.

Plethora of paleoclimate studies using trace elemental geochemistry of the marine sediments revealed variations in chemical weathering (Tripathy et al., 2014), paleo-productivity (Agnihotri et al., 2003), paleo-redox conditions (Pattan and Pearce, 2009) and its implications on changing monsoon. Temporal variations of the trace elements from the Arabian Sea as a function of changing monsoonal intensity, atmospheric circulation and hydrographic conditions during last 25000 years by Sirocko et al., (2000) has been reported based on sediment core from western Arabian Sea. Weakening of ISM during LGM with high dust discharge from the north-westerly winds has been observed by Sirocko et al., (2000). A multi proxy study on a sediment core raised from the western Arabian Sea suggested that the low calcareous productivity could be due to the favoring of silicate over carbonate productivity as a function of ISM strengthening (Tiwari et al., 2010).

In the Arabian Sea, the depth of Aragonite Compensation Depth (ACD) (250–700 m) generally falls within the Oxygen Minimum Zone (150–1250 m). Above conditions in the Arabian Sea are sustained by overhead productivity, carbon respiration within the water column and sediments and water mass ventilation thereby causing an interconnection between aragonite preservation and intensity of OMZ (von Rad et al., 1999). However, in the present day conditions, aragonite preservation is poor in the Arabian Sea due to the occurrence of intense OMZ environment (Naidu et al., 2014). To study the relationship between ACD and Antarctica Intermediate Water (AAIW) ventilation in the Arabian Sea, Naidu et al., (2014) estimated aragonite contents and pteropods abundance in a sediment core within the oxygen minimum zone of the eastern Arabian Sea. Compared to

present day condition, deepening of ACD in the eastern Arabian Sea persisted during glacial period and stadials (Heinrich events) as suggested by enhanced aragonite content and pteropod abundances. Such changes in ACD result as a function of declining local monsoon driven productivity accompanied by improved ventilation caused by intrusion of glacial AAIW (Naidu et al., 2014). Thus, the ISM intensity directly influences the overhead productivity in the western Arabian Sea. But the NE monsoonal wind intensification during LGM in the eastern Arabian Sea documented ACD deepening which lead to enhanced productivity and better preservation of aragonite and pteropods.

The Bay of Bengal witnessed sedimentation since early Miocene and is known to have archived paleoclimatic signatures experienced in various catchment regions of different fluvial sources such as Himalaya, peninsular regions, Andaman group of islands and Myanmar (Sarin et al., 1979; Fontugne and Duplessy, 1986). Unlike the Arabian Sea, the Bay of Bengal and the Andaman Sea is highly influenced by riverine influx and sediment (2000 million tons/year) from the Himalayan and Indian peninsular rivers (Chauhan and Vogelsang, 2006) and rainfall during ISM (Govil and Naidu, 2011). The Bay of Bengal is known to experience extensive river discharge during ISM with strongly stratified surface layer causing abrupt decrease in surface salinity of the order of 4 psu in the northern Bay of Bengal (Wyrtki, 1973). The past (~32 kyr) sea surface salinity and temperature reconstruction based on paired measurement of planktonic foraminiferal Mg/Ca and $\delta^{18}O$ in a sediment core from western Bay of Bengal was studied by (Govil and Naidu, 2011). The study demonstrated ~3.2 °C cooler SST of the Bay of Bengal during LGM. But low salinity indicated by low $\delta^{18}O_{sw}$ during Bolling-Allerod (B-A) event signified the onset of ISM intensification. Alike B-A event, Holocene also reflected strong ISM with enhanced freshwater discharge (Govil and Naidu, 2011). A similar observations of ISM weakening/strengthening during LGM/ Holocene as a consequence of low/high freshwater influx in the northern Bay of Bengal has been evidenced from foraminiferal $\delta^{18}O$ (Kudrass et al., 2001). Although, sediment sources to the Bay of Bengal has been dominated by both Higher and Lesser Himalaya, on

million-year time scale source of sediment has remained nearly consistent since Miocene (Bouquillon et al., 1990; France-Lanord, 1993).

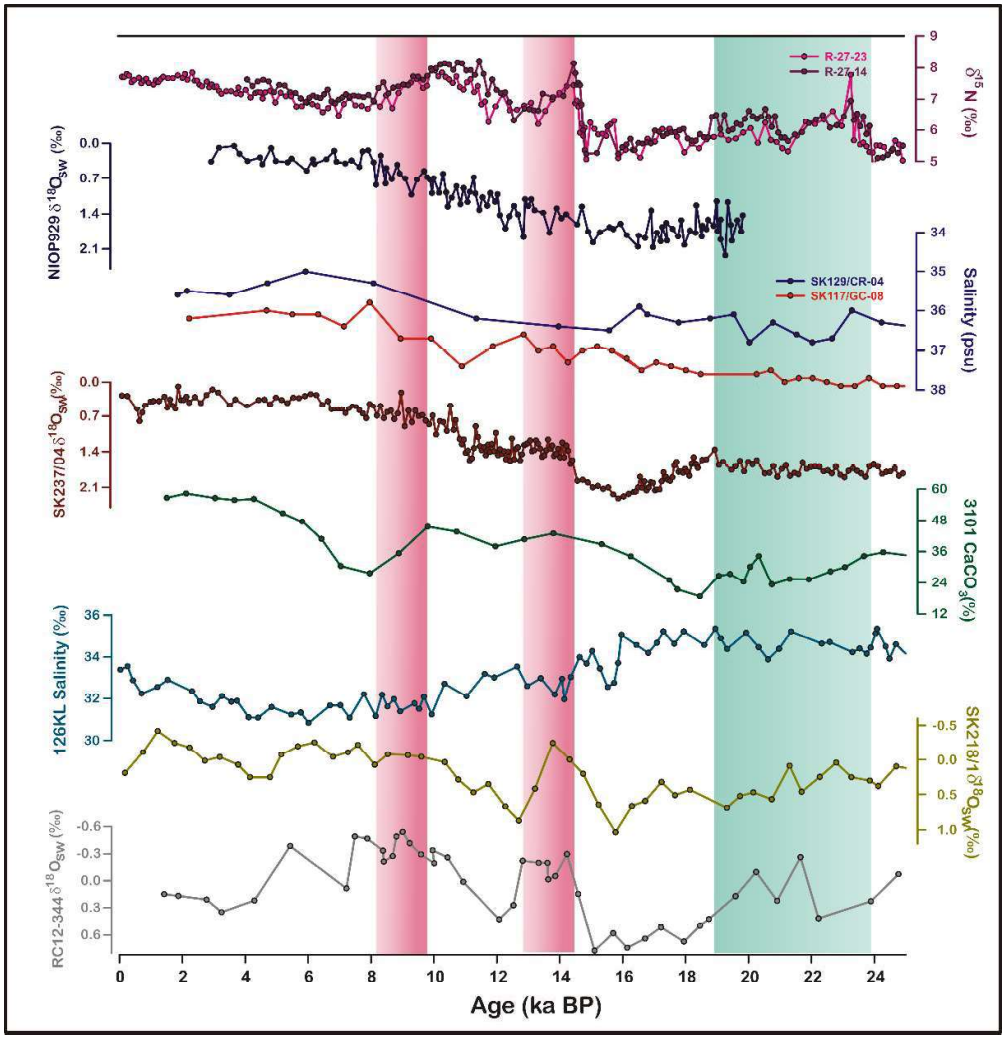

Figure 1.2: Reconstructed high resolution paleomonsoon records from the northern Indian Ocean for the last glacial-interglacial transition. RC27-14, RC27-23 $\delta^{15}N$ (Altabet et al., 2002); NIOP929 $\delta^{18}Osw$ (Saher et al., 2007); SK129/CR-04 & SK117-GC-08 (Mahesh and Banakar, 2014); SK237-GC04 $\delta^{18}Osw$ (Saraswat et al., 2013); 3101 (Agnihotri et al., 2003); SK218/1 (Govil and Naidu, 2011); 126KL Salinity (Kudrass et al., 2001); RC12-344 (Rashid et al., 2007). Pink band in the plot represents ISM strengthening and green band indicative of ISM weakening.

Evidence of changing provenance of sediment as a function of changing climate on millennial timescale has been addressed extensively (Ahmad et al., 2005; Clift et al., 2008; Rahaman et al., 2009). The isotopic study of the sediment from western Bay of Bengal revealed ISM weakening and expansion of glaciation over Higher Himalaya that reduced the erosion rate over the Himalaya resulting in relatively lower $^{87}Sr/^{88}Sr$ and higher ε_{Nd} during LGM (Tripathy et al., 2011).

The sediment records of the Andaman Sea indicates low riverine flux and cooler SST during LGM and Younger Dryas with subsequent warmer SST and enhanced riverine influence from Irrawaddy river during B-A and early Holocene as suggested by $\delta^{18}O_{sw}$ (Rashid et al., 2007). Based on stable carbon and oxygen isotopic variation of the planktonic foraminifera from a deep sediment core in the Andaman Sea indicated increased salinity/ decrease temperature during glacial period attributed to cooling event or sudden decline in fresh water flux as recorded from $\delta^{18}O$. Simultaneous enrichment in $\delta^{13}C$ values during glacial periods is indicative of enhanced productivity due to NE monsoon intensification in the Andaman Sea (Ahmad et al., 2000). Weak ISM resulted in low fresh water influx to the Bay of Bengal and Andaman Sea which lead to increase in SST and overhead productivity during LGM. With the re-establishment of ISM during B-A event and Holocene, high fresh water influx with depleted SST has been witnessed in the Bay of Bengal and Andaman Sea.

A low salinity tongue formed by the inflow of low salinity surface water from the Bay of Bengal to the eastern Arabian Sea is largely driven by the higher sea level in the Bay of Bengal than in the Arabian Sea (Mahesh and Banakar, 2014). To assess absolute sea surface salinity changes during the last glacial period, Mahesh and Banakar (2014) collected two cores along a north–south transect in the eastern Arabian Sea. Based on paired measurement of $\delta^{18}O$ and Mg/Ca in surface dwelling planktonic foraminifera, suggested decrease in intensity of ISM resulted in low freshwater discharge in the Bay of Bengal during the last glacial period.

The SST reconstruction based on oxygen isotopic composition in foraminifera has been extensively explored but the technique of studying the abundance ratios of unsaturated alkenones in phytoplankton as preserved in

sediments has recently developed in past few decades (Prahl and Wakeham, 1987). The paleotemperature record based on alkenone and oxygen isotopes in foraminifera from Maldives inferred high salinity during glacial stages characterized by increased evaporation and/or decreased precipitation, is attributed to enhanced dry NE winds and/or reduced SW monsoon (Rostek et al., 1993). Unlike other paleoclimatic records from the Arabian Sea, enhanced primary productivity was observed during the glacial periods while interglacial periods witnessed low productivity as attributed to increased convective overturning due to stronger NE monsoon winds (Rostek et al., 1993). Similar observation of enhanced productivity during LGM in the equatorial Indian Ocean was suggested by (Punyu et al., 2014) based on marine productivity indicators such as phytol, brassicasterol and organic carbon. Such enhanced productivity during LGM is combined impact of intensified inter-monsoon Wyrtki Jets and NE winds which triggered the nutrients levels in the photic layer. Conversely, the oxygen isotopes of planktonic foraminifera from equatorial Indian Ocean suggested strengthening of NE wind during early deglacial period instead of LGM (Tiwari et al., 2005). Based on Mg/Ca on planktonic foraminifera from the equatorial Indian Ocean for the SST reconstruction of last 137 kyr, it has been observed that SST was 2.1 °C cooler during LGM compared to the present (Saraswat et al., 2005). On comparing the equatorial Indian Ocean SST with Antarctic δD and Greenland $\delta^{18}O$ records, presence of major high-latitude cooling/warming events in the equatorial Indian Ocean is noticed (Saraswat et al., 2005). Based on these studies, it can be suggested that the equatorial Indian Ocean is characterized by high SSS and overhead productivity accompanied by low SST during LGM lead by strengthened NE monsoon winds during LGM.

1.2.2 Holocene (10 ka-present) records of ISM

Holocene period is known to have witnessed great fluctuations in ISM precipitation. The wind reversal associated with the ISM and winter monsoon results in a unique environment with upwelling, large freshwater influx and a seasonal bottom water anoxia (Agnihotri et al., 2008) thereby leading to enhanced phytoplankton productivity in the eastern Arabian Sea (Parab et al., 2006). The Arabian Sea is known to witness bacterially mediated denitrification in the

suboxic conditions which in turn depends on the surface productivity. Sediment record of past 700 yr from the eastern Arabian Sea revealed reduced denitrification during 1750 to 1650 AD (Little ice age) associated with low upwelling as a result of reduced ISM (Agnihotri et al., 2008). However, increased productivity with depleted sedimentary $\delta^{15}N$ for the last 150 years (the Anthropocene) resulted due to the dilution by isotopically lighter nitrogen supply from the land (Agnihotri et al., 2008). Likewise, the study of other productivity proxies ($\delta^{13}C_{org}$, $\delta^{13}C_{ruber}$ and OC) from the eastern Arabian Sea also suggests enhanced productivity since 7 ka as a result of increase in upwelling intensity/ winter convective mixing (Naik et al., 2014). Temporal variation of high resolution terrigenous contribution in the eastern Arabian Sea suggests monsoon intensification during 9.5 and 9.1 ka followed by monsoon weakening events recorded at 8.2, 7.0, 5.5 and 3.5 ka (Thamban et al., 2007).

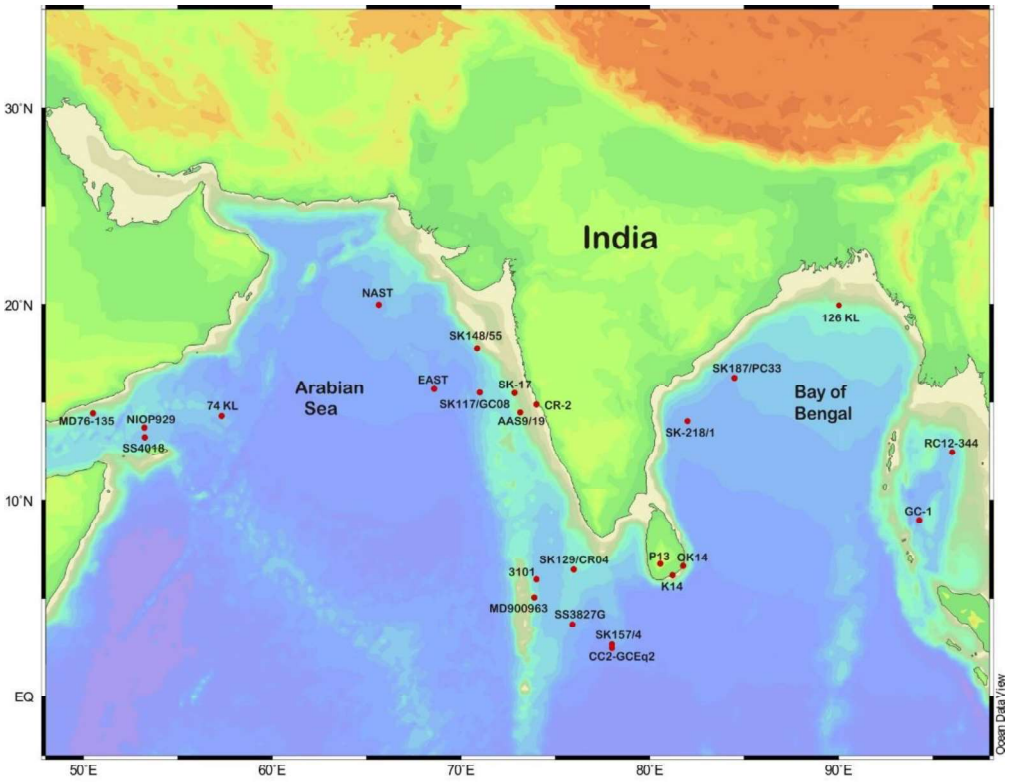

Figure 1.3: Location of the cores discussed in the section is represented by filled circles.

Exploring the Holocene records from equatorial region of the Indian Ocean is skeptical, but the continental shelf of Sri Lanka can be examined to have better understanding of the paleoceanographic processes for the Holocene. And the southeastern coast of Sri Lanka is mainly affected by winter monsoon, as it is the shadow region for ISM and thus archives winter monsoon variability. Investigation based on sediment cores from coastal estuaries and lagoons underscored climate aridification intervals from 7.3–6.7, ~4.0–3.0 and ~1.1–0.5 ka interspersed with semi-arid conditions from ~6.2–4.6 ka, and short-wet intervals of ~6.5–6.2 ka and ~3.0–1.5 ka. Statistical similarity between Indian winter monsoon and Indian summer monsoon variability suggests control of similar forcing mechanism (Ranasinghe et al., 2013).

1.3 Motivation

Over the last several decades, the paleoclimatic and paleoceanographic understanding for the northern Indian Ocean since LGM has expanded. Such extensive and pioneering studies provide an excellent portrayal of ISM variability since LGM. The past climate variability as a function of ISM intensification from several paleorecords on different time scales from northern Indian Ocean indicate ISM weakening during glacial periods such as LGM (~23 ka) and Younger Dryas (~12.5 ka) interrupted by ISM strengthening post LGM (~17 ka). The temporal variability of ISM during Holocene suggested monsoon strengthening during early Holocene (~10 ka) followed by gradual weakening towards mid-late Holocene (~8–4 ka). The observation based on various studies primarily opines two concepts of the past ISM variability in the northern Indian Ocean: a) the productivity variation in the Arabian Sea, and b) the change in SST/salinity in the Bay of Bengal, as a function of the ISM intensity during glacial-interglacial periods. The western Arabian Sea witnessed high productivity due to enhanced upwelling driven by improved ISM intensity during interglacial period, whereas, the eastern Arabian Sea experienced high productivity during LGM due to mixed layer deepening caused by intensified NE monsoon. Similar to the eastern Arabian Sea, the Andaman Sea also witnessed enhanced productivity during LGM triggered by NE monsoon intensification. Whereas, during B-A event and

Holocene, low salinity signifies improved ISM with enhanced freshwater influx in the Bay of Bengal and the Andaman Sea, while during LGM low temperatures invokes ISM weakening in the region. In the equatorial Indian Ocean, dry NE winds and reduced ISM resulted in high salinity in the region during glacial period. Further, a combined impact of intensified inter-monsoon, Wyrtki Jets and NE winds triggered productivity during LGM near central equatorial Indian Ocean.

Summarizing these studies, it can be underscored that emphasis is being made on paleoclimatic and paleoceanographic reconstruction of the Arabian Sea, the Bay of Bengal and the Andaman Sea. However, the intermixing zone of the Arabian Sea and the Bay of Bengal near the equatorial region off Sri Lanka with limited studies still remains an enigma and needs to be addressed in terms of the oceanographic processes since LGM. Further it has also been observed that past climate bracketing the major events of last few centuries for the northern Indian Ocean is the major impediment in the compilation of data for rapid climate change of late Holocene and future climate changing trends. In view of this, the study area is off Sri Lanka, which forms a major and distinctive part of the northern Indian Ocean. The study region is suitable for monsoonal studies as it experiences both the monsoons (SW and NE) and records associated biogeochemical changes. Additionally, the region is in the intermixing zone and transports water between both the basins, the Arabian Sea and the Bay of Bengal during different monsoon periods. Thus, the present study attempts to reconstruct the late Quaternary climatic variability near central equatorial Indian Ocean, off Sri Lanka with multi-proxy geochemical approach. The following objectives will be addressed:

- To obtain the past monsoon variations for the Late Quaternary period (~25,000 to 2000 yr BP) on millennial timescales by high-resolution sampling using various geochemical tracers with demarcation of the onset of deglacial period in the northern Indian Ocean.
- Reconstruction of the paleoproductivity and nutrient utilisation during glacial-interglacial periods from the northern Indian Ocean.

- Reconstruction of paleoredox conditions by identifying simultaneous interplay of the bottom water ventilation and productivity variations during the last 25 kyrs BP.
- To investigate the influence of Total Solar Irradiance (TSI) on ISM and to identify the solar periodicities engrossed in the sediments of intermixing zone of Arabian Sea and the Bay of Bengal from Northern Indian Ocean.

1.4 Study Area

Geochemical investigations have revealed that the equatorial Indian Ocean, off Sri Lanka is largely composed of calcareous and smectite clays (Nath, 2001). The sediment trap study carried out for estimating biogenic fluxes in the Arabian Sea, the Bay of Bengal and the equatorial Indian Ocean found predominance of opal fluxes in the western Arabian Sea and the Bay of Bengal. Based on the sediment trap data, the eastern Arabian Sea, the Southern Bay of Bengal and the Equatorial Indian Ocean are dominated by carbonate fluxes (Ramaswamy and Gaye, 2006). Strong seasonality in the biogenic fluxes has been observed at SBBT, while EIOT remained deprived of such seasonal variations (Vidya et al., 2013).

Sri Lanka is uniquely located within the equatorial belt of the northern Indian Ocean and experiences seasonal reversal of wind and is exposed to both monsoon periods, with the Arabian Sea on its western side and Bay of Bengal on eastern side (Fig 1.4). The southwest region of Sri Lanka mainly receives rainfall during summer monsoon, as the southwest part is directly exposed to the SW monsoon winds, whereas northeast region of Sri Lanka receives rainfall during NE monsoon. This is due to the rain shadow effect of the Central Highlands of Sri Lanka that acts as the physiographic climate barrier and controls the prevailing moisture winds and confines rainfall over the region between the two monsoons. Based on this two major climatic zones are defined: the Wet Zone to the west and Dry Zone to the east of Central Highlands (Fig 1.4) (Malmgren et al., 2003; Ranasinghe et al., 2013). Apart from this, during both monsoon periods, the flow of currents along the eastern and western coast are southward converging along the southern coast (de Vos et al., 2014).

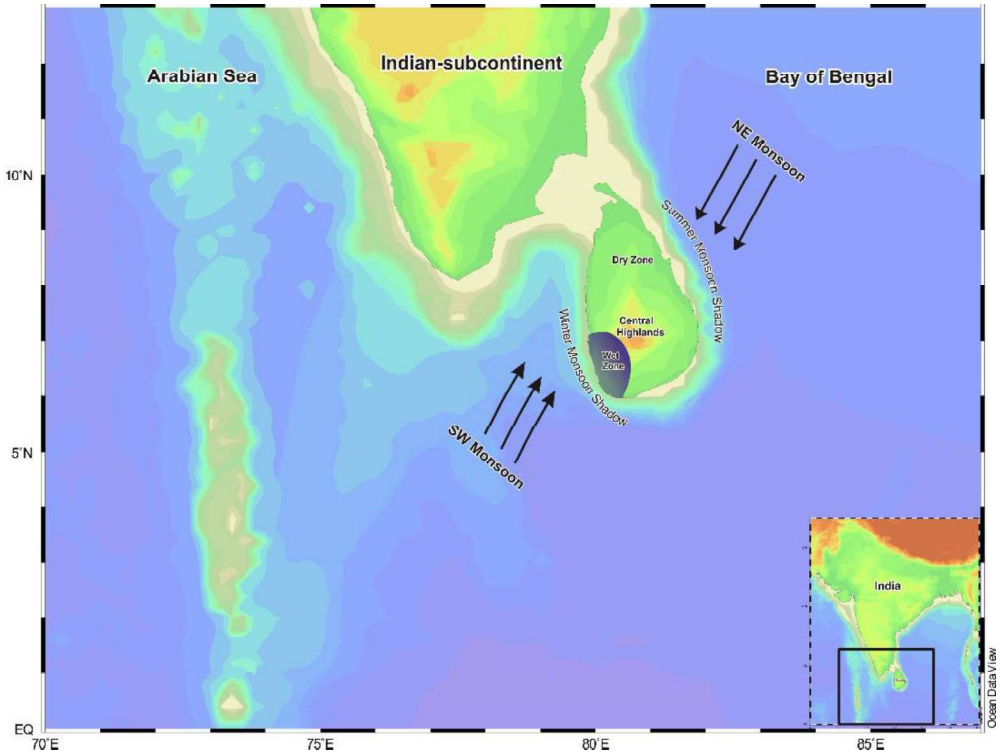

Figure 1.4: Climatic zones (Wet and Dry zones) and Shadow areas of Sri Lanka produced by Central Highlands during the monsoons.

The upwelling system along the southern coast of Sri Lanka is driven by interaction of wind driven circulation around the island, rather than by Ekman dynamics. This results in a converging coastal current system that flows offshore and causes divergence associated with offshore transport of water, which in turn results in upwelling along the southern coast during both the monsoon periods. The upwelling center along the eastern and western coasts depends upon the flow convergence and strength of the wind driven flow. Higher sea surface chlorophyll and lower sea surface temperature were observed to the southeastern Sri Lanka during SW monsoon. While, low sea surface temperature and high sea surface chlorophyll was observed towards southwestern Sri Lanka during NE monsoon. Thus, during SW monsoon the upwelling center shifts towards east as the flow along the western coast is stronger, and when the flow along the eastern coast is stronger, the upwelling center shifts towards west during NE monsoon.

1.5 Outline of the thesis

In addition to this chapter, thesis contains five other chapters. **Chapter 2** deals with procedures and protocols followed for the geochemical analysis of different parameters conducted in the study. **Chapter 3** demonstrates the control of monsoon over changing in situ productivity **Chapter 4** describes the influence of productivity and low bottom water ventilation on behavioral change of redox sensitive elements during last late quaternary period. **Chapter 5** explains the role of Total Solar Irradiance over geochemical proxies and climate. **Chapter 6** concludes the paleoclimatic and paleoproductivity variations and its forcing factors derived from the present study.

CHAPTER 2

MATERIAL AND METHODS

2.1 Sample collection and location of the sediment core

During the oceanographic expedition onboard ORV Sagar Kanya in the cruise 304A during 2013, a gravity core SK-304A/05 was collected from a water depth of 3408 m off Sri Lanka (05°45.622′N; 79°24.763′E:4.1 m long) from the equatorial Indian Ocean region (Fig 2.1). This was the maiden cruise organised as part of the GEOTRACES (Indian Ocean) for sampling the GI03 in the Indian Ocean for detailed investigation of various trace element and their isotopes both in water column and sediments for understanding various ocean processes.

The sediment core SK-304A/05 sampled in a perspex cylindrical tube was further was sub-sampled at 1 cm interval using perspex knife to avoid any metallic contamination. Nearly 3 cm of the top section was mixed and was sampled together and next ~8 cm of the core showed slight mixing, which was sampled carefully to avoid cross contamination. The sub-samples were sealed in cleaned ziplock bags immediately after sectioning and stored. In laboratory, one aliquot of the sample was dried at 80°C, finely powdered using agate mortar-pestle and kept in precleaned vials for further analysis. Other aliquot of wet sediment sample was preserved to separate planktonic foraminifera for ^{14}C measurements.

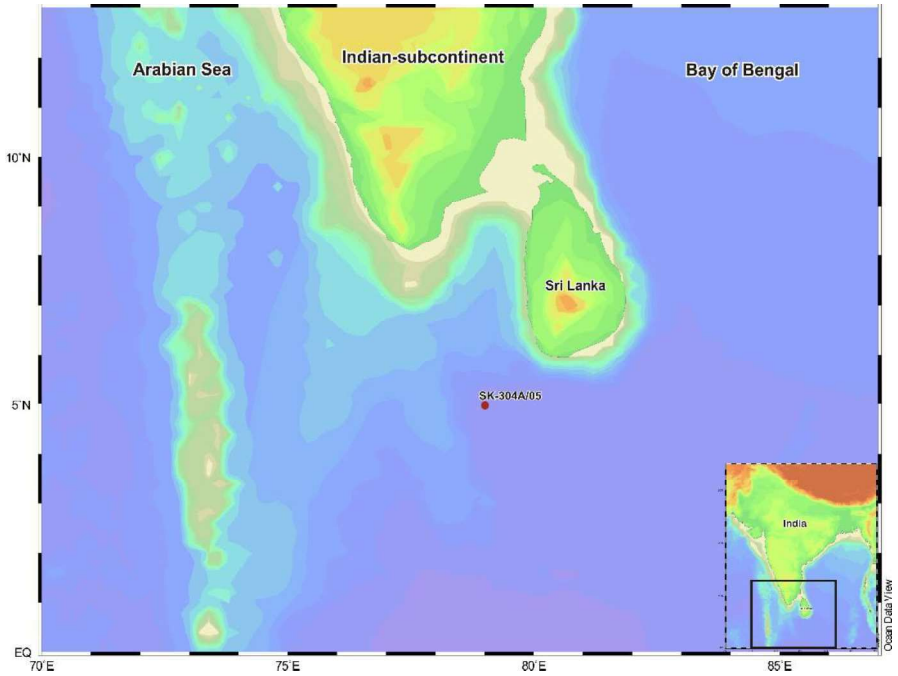

Figure 2.1: Location map of the studied sediment core SK-304A/05

2.2 Foraminifera Separation for Radiocarbon Measurements

Foraminifera are single celled eukaryotes, characterized by the absence of organs or tissues, belonging to Phylum *Protozoa*. The organisms live either on the sea floor or as planktons. The foraminiferal cell consists of protoplasm which is mostly bounded within a shell called *test*. The foraminiferal test is mainly composed of secreted organic matter; secreted minerals such as *calcium carbonate* or aragonite; or agglutinated particles, which gets preserved in marine sediments as fossils. The test consists of a single chamber (*unilocular*) or multiple chambers (*mulitilocular*). In multilocular forms, each chamber is separated by a wall called *septum*. These chambers are interconnected with a small opening in septum called *foramen*, which acts as passage for protoplasm to extend throughout the shell. At the wall of the final chamber an opening called *aperture* is found which connects protoplasm with the external pseudopodia. Apertures can be classified as primary or secondary, primary may be single or multiple in number and their position can vary while secondary apertures are along the sutures or periphery of the test. The typical life span of foraminifera are 2-4 weeks and their size ranges from 10 μ to 10 mm, with an average size ranging between 100 μ to 1 mm. Depending on the test morphology, foraminifera are divided into *Spinose* (bearing spines) and *Non-spinose* (lack of spines) forms. Generally, spines get broken and are not fossilized.

Foraminifera are important as biostratigraphical indicators. They are both planktonic and benthic. Planktonic foraminifera are wide spread and are passive dwellers in the surface water currents. They are the most recent in origin than benthics and existed since Jurassic (~200 Ma). Benthics are bottom dwelling species mostly sessile (attached to the sea bed) and existed since Cambrian (~570 Ma). They inhabit from continental shelf to abyssal plains. The planktonic species inhabit at different water depths from top 150 to 1000 m, and the absolute depth habitat of a particular species may vary greatly from one location to another depending on the position of the seasonal thermocline. Based on depth habitat, they can be classified as *Shallow-water*, *Intermediate-water* and *Deep-water* dwelling species. Shallow-water species live mainly in the upper 50 m of the photic zone, mainly spinose forms with long spines and globular chambers that

help them to improve buoyancy. They include all types of species of genus *Globigerinoides* and few *Globigerina*. Intermediate-water species mainly live within 50-100 m of the water column and include both spinose forms with symbionts and non-spinose forms without symbionts (hosting algae). Deep-water species live below 100 m (except as juveniles) with club shaped chambers or lack of spines. These species are adapted to cooler denser water masses.

2.1.1 Separation of foraminifera

Nearly 5-10 g of wet sediment sample was taken in a 200 ml beaker. For dispersing the agglutinated inorganic particles from foraminifera, 4 M sodium hexametaphosphate (calgon powder) was added, which acts as a dispersing agent. Thereafter, the samples were kept overnight for total disintegration of the sediments. The samples were wet sieved using sieves of the sizes 63 and 150 μ. The size fractions 63 and 150 μ were transferred to the beakers and shells were dried at 80°C. The dry fraction obtained was stored in pre-cleaned vials. The planktonic foraminifera species were handpicked Under stereoscopic microscope from the dry bulk fraction. Enough care was taken while picking to ensure that all separated shells are of similar size and not broken.

For AMS radiocarbon dating, ~1 mg of carbon from foraminifer separates is required. About 20 mg of select planktonic foraminifera were handpicked, namely *Globigerinoides ruber*, *Globigerinoides sacculifer* and *Globorotalia menardii*. These planktonic foraminifera were selected for the study as they reside mainly at the surface and near surface oceans (upto ~100 m) and readily incorporate changes occurring in the surface ocean into their calcite shells.

2.2 Radiocarbon dating

The chronology of the sediment core has been obtained using Radiocarbon dating method as part of this present work (Libby, 1955). The radiocarbon (^{14}C) is produced in the upper atmosphere, where cosmic ray produced slow neutrons produced react with ^{14}N atoms. The ^{14}C so produced gets oxidized to $^{14}CO_2$ in the atmosphere and follows the pathways of CO_2 and gets mixed and deposited in

various earth reservoirs. The seawater carbonate chemistry is governed by a series of equilibria as shown below:

$$^{14}CO_{2(atm)} \leftrightarrow {}^{14}CO_{2(aq)} + H_2O \leftrightarrow H_2{}^{14}CO_3 \leftrightarrow H^+ + H{}^{14}CO_3^- \leftrightarrow 2H^+ + {}^{14}CO_3^{2-}$$

At pH ~8.1, ~90 % of the inorganic carbon is present as bicarbonate ions (HCO_3^-), ~9 % as carbonate ions (CO_3^{2-}) and 1 % as dissolved CO_2 (Doney et al., 2009). The dominant fraction is taken up by marine microorganisms to secrete calcium carbonate shells. The foraminifer species form calcareous shells mainly comprising calcite. These calcite shells of microorganisms have radioactive carbon incorporated in them in equilibrium with surface seawater and can be used for radiocarbon dating. From nine (9) depths, mixed planktonic foraminifera species were separated for radiocarbon measurement. The radiocarbon dating was done using the Accelerator Mass Spectrometer (AMS) at NSF Arizona AMS Facility, University of Arizona, USA in collaboration with A.J.T. Jull (Linick et al., 1986; Jull et al., 1989; Somayajulu et al., 1999). In AMS technique atoms are counted, while in conventional method decay of atoms is counted. The conventional method is time consuming and takes nearly 5 days for analysis of one sample, whereas AMS takes less than an hour for the analysis and more samples can be analysed at the same time (Agnihotri, 2001). This allows AMS to measure even small samples, which assists in improving the accuracy relative to the bulk method by the absence of various contaminants that are usually present in the bulk samples. In typical mass spectrometers, the energies to which the ions are accelerated are in thousands of eV (keV) whereas in the AMS the energies are in millions of eV (MeV). The uncertainties in the identification of the atomic and molecular ions with the same mass (isobaric effect) are removed with such higher energies. Thus, we can measure isotopic ratio for specific elements to a level of 1 in 10^{15} (Agnihotri, 2001).

The ^{14}C ages of marine foraminifera are ~400 years older than the contemporary terrestrial wood, as it derives carbon with depleted $^{14}C/^{12}C$ ratios compared to the atmosphere from the oceanic reservoir (seawater). This depleted radiocarbon signatures of seawater results due to the long time taken by huge oceanic reservoir for mixing. At any given time for a region, the difference

between the regional marine ^{14}C age and global model marine ^{14}C age is given by ΔR (Stuiver and Braziunas, 1993; Bhushan et al., 2001).

Table 2.1.Radiocarbon ages and calibrated age ranges of the samples for the core SK-304A/05 from the equatorial Indian Ocean

S.No.	Sample ID	Laboratory ID	Depth range (cm)	Radiocarbon age (yr BP)	Calibrated age Range (cal yr BP)	
1	PRL-AS-01	AA104059	4	2793 ± 32	2338	2528
2	PRL-AS-02	AA104060	11	3209 ± 32	2844	3013
3	PRL-AS-03	AA104061	21	4173 ± 33	4071	4257
4	PRL-AS-04	AA104062	40	5787 ± 35	6050	6217
5	PRL-AS-05	AA104063	60	8014 ± 38	8347	8476
6	PRL-AS-07	AA104065	101	10372 ± 44	11192	11427
7	PRL-AS-08	AA104066	119	12172 ± 49	13459	13648
8	PRL-AS-09	AA104067	149	16642 ± 63	19399	13639
9	PRL-AS-10	AA104068	201	21910 ± 120	25646	25881

The ΔR value is the reservoir age correction, which is applied for all radiocarbon ages of marine samples before calibrating ^{14}C ages. In the present study, the radiocarbon ages obtained are calibrated to calendar ages using calibration program calib 7.0.2 using Marine13 (Stuiver et al., 1998; Reimer et al., 2009; 2013). The radiocarbon dates were corrected using a reservoir age (ΔR) of 60±52 yrs applicable for marine samples from southern Bay of Bengal (Dutta et al., 2001; Southon et al., 2002). The errors reported for the calibrated ages of the samples are one standard deviation (1σ).

The age-depth model for the Core SK−304A/05 was constructed based on the calibrated radiocarbon dates of foraminifers at various depths (Table 2.1). The sediment accumulation rate of the core varies from ~5 to 13.8 cm.kyr^{-1} with highest and lowest sediment accumulation rate between ~8 to 11 ka and ~13.5 to 19.5 ka respectively. Average sediment accumulation rate for the last 25 kyr was ~8 cm.kyr^{-1}(Fig 2.2).

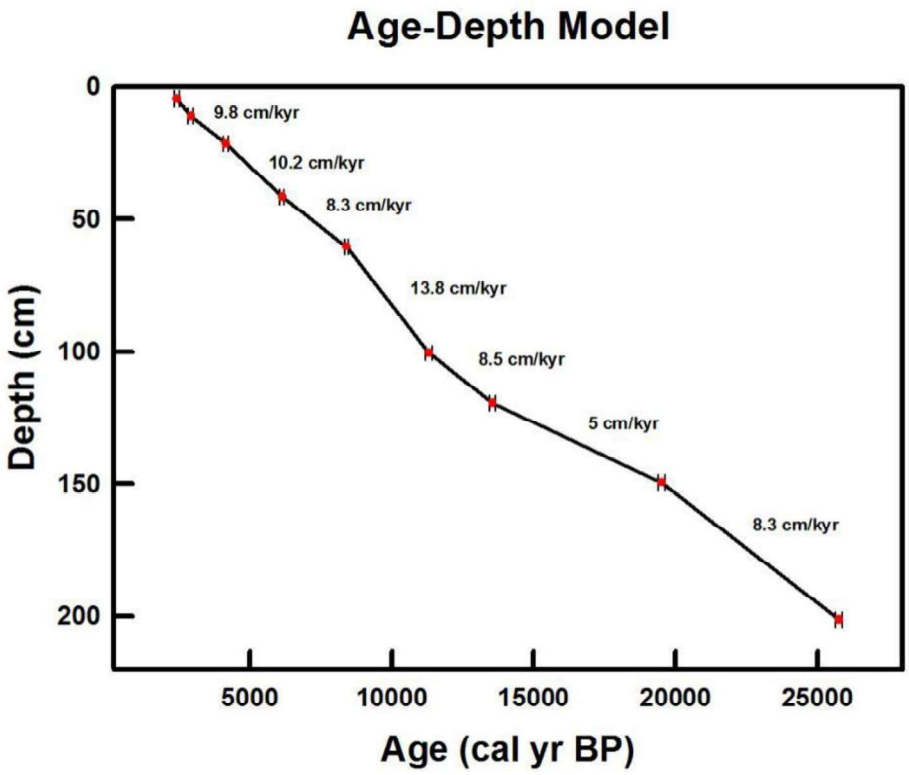

Figure 2.2: Age-depth model of the sediment core SK-304A/05. The values shown between the dated sample points indicate corresponding sedimentation rate

2.3 Paleoclimate proxies

The signatures of surface productivity, bottom water redox conditions, terrestrial contribution and nutrient utilisation in marine sediment from the equatorial Indian Ocean has been elucidated using various paleoclimate proxies.

2.3.1 Productivity proxy

I. Organic carbon (OC) and nitrogen (N)

Organic carbon (OC) and nitrogen (N) preserved in the sediments are mainly derived from settling of biogenic debris and is a manifestation of the overhead surface productivity provided there are no alterations after deposition (Müller and Suess, 1979; Schulz et al., 1998). Around 5 % of the fixed OC by photosynthesis in the euphotic zone is transported to the deeper waters, where it undergoes degradation before reaching the ocean bed. At sediment water interface, most of the OC and N gets oxidized at the top 5-10 cm of the

sedimentary column due to availability of oxygen. Thus, 0.05-0.1 % of the total surface productivity gets eventually preserved (Chester, 2003). The regions underlying oxygen minimum zone (OMZ) and the regions with reducing conditions at the sediment water interface experience enhanced OC preservation. High sedimentation rate also reinforces the enhancement of OC preservation, as it shields the organic matter from diagenesis (Heinrichs, 1992). As the organic matter is prone to degradation, downcore variation of OC and N does not manifest overhead productivity. The Cu, Ni acts as micronutrients and are scavenged by OC from the water column. The Cu and Ni are retained within the sediments, whereas the OC gets remineralised by bacterial activity. Thus, their downcore variation serves as an organic carbon productivity proxy (Schnetger et al., 2000; Tribovillard et al., 2006).

Organic carbon in the sediments is derived from both terrestrial and marine sources. It is essential to ascertain the source of the organic carbon, before using it as a surface productivity indicator. C/N ratio has been used as tracer for delineating marine vs terrestrial components with marine organic matter having C/N ratio of ~7 (Redfield AC, 1934; 1958). The average C/N ratio of the recent marine sediments varies between 8-10 whereas ancient sediments varies between 12-15 (Mackenzie, 1980). Land derived plants has C/N ratio ranging between 20-100 (Premuzic et al., 1982; Meyers, 1994).

II. Calcium carbonate ($CaCO_3$) and Biogenic silica (BSi)

The calcitic shells forms the major constituent of marine sediments and are mainly composed of foraminiferal shells called as carbonate ooze. The $CaCO_3$ flux acts as an indicator of overhead calcareous productivity (Shimmeld,1992; Reichart, 1997). The $CaCO_3$ content in the sediments can serve as a proxy for productivity provided the core is from the depth above regional lysocline (4000 m for equatorial Indian Ocean) (Schulte and Bard, 2003)) with no contribution from detrital carbonate (Sirocko et al., 1993, 2000. The concentration of Sr and Ca due to its association with $CaCO_3$ and biogenic Ba (BioBa) corrected for the detrital component also serves as calcareous productivity indicator. Bio Ba is formed through barite precipitation by decaying organic matter (Reichart et al., 1997;

Goldberg and Arrhenius, 1958; Ganeshram and Pedersen, 1998; Dymond et al., 1992; Sirocko et al., 1996; Agnihotri et al., 2003).

Biogenic silica also known as biogenic opal is a chemical determination of the amount of amorphorous hydrated SiO_2. They are mainly produced in the upper water column and is composed of biological components such as diatoms, radiolarians, silicoflagellates (Gehlen et al., 2002; Conley, 1998). BSi is one of the major component of the marine sediments and its downcore sedimentary records provide information of past ocean productivity variations.

III. Detrital proxy

The major components of aluminosilicate phases are Al, Ti, Fe and Mg, and hence are tagged as detrital inputs to the sediments (Agnihotri et al., 2003). Except Fe, the concentration of these elements is not affected by the changing redox conditions in the water column and in the sediments. Thus, the depth profiles of these elements can be used to infer the detrital contribution to the sediments, as they are predominantly controlled by changing supply of detrital contribution as a function of river discharge/aeolian transport linked with monsoon during the past (Agnihotri et al., 2003; Tripathy et al., 2014).

IV. Redox sensitive elements

The organic carbon (Shetye et al., 2014) and Mn-Fe oxy-hydroxides (Tribovillard et al., 2006) are the major sources for the transportation of the trace elements from water column to the sediments. The trace elemental concentration (Mo, V, Mn, Cr) in the sediments are used to infer the redox conditions in the water column and at the sediment water interface. In oxic and anoxic environments, the trace elements have different behavior based on their oxidation states which is influenced by the redox conditions (Shetye et al., 2014). In oxic waters, Mn gets precipitated as Mn-oxides into the sediments, while V, Mo, Cr, U are found to be depleted. But under anoxic conditions V, Mo, Cr, U are highly enriched in sediments where bottom water oxygen is zero (Calvert and Pedersen, 1993; 1996; Algeo and Lyons, 2006; Tribovillard et al., 2006; Pattan and Pearce, 2009). Thus, an inverse relation can be observed between Mn, Cr, V, Mo in sedimentary column.

2.3.2 Stable isotopes

The stable isotopes Carbon, Nitrogen and Sulphur have been extensively used for past climate reconstruction. Generally, variation in stable isotope is expressed using delta (δ) notation in per mil (‰). And is defined as the ratio of ratio of less abundant (heavy) isotope to more abundant (lighter) isotope.

$$\delta = (\frac{\boldsymbol{R}sample}{\boldsymbol{R}std} - 1) \times 1000$$

Where, Ra is ratio in sample and Rstd is ratio in standard, and **R**= $^{13}C/^{12}C$, $^{15}N/^{14}N$, $^{34}S/^{32}S$

I. Carbon isotopes ($\delta^{13}C$)

The carbon has two stable isotopes ^{12}C and ^{13}C with natural abundance of 98.89 % and 1.11 % respectively. The standard used for measurement is Vienna-Peedee Belemnite (PDB). On the Earth, the carbon has two reservoirs, organic matter and sedimentary carbonates. To ascertain the organic carbon source, $\delta^{13}C$ of the sedimentary organic matter is measured along with OC/N (Lamb et al., 2006). The marine $\delta^{13}C$ values for OC ranges between -19 ‰ to -22 ‰ (Sarkar et al., 1993; Agnihotri, 2001), whereas, the terrestrially derived organic matter ranges between -26 ‰ to -28 ‰ (Fontugne and Duplessy, 1986). A mixture of both terrestrial and marine organic matter can result values in between these two limits. By using $\delta^{13}C$ and C/N as tracers, it is possible to delineate the proportion of marine and terrestrial components of the organic matter in the sediments.

II. Nitrogen isotopes ($\delta^{15}N$)

The nitrogen has two stable isotopes, ^{15}N and ^{14}N with natural abundance of 99.64 % and 0.36 % respectively. The standard used for measuring nitrogen isotopes is atmospheric nitrogen. In oceanic regimes, the nitrogen fixing bacteria called as diazotrophs, fixes N_2 to ammonia (NH_3) and NH_4^+ through photosynthesis process. The NH_3 and NH_4^+ is converted to nitrate (NO_3^-) and nitrite (NO_2^-) by the bacteria *Nitrosamonas* and *Nitrobacter*. Nitrate is the major nutrient consumed by the phytoplankton. Phytoplankton preferentially consume NO_3^- with lighter ^{14}N, thus enriching the residual nitrate. Thereby, depleted $\delta^{15}N$ of the organic matter indicates conditions of low relative nutrient utilization,

whereas enriched $\delta^{15}N$ of the organic matter implies high relative nutrient utilization (Müller and Opdyke, 2000). Thus, sedimentary $\delta^{15}N$ records the relative nitrate utilization in the region (Farrell et al., 1995; Holmes et al., 1997).

III. Sulphur isotopes ($\delta^{34}S$)

The Sulphur has four naturally occurring isotopes ^{32}S, ^{33}S, ^{34}S, and ^{36}S with abundance of 95.02 %, 0.75 %, 4.21 % and 0.02 % respectively. The sulphur isotopes are used to ascertain the Earth's environment over the past such as rise of the atmospheric oxygen, ocean oxygenation and mass extinction (Riccardi et al., 2006; Jones and Fike, 2013), through a variety of abiotic and biotic reactions, where sulphate reduction and the formation of pyrite in marine environments takes place (Berner, 1970; Jorgensen, 1983; Canfield et al., 2000). The oceanic sulphate isotope composition ($\delta^{34}S$) ranges from +35 ‰ to +5 ‰ with an average of +20 ‰ (Thode, 1970; Strauss, 2003; Bottrell and Newton, 2006).

2.4 Analytical techniques

2.4.1 $CaCO_3$, OC and N measurement

Calcium carbonate ($CaCO_3$) in the sediment samples was estimated using Coulometer (*UIC Coulometer; 5012*) and organic carbon (OC) and nitrogen (N) were measured using NC elemental analyser (*Flash 2000*) at Physical Research Laboratory (PRL), Ahmedabad.

Total organic carbon (OC) along with nitrogen (TN) were estimated using NC organic elemental analyzer (*Flash 2000*). To estimate the organic carbon, the sediment samples were decarbonated using 10 % HCl and washed thoroughly with deionised water and dried at 80°C to remove the inorganic carbon fraction. Nearly about 20-25 mg of the decarbonated powdered sample was packed in a tin capsule and was introduced into a combustion chamber at 1020°C through an autosampler of the elemental analyser. Immediate combustion of the sample at high temperature (1020°C) in presence of high purity oxygen gas leads to flash combustion. High purity helium gas is used as a carrier gas. The gases thus evolved as part of the combustion comprises CO_x, NO_x, SO_x and halides. Except CO_x and NO_x, all other impurities are removed by various scrubbers. Only CO_x

and NO_x are allowed to pass through the reduction column containing metallic copper, maintained at a temperature of 650°C. Further the reduced gases (CO_2 and N_2) are passed through a magnesium perchlorate filter to remove moisture. And finally, the purified gases are passed through a gas chromatographic column, where they are released sequentially, and enters the Thermal Conductivity Detector (TCD). The electrical signal generated are proportional to the concentrations of the gases present and the peak area is integrated for the quantitative estimation. The calibration is done with standards supplied by Elemental Microanalysis using High Organic Soil Sample (HOSS) (OC: 6.72 %; TN: 0.5 %) and Low Organic Soil Sample (LOSS) (OC: 1.65 % TN: 0.14 %) as standard reference material (Bhushan et al., 2001). The measurement precision for carbon estimation with HOSS & LOSS is 0.2 % and 5 % respectively. The precision of measurement for nitrogen estimation with HOSS & LOSS is ~2 % (Table 2.2).

The inorganic carbon in the form of calcium carbonate ($CaCO_3$) was estimated using Coulometer (*UIC Coulometer, Model 5012).* Nearly 15-20 mg of the finely powdered sediment sample was treated with 5 ml of 40 % Orthophosphoric acid in a closed system at a temperature of 80°C using Acidification Module (CM5130). The liberated CO_2 is flushed from the system by the carrier gas (CO_2 free air) and is allowed to pass through a column containing silica gel for drying. Thus, the obtained CO_2 is passed through the coulometer cell filled with a solution containing monoethanolamine and a pH indicator. A Pt cathode and an Ag anode are positioned between a light source and a photodetector in the coulometer. The CO_2 is estimated based on Faraday's law of electrolysis, which states that 1 F of electricity will result in alteration of 1 GEW (Gram Equivalent Wt) of a substance during electrolysis. In the coulometer, each F of electricity is expended to electrolyse equivalent to 1 GEW of CO_2 titrated. As the CO_2 gas passes into the cell, the CO_2 is absorbed, reacting with the solution to form titrable acids, which causes the color indicator to fade. Photodetection monitors change in color of the solution as %Transmittance (%T). As %T increases, the titration current is automatically activated to electrochemically generate base at a rate proportional to %T. When solution returns to its original

color the current stops. The calibration was done using pure and dried Na_2CO_3 as a standard material. The precision for $CaCO_3$ measurement is < 1 % (Table 2.2).

2.4.2 Biogenic silica (BSi)

The Biogenic Silica (BSi) was estimated using single-step wet-alkaline leach method (Carter and Colman, 1994). Nearly 50 mg of the finely powdered sample was treated with 5 ml of 10 % H_2O_2 to remove organic fraction, while the inorganic fraction was removed by adding 5 ml of 1N HCl and was allowed to react for few hours. Later the samples were centrifuged by adding 20 ml of Milli-Q water for 5 mins and the supernatant was discarded and dried. The dried samples were digested by adding 30 ml of 2 M Na_2CO_3 solution which was further heated in a hot water bath for 5 hours at 95°C. After 5 hours, the samples were immediately centrifuged, and 3 ml of each sample diluted with 30 ml of Milli-Q. Each of the diluted samples were acidified by adding 0.9 ml concentrated HNO_3 and the final solution was used to measure the amount of Si extracted using ICP-AES (Jobin-Yvon, Model 38S). The measured Si concentration was corrected for clay mineral dissolution during leaching using the molar ratio of Si:Al (0.66) in clay mineral. The precision for BSi is found to be ± 3 %. The calculated Si concentration was converted to Biogenic Silica concentration by using the following formula

$$BSi = 2.4 *[X- (0.66Y)]$$

Where, BSi is Biogenic Silica concentration, X is the measured Si concentration and Y is the measured Al concentration.

2.4.3 Major and trace elemental analyses

For elemental chemistry, the sediment samples were dried at 80°C which was further crushed and homogenized to fine powder using agate mortar and pestle to avoid metallic contamination. Nearly 300 mg of finely powdered samples were subjected to closed digestion by treating them with mixture of concentrated HNO_3, HCl, and HF in microwave digestion system (*Milestone Digestion System, Model*). Following this, the mixture was evaporated, and the samples was treated with aqua-regia for complete digestion and dried. The samples were dissolved in 2 % HNO_3 and the final solution was made to 50 ml

(Dalai et al., 2004; Das and Krishnaswami, 2007). All the reagents used in the study were of analytical grade. Major (Al, Fe, Mg, Ca) and trace (Sr, Cu, Ni, Ti, Cr, Co, Mn, V, Mo) elements for each of the diluted sediment samples were measured by aspirating the samples in ICP-AES (*Jobin-Yvon, Model 38S*) and Q-ICP-MS (*Thermo fisher*) respectively. The precision of the instrument was obtained by repeat measurements for the elements analysed. The accuracy was estimated using Marine Sediment (MAG-1) and NOVA certified reference sediment standards. NOVA is deep sea clay sediment collected from north Pacific Ocean at a depth of 5351 m (Amin et al., 1972) and MAG-1 is a fined grained gray-brown clayey mud with low carbonate content from the Wilkinson Basin of the Gulf of Maine (Abbey, 1983; Gladney and Roelandts, 1987; Govindaraju, 1994).

2.4.4 Estimation of Burial flux (BF)

Burial flux (BF) of biogenic proxies is obtained by:

$$BF = C \times DBD \times s$$

where C is concentration (g/g); DBD is dry bulk density (g/cm^3) calculated using an empirical formula given in (Clemens et al., 1987) and s is sedimentation rate (cm/ka).

2.4.5 Carbon, Nitrogen and Sulphur isotopes

The carbon, nitrogen and sulphur isotope measurements were carried out at National Physical Laboratory, New Delhi using isotope ratio mass spectrometer (*Isoprime 100, Isoprime UK®*) coupled with an elemental analyser (*Pyrocube, Elementar®*). The pre-processing of samples was done in laboratory at PRL. The inorganic carbon fraction was removed from the sediments by decarbonation using 10 % HCl and washed with deionized water and dried at 80°C to measure $\delta^{13}C$, $\delta^{14}N$ and $\delta^{34}S$ in the organic fraction. Nearly 20-25 mg of the dried sample was packed in tin cups and was introduced in to the combustion tube maintained at 1120°C of Pyrocube EA (Agnihotri et al., 2015). The tungsten oxide padded with corundum balls and quartz wool filled in the combustion tube acts as catalyst for CNS mode of the instrument. The gases then evolved are allowed to pass through the reduction column filled with metallic copper, which is maintained at a

temperature of 850°C. N_2 is directly passed through an open slit orifice of IRMS, meanwhile CO_2 and SO_2 are held on two columns kept at temperatures 20 to 25°C and 55°C respectively. Once N_2 analysis is done, the CO_2 column temperature is raised to 240°C for desorption of CO_2 gas. Similarly, after CO_2 analysis, temperature of SO_2 column is raised to 220°C and SO_2 gas is allowed to be desorbed from the column (Agnihotri et al., 2015).

Table 2.2: Comparison of average concentration of various elements measured in the present study with that of the reported values

	MAG			**NOVA**		
Elements (%)	**Reported**	**Present Study**	**No. of readings**	**Reported (Agnihotri, 2001)**	**Present Study**	**No. of readings**
Al	8.21±0.16	7.9±0.7	17	8.4±0.29	8.2±0.4	13
Ca	0.978±0.071	1.02±0.1	13	–	–	–
Fe	4.76±0.42	5.0±0.4	14	5.41±0.23	5.6±0.4	14
Mg	1.8±0.06	1.8±0.2	17	2.34±0.09	2.3±0.2	8
Elements (ppm)						
Ti	4494±420	4452±212	23	3810±245	3810±235	18
Cr	97±8	97±9	18	63±4	67±3	21
Mn	759±68	741±28	18	7192±366	7184±378	18
Co	20±1.6	20±1.9	22	104±7	104±8	23
Ni	53±8	47±3	15	206±15	206±19	21
Cu	30±3	30±5	15	392±20	392±15	13
Zn	130±6	134±5	13	152±10	158±14	13
Sr	150±15	151±11	24	182±6	180±10	19
Ba	480±41	476±29	22	1635±52	1635±64	14
V	140±6	137±8	22	147±10	137±7	14
Mo	1.6	1.3±0.2	5	22±2	22±2	6
	HOSS			**LOSS**		
Elements (%)	**Reported**	**Present Study**	**No. of readings**	**Reported**	**Present Study**	**No. of readings**
C	6.72	6.74±0.14	33	1.62	1.71±0.04	7
N	0.5	0.49±0.02	15	0.14	0.14±0.01	7

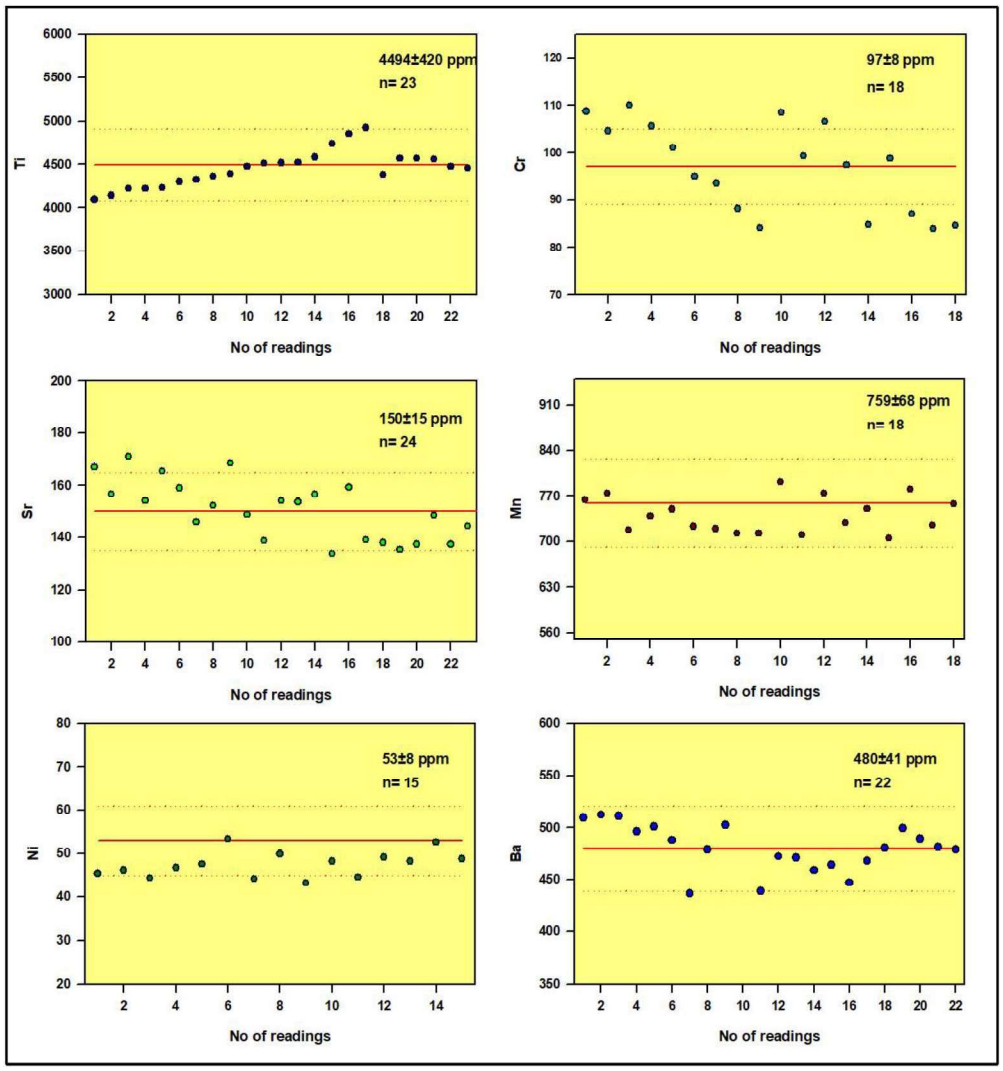

Figure 2.3: Variations in trace elements of reference standard MAG-1 during measurement on Q-ICPMS.

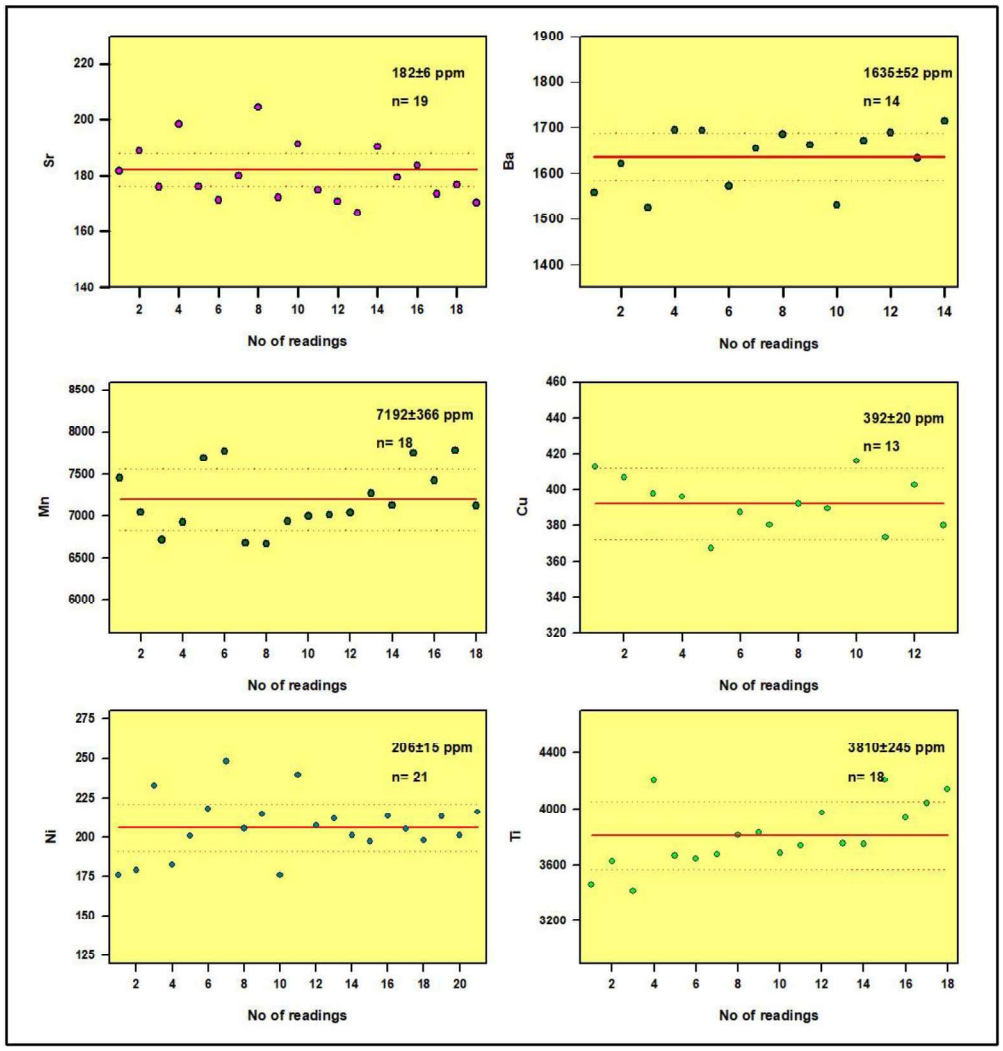

Figure 2.4: Variations in trace elements of reference standard NOVA during measurement on Q-ICPMS.

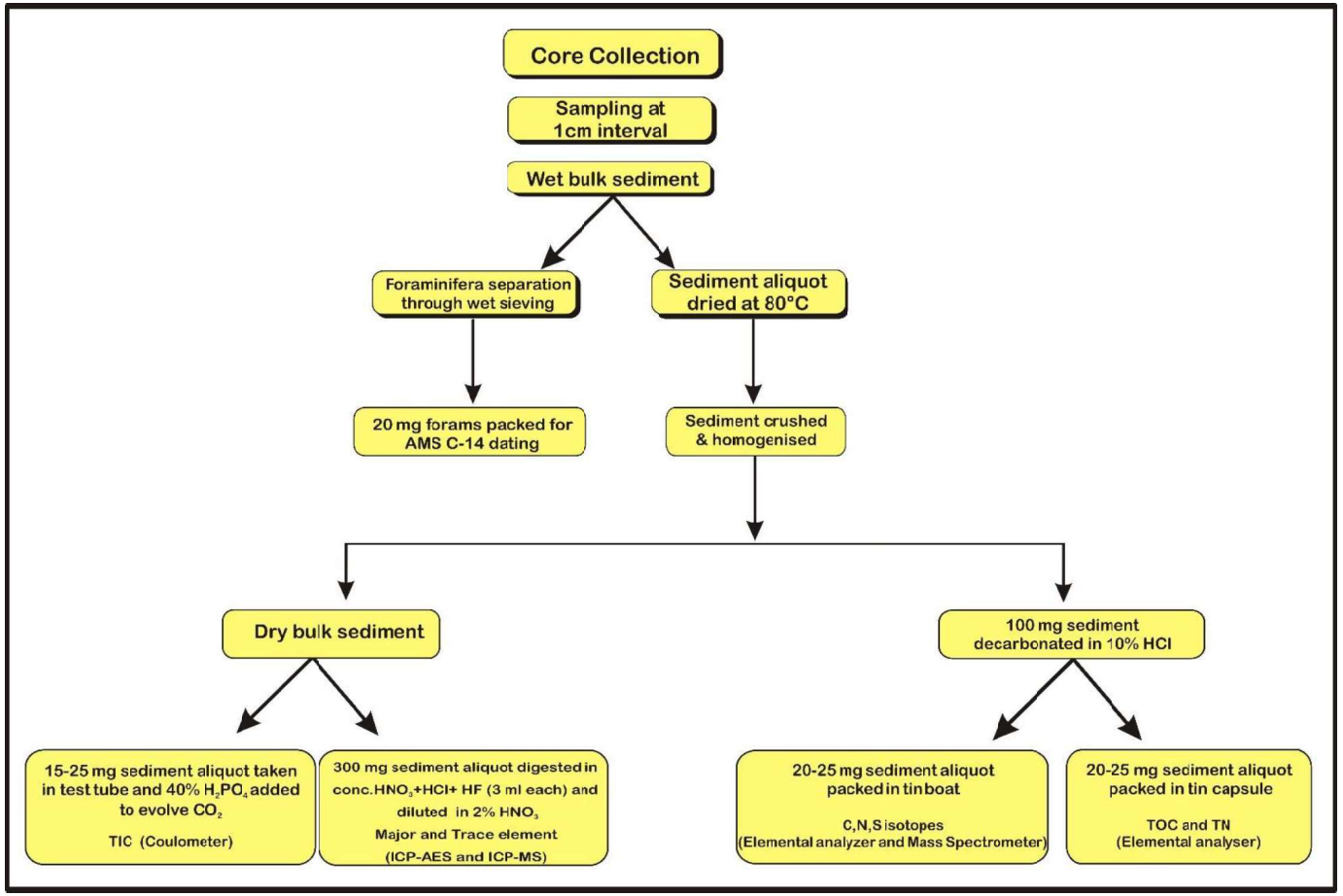

Figure 2.5: Schematic diagram of sampling and processing protocol followed for the measurement of various elemental and isotopic proxies.

CHAPTER 3

PALEOMONSOONAL RECONSTRUCTION FOR THE CENTRAL EQUATORIAL INDIAN OCEAN

3.1 Introduction

Instrumental and historical records for last several decades and centuries have demonstrated a considerable variation in the monsoon over Indian subcontinent and neighboring regions. Additionally, high resolution paleoclimatic reconstructions based on sediment cores (Bhushan et al., 2001; Saraswat et al., 2013; Banerji et al., 2017; Chandana et al., 2017; Panmei et al., 2017), speleothems (Sinha et al., 2005; Yadava and Ramesh, 2005; Fleitmann et al., 2007), corals (Ahmad et al., 2011), peat sections (Sukumar et al., 1993; Hong et al., 2003; Rühland et al., 2006) etc. with well constrained chronologies has led to significant advancement in the understanding the monsoon. The thermal contrast between land and ocean in the northern Indian Ocean plays a key role in seasonal reversal of the wind systems, resulting in monsoons which has a significant role in the socio-economic development of Indian subcontinent and adjoining regions. The monsoon over Indian subcontinent is controlled by migration of narrow latitudinal wind convergence zone termed as intertropical convergence zone (ITCZ). During summer (June–September), a northward shift of the ITCZ induces moisture laden south-westerly (SW) winds resulting into strong SW monsoon or Indian Summer Monsoon (ISM) (Saher et al., 2007). ISM is an important component of global climate, and responsible for transporting heat and moisture from tropical ocean to higher latitudes across the equator (Clemens et al., 2003; Govil and Naidu, 2010; Kessarkar et al., 2013). Southward shift of the ITCZ during winter (November–February) results in dragging of north-easterly (NE) winds causing winter precipitation towards southern India (de Vos et al., 2014) (See Fig 1.1).

The convergence of the easterly trade winds along the equatorial ocean leads to the formation of ITCZ that creates Ekman transport of the surface water causing surface divergence with upwelling of cold nutrient rich water. Such strong upwelling of cold nutrient rich water in the Pacific and the Atlantic Oceans causes enhanced biological processes contributing to high carbon export into the deeper oceans (Schott et al., 2002; Bradtmiller et al., 2007; Vidya et al., 2013). Studies from the Pacific Ocean to decipher the past productivity variation showed enhanced productivity compared to Holocene during LGM, whereas the equatorial

Atlantic Ocean showed opposite trend (Bradtmiller et al., 2006; 2007). Unlike other equatorial oceanic regimes, the equatorial Indian Ocean presently does not witness such upwelling due to its unique geographical settings. The northern Indian Ocean with two contrasting basins viz. the Arabian Sea and the Bay of Bengal separated by Indian subcontinent mostly experiences monsoon-induced upwelling with certain zones exhibiting perennially intense Oxygen Minimum Zone (OMZ) and denitrification due to the combination of high productivity and moderate ventilation at water depths 150–1200 m (Naqvi, 1987).

Compared to other contemporary oceanic basins, limited number of studies has attempted to demonstrate the past upwelling processes from the equatorial Indian Ocean. Based on oxygen isotopic composition of *G. ruber* from eastern Maldives in equatorial Indian Ocean, Rostek et al., (1993) demonstrated increased evaporation and/or decreased precipitation during glacial stages attributing it to enhanced dry NE monsoon and/or reduced SW monsoon. Tiwari et al., (2006) studied paleo-productivity variations as a function of the Indian Ocean Equatorial Westerlies (IEW) and its connection with Southern Oscillation Index (SOI), a measure of El Nino. Reduced productivity due to low nutrient availability has been linked with ISM weakening during glacial periods corroborating well with maximum El Nino frequencies. Thus, ocean productivity is strongly influenced by nutrient availability and plays a significant role in controlling the CO_2 sequestration between ocean and atmosphere by effective utilisation dissolved inorganic carbon and transforming it into organic compounds (Elderfield and Rickaby, 2000).

3.2 Surface circulation in the study area

The surface and the coastal currents in the equatorial Indian Ocean reverses their direction in response to wind reversals (Fig 1.1). During summer, the Summer Monsoon Current (SMC) and East Indian Coastal Current (EICC) flows eastward from the Arabian Sea to the Bay of Bengal, while during winter, the winter monsoon current (WMC)/ northeast monsoon current (NMC) and West Indian Coastal current (WICC) flows from the Bay of Bengal to the Arabian Sea (Schott and McCreary, 2001; Shankar et al., 2002; de Vos et al., 2014). These

surface currents along with the coastal currents plays an important role in nutrient and chlorophyll distribution in the equatorial regions (Vinayachandran et al., 2004; Vidya et al., 2013).

The WICC in the Arabian Sea flows southwards transporting high saline water and merges with the eastward flowing SMC between equator and the Sri Lanka during summer monsoon (Schott et al., 1994). After crossing Sri Lanka coast, this current forms an anticlockwise eddy identified as Sri Lanka Dome (SLD) (Vinayachandran and Yamagata, 1998). The eddy current splits into two with one arm of the current flowing southward along the eastern coast of Sri Lanka and again merging with SMC flowing eastward, while the other arm flows northward along the East Indian coast as EICC (de Vos et al., 2014) (Fig 1.1B).

During winter monsoon, the surface and boundary current reverses its direction. The EICC along the eastern Indian coast flows southward and merges with NMC flowing from east to west transporting low salinity water from the Bay of Bengal to the Arabian Sea. After crossing Sri Lanka coast, the currents flow around the clockwise Lakshadweep eddy and northward along the western Indian coastline as the West Indian Coastal Current (WICC) (Schott et al., 1994; de Vos et al., 2014) (Fig 1.1A). Thus, reversal of surface currents during summers and winters results in productivity variations in the equatorial Indian Ocean, an interlinking zone between two contrasting basins of northern Indian Ocean. Thus, it necessitates to comprehend the overhead productivity variation during glacial-interglacial periods as a function of changing strength of ISM and winter precipitation.

3.3 Results and Discussion

3.3.1 Influence of monsoon on detrital proxy

The sediment core (SK-305A/05) raised from the intermixing zone of Arabian Sea and Bay of Bengal near the equatorial Indian Ocean off Sri Lanka mainly receives detrital contribution from the southern India and Sri Lanka. Presently, southern India and Sri Lanka receive high precipitation and freshwater influx during the SW monsoon, which potentially influences the sedimentation rate of the study area (See Fig 1.4). With increased precipitation in the study area

leading to enhanced detrital contribution, the downcore variation of detrital proxy such as Titanium (Ti), Aluminium (Al) and Iron (Fe) concentrations are expected to reflect changes in precipitation during glacial-interglacial period. Since the region remains deprived from NE monsoon precipitation, the detrital elemental concentration would mimic invariably as a function of SW monsoon. The Ti content varies between 2000–4000 ppm (Fig 3.1) with low values during 25–17.5 ka. Post 17.5 ka, an increased Ti concentration till 11 ka with two conspicuous declines at 16.8 ka and 13 ka has been observed. A sudden increase in Ti between 11–9 ka with a prominent peak around 10 ka was observed. Later, consistent values between 7–3 ka with a gradually increasing trend till 2 ka has been showed by Ti. The Al content varies between 2–5 % and Fe varies between 1–4 % with consistent values till 13 ka. Post 13 ka, a sudden decrease in Al and Fe concentrations is observed till 11 ka. Similar to Ti, a sudden increase in Al and Fe between 11–9 ka was observed.

Presently, the study area is significantly influenced by SW monsoon winds (Malmgren et al., 2003) accompanied by high freshwater influx from Gin Ganga and Kalu Ganga rivers. During LGM (24–19 ka), the downcore variation of Ti shows low concentrations (Fig 3.1) suggesting reduced detrital contribution as a result of low precipitation in the region.

Sea surface temperature (SST) variations in the equatorial Indian Ocean shows increasing trend of temperature from west to east, unlike in other world oceans (Webster et al., 1999). In different regions of the Indian Ocean, alkenones based SST reconstruction suggest temperature difference of ~1.5–2.5°C between present day and the LGM (Sonzogni et al., 1998). Similar SST reconstruction from the equatorial Indian Ocean for the last 137 kyr based on Mg/Ca of the planktonic foraminiferal species showed that the equatorial Indian Ocean SST was 2.1°C cooler than the present during last glacial maximum (Saraswat et al., 2005). While comparing the GISP2 temperature record (Alley, 2004) with SST record from the equatorial Indian Ocean, it is observed that the high latitude cooling and warming events were also documented in the equatorial ocean records (Fig 3.1), which fluctuated in sync with the mid-summer low latitude solar insolation (Berger and Loutre, 1991; Laskar et al., 2004).

To comprehend the influence of solar insolation on monsoon, detrital flux in the study area, the Ti, Al and Fe variation has been investigated with the mid-summer low latitude solar insolation (Berger and Loutre, 1991; Laskar et al., 2004) and monsoon index (Fig 3.1). The low solar insolation induced SW monsoon weakening during LGM which caused low freshwater influx is evidenced by low detrital contribution to the study area (Fig 3.1). Previous studies from the AS and the BOB also inferred weakening of SW monsoon during LGM associated with reduced land contribution (Nigam and Khare, 1995; 1999; Naidu and Malmgren, 1996; Rashid et al., 2007; Anand et al., 2008).

The equatorial Indian Ocean cooling during LGM has consequences on the ITCZ migration and subsequent monsoonal rainfall over the region, and low latitude insolation (Govil and Naidu, 2011; Kessarkar et al., 2013; Saraswat et al., 2013). Southward migration of ITCZ (towards equator) during LGM (Fig 3.5) resulted in SW monsoon weakening and less moisture over the region (Wang et al., 2001; Sinha et al., 2005; Broccoli et al., 2006; Fleitmann et al., 2007; Yancheva et al., 2007; Saraswat et al., 2013). The low Ti during LGM is thus indicative of reduced terrestrial flux suggesting weakened SW monsoon associated with low summer insolation and southern shift of ITCZ.

The initiation/onset of deglacial period (18–11 ka) and intensification of SW monsoon in the northern Indian Ocean is an event which is not continuous but has been interrupted by abrupt climatic events. This period is generally characterized by rise in global sea level, rapid climatic fluctuations (Rao et al., 2010). The increase in Ti and Fe concentration in the present study between ~17.5–16.8 ka represents high terrestrial influx to the core location, which can be linked with synchronous increase in solar insolation and monsoon index (Fig 3.1). The period ~17.5–16.8 ka thus can be marked as initiation of deglacial period with strengthened SW monsoon. The SW monsoon intensification during ~17.5–16.8 ka corroborated well with the study carried out by (Anand et al., 2008) on Mg/Ca of planktonic foraminiferal species from the eastern Arabian Sea. Based on $\delta^{18}O$ of planktonic foraminifera from the Bay of Bengal, (Govil and Naidu, 2011) suggested initiation of deglaciation around 15.8 ka. A significant decrease in Ti and Fe during 16.8–15 ka implies reduced monsoonal activity. The

study on $\delta^{18}O$ of stalagmites from India and China by (Pausata et al., 2011) and on Ba/Ca and $\delta^{18}O$ of planktonic foraminifera from eastern Arabian Sea by (Saraswat et al., 2013) too demonstrated reduced monsoonal activity, coinciding with Heinrich event 1 observed in North Atlantic region referred as cooler climatic episode (Bond, 1997). Thus, variations in Ti and Fe concentrations implies strengthening or weakening of both SW and NE monsoonal rainfall. This has been validated well in previously documented monsoon fluctuations from the eastern Arabian Sea (Govil and Naidu, 2010; Saraswat et al., 2013) and the Bay of Bengal (Govil and Naidu, 2011).

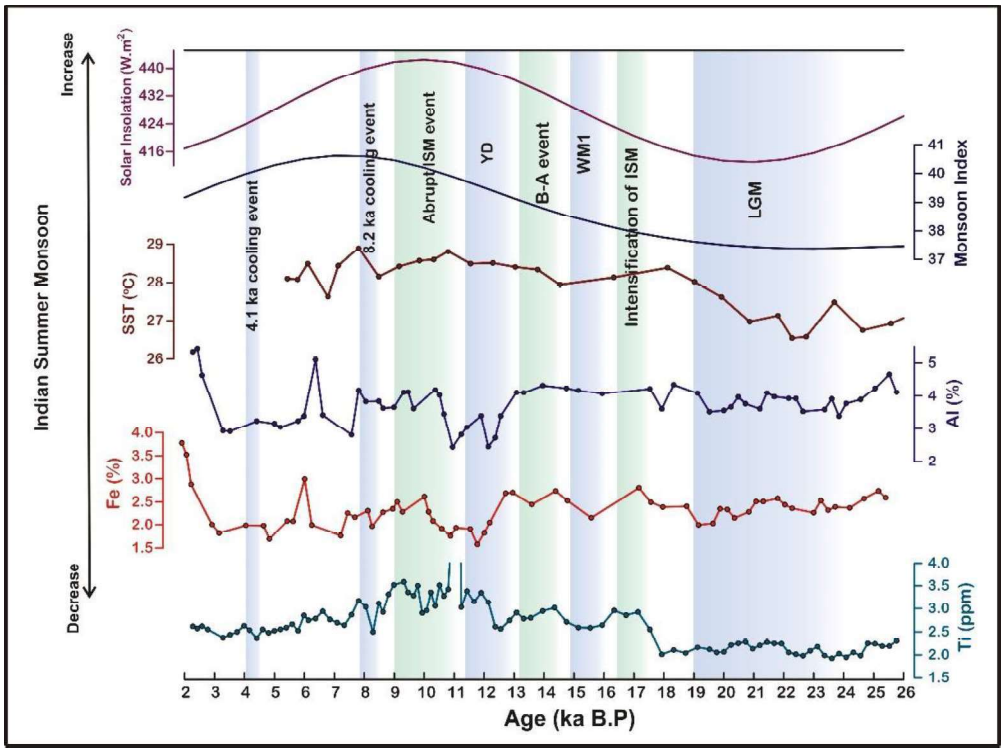

Figure 3.1: Comparison of Ti, Al and Fe record of core SK-304A/05 with Indian summer monsoon index, mid-summer solar insolation, Sea Surface Temperature record from equatorial Indian Ocean (Saraswat et al., 2005) and GISP2 temperature records (Alley, 2004). The blue bar indicates cold periods and green bar indicates warm periods.

Bolling-Allerod (B–A) event is a short-lived interglacial phase between 15–13 ka globally, which influenced northern Indian Ocean with SW monsoon strengthening (Saraswat et al., 2013) and is well documented in various sediment cores from northern Indian Ocean (Altabet et al., 2002; Tiwari et al., 2005; Singh et al., 2006; Rao et al., 2010; Kessarkar et al., 2013). SW monsoon intensification during 15–13 ka has also been documented in the speleothem $\delta^{18}O$ of Timta Cave (Sinha et al., 2005) and Hulu Cave (Wang et al., 2001) in north India and China. In the present study, the high Ti and Fe concentration during 15–13 ka thus implies enhanced terrestrial contribution associated with rainfall due to the intensification of SW monsoon.

An increase in the Ti concentration between 13–8.2 ka peaking at ~10 ka implies an increase in the detrital contribution as a function of SW intensification. Onset of Holocene period is known for monsoon intensification as a result of maximum solar insolation in the Northern Hemisphere which played significant role in improved SW monsoon intensity (Ramisch et al., 2016). This observation supplements previous studies based on geochemical and isotopic analyses where in increased SW monsoon has been observed (Sirocko et al., 1993; Naidu and Malmgren, 1996; Gasse, 2000; Govil and Naidu, 2011). Though, the Al concentration remained nearly consistent between 25–13 ka, a gradual decline in Al and Fe between 13–11 ka has been observed which can be attributed to onset of Younger Dryas (YD) associated with decrease in SW monsoon intensity. The $\delta^{18}O$ records of foraminifers from the Andaman Sea (Rashid et al., 2007), the northern Bay of Bengal (Kudrass et al., 2001), the eastern Arabian Sea (Anand et al., 2008; Kessarkar et al., 2013) and $\delta^{18}O$ speleothem records from Timta caves (Sinha et al., 2005) suggested weak SW monsoon rainfall during YD.

During early Holocene, a conspicuous decrease in the terrestrial signals between 8.5–7.5 ka (Fig 3.2) is correlated well with the low Total Solar Irradiance (TSI) (Steinhilber et al., 2009) corresponding to 8.2 ka global cooling event prevailed as a consequence of increased melting of ice sheets along with enhanced dryness and windiness in the Northern Hemisphere (Törnqvist et al., 2004). The 8.2 ka cooling event is also associated with glacial outburst flood in North Atlantic (Bond, 1997), which triggered SW monsoon weakening in the northern

India Ocean (Dixit et al., 2014a). Such reduced monsoon intensity has also been documented in the dolomite (an aridity proxy) (Sirocko et al., 1993) and upwelling record (Gupta et al., 2003; 2005; Thamban et al., 2007) from the Arabian Sea. All the detrital tagged elements (Fe, Ti, and Al) showed marginal enhancement between 7.5–6.5 ka suggesting mild amelioration in the monsoon triggered by increased TSI.

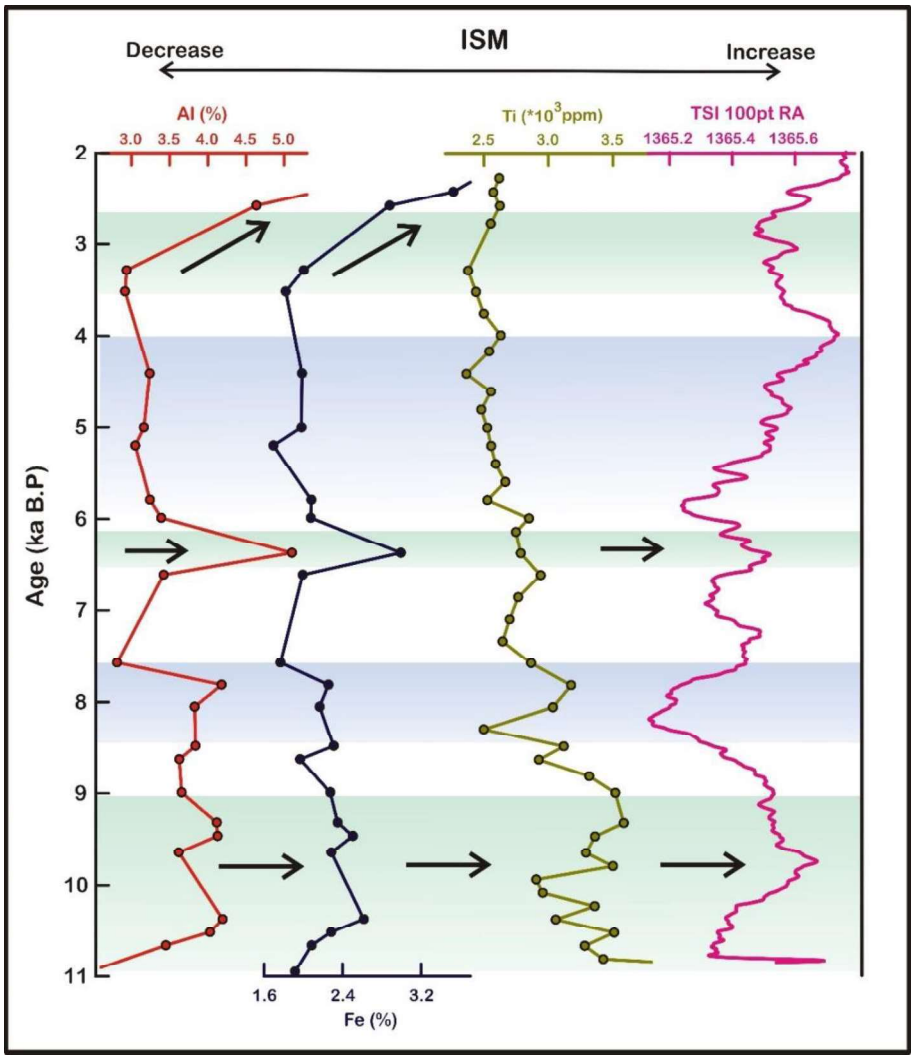

Figure 3.2: Comparison of Ti, Al and Fe record of core SK-304A/05 with Total Solar Irradiance (TSI). The blue bar indicates cold periods and green bar indicates warm periods.

Recent study from the SE Sri Lanka based on clay mineralogy on coastal cores demonstrated an arid climate with short wet intervals between 6.5-6.2 ka (Ranasinghe et al., 2013). Post 6.5 ka till 3.5 ka, low values of Ti, Al and Fe suggest dry climate with low precipitation. The $\delta^{18}O$ records and clay mineralogy from SE Arabian Sea and SE Sri Lanka sediment cores (Sarkar et al., 2000; Thamban et al., 2001; 2007; Ranasinghe et al., 2013) respectively have also shown dry climatic period during 6.5 to 3.5 ka. A significant drought event at 4.1 ka during mid-late Holocene played a significant role in transformation of Indus civilisation (Staubwasser et al., 2003; Dixit et al., 2014b). A noticeable decline of Ti from 4 ka probably marks this drought event. Post 3.5 ka, the terrestrial proxies (Ti, Al, Fe) display increase with simultaneous high TSI indicating wet conditions with improving rainfall conditions.

The solar forcing on SW monsoon variation has been evident based on various observations. The weakening of SW monsoon during LGM in the equatorial region of Indian Ocean resulted in low detrital input in response to low solar insolation. With the gradual increase in the solar insolation post 17.5 ka, SW monsoon strengthened thereby triggering increase in detrital contribution to the core location. During early Holocene, sudden increase in detrital input is observed in response to the high Northern Hemisphere solar insolation. This was followed by a gradual decrease around 8 ka corresponding to North Atlantic cooling event, and subsequent amelioration of SW monsoon after 3.5 ka. The present study site located off Sri Lanka in the equatorial Indian Ocean region documented global climatic events along with the regional climatic changes.

3.3.2 Biogenic proxies and evidences of ITCZ migration

The realisation of crucial role being played by oceanic productivity and biogeochemical cycle of carbon in regulating global climate change reinforced extensive studies on the reconstruction of paleoproductivity variations (Nath, 1999). Numerous studies have described noteworthy changes in the productivity during glacial-interglacial cycles. The bulk biogenic fraction of sediment encompasses mainly sedimentary organic matter, calcium carbonate and opal (biogenic silica) which are collectively used to infer ocean surface productivity.

Sedimentary OC is potential proxy used as an index of overhead surface water productivity being the basic component for all biota. To exploit OC as overhead productivity indicator, it is important to ascertain the source of OC. Thus, C/N ratio has been extensively used in addition to $\delta^{13}C$ to delineate marine vs terrestrially contributed OC. Generally, the C/N ratio for marine organic matter has been estimated to be ~7 (Redfield AC, 1934; 1958) with an average C/N ratio of the recent marine sediments ranging between 8–10, as more proteins and nucleic acids (rich in organic nitrogen) are present in marine plants (Blackburn, 1983). On the contrary, the land derived plants are composed of lignin and cellulose and poor in organic nitrogen resulting in C/N ratio >12 (Premuzic et al., 1982; Meyers, 1994; Prahl et al., 1997). $\delta^{13}C$ is generally enriched in labile marine organic matter (amino acids and carbohydrates) compared to terrestrially derived organic matter (lignin and lipids) which leads to shift in isotopic composition as a function of provenance of OC (de Lange et al., 1994; Prahl et al., 1997; Böttcher et al., 1998; Ogrinc et al., 2005; Vizzini et al., 2005). Thus, the typical isotopic composition of marine phytoplankton ranges from -19 ‰ to -21 ‰ for $\delta^{13}C$ (Gearing et al., 1984) while, for terrestrial organic matter the values ranges between -26 ‰ to -28 ‰ (Hoefs, 1996). The OC, C/N and $\delta^{13}C$ content in the present study varied between 1.3–5.1 wt%, 9–18 and -17 ‰ to -24 ‰ respectively. The OC shows enhancement between 24–18 ka, followed by a declining trend prevailing till 11 ka (Fig. 3-3). During 24–18 ka, the marine values of nearly -18 ‰ and ~12 are observed for $\delta^{13}C$ and C/N respectively (Fig 3.3 & 3.6), underpinning OC as a result of overhead productivity during LGM. Onset of early Holocene (11–8 ka) showed conspicuously high OC content and C/N>12 with depleted but fluctuating values of $\delta^{13}C$ indicating substantial contribution from the terrestrially derived organic matter as a result of improved SW monsoon. This period also displays enhanced TSI and solar insolation demonstrating solar forcing of SW monsoon. As the variation in OC being prone to degradation, affected by various processes such as overhead productivity or changes in sedimentation rates or the dust influx (Reichart et al., 1997), the other geochemical proxies need to supplement this information to infer past organic productivity. The Ni and Cu acts as micronutrients and are scavenged by OC from

the water column, they are retained within the sediments despite OC getting remineralised by bacterial activity. The downcore variation of Ni and Cu thus can serve as a potential tracer for OC productivity (Schnetger et al., 2000; Tribovillard et al., 2006). The Ni and Cu concentration normalized to Ti indicates their contribution other that detrital. The Ni/Ti and Cu/Ti ratios vary between 28–366 and 26–327 respectively. In the present studied sediment core SK-304A/05, Ni/Ti and Cu/Ti shows higher values similar to OC suggesting enhanced paleo productivity during LGM.

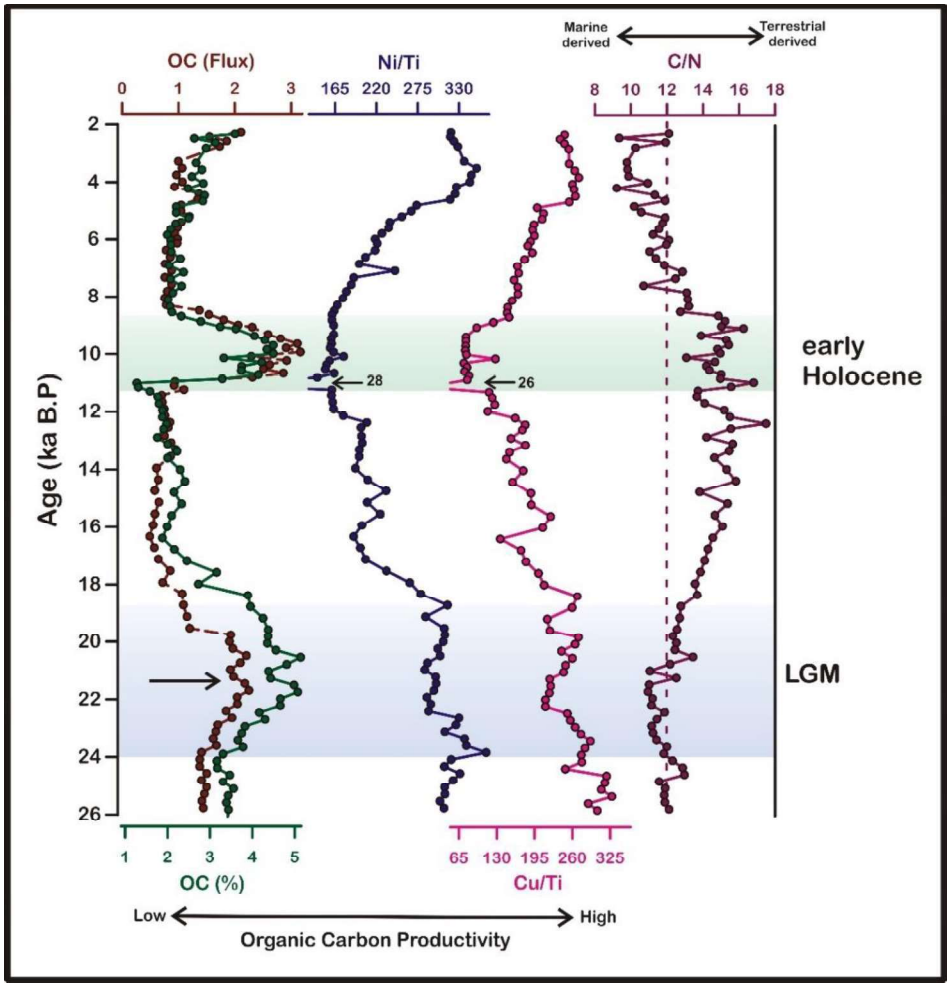

Figure 3.3: Downcore variation of Ti normalised productivity proxies (Ni & Cu), OC and OC Flux in the sediment core SK-304A /05. High values OC are observed during LGM and early Holocene.

Unlike OC, Ni/Ti and Cu/Ti didn't show any conspicuous peak during 22–20 ka, which indicates that besides overhead productivity some other

mechanism has played significant role in regulating OC content and peaking at 22–20 ka (discussed in Chapter-4). Since early Holocene to present, Cu/Ti and Ni/Ti trend are comparable with OC except an abrupt peak observed in the case of OC during 11–8 ka. The abrupt peak of OC during early Holocene (Fig 3.3) occurred as a result of greater terrestrial influence due to high sediment accumulation rate thereby leading to enhanced preservation of OC (Fig 2.2). These observations corroborate well with the ISM intensification of early Holocene that caused high terrestrially derived OC to the studied region.

The calcium carbonate accumulation at sea floor is predominantly controlled by three factors: the overhead surface productivity, the rate of dissolution through the water column and the dilution by means of the non-carbonate fraction and detrital input. The regional lysocline depth in the equatorial Indian Ocean is ~4000 m (Schulte and Bard, 2003), while the water depth of the present core location is ~ 3400 m, much less than that of regional lysocline depth and hence will result in negligible $CaCO_3$ dissolution. Thus in the present core, the $CaCO_3$ can be used as a potential proxy for the calcareous productivity. The $CaCO_3$ concentrations varied between 25.3–48.9 wt% (Fig 3.4) with high but consistent values between 25–12.5 ka followed by a declining trend till present. In general, the Ca and Sr gets associated with biogenic particles such as $CaCO_3$ (Reichart et al., 1997; Schnetger et al., 2000; Sirocko et al., 2000) and are extensively used as a contemporary proxy of calcareous productivity. The Ca/Ti and Sr/Ti ratio varies from 1.4–7.2 and 79–503 respectively throughout the core. The detrital corrected Ca/Ti and Sr/Ti trend are analogous to $CaCO_3$ downcore variations (Fig 3.4). The enhanced calcareous productivity during LGM has been indicated by the proxies ($CaCO_3$, Ca/Ti and Sr/Ti), which is in good agreement with the organic carbon productivity indicators (OC, Cu/Ti and Ni/Ti).

Apart from organic and calcareous productivity, one of the productivity components is Biogenic Silica (BSi) represented by siliceous phytoplanktons such as diatoms, silicoflagellates, sponges etc. The BSi is believed to be less prone to dissolution and sedimentation effects thus providing a crucial platform to reconstruct paleoproductivity variation. In the present study, BSi varies between 1.63–10.68 wt%. Generally, detrital corrected Ba (Ba/Ti) content is widely used

as a productivity tracer. In the present study, the BSi and Ba/Ti has been used to infer siliceous productivity variations (Fig 3.4). The BSi does not show significant variation like $CaCO_3$ till 12.5 ka. While, Ba/Ti show a downcore variation nearly similar to BSi with slightly enhanced values during LGM and with a declining trend till 11 ka.

Post 11 ka, both siliceous proxy Ba/Ti and BSi showed a marginal increase (Fig 3.4). The accumulation rate for OC, $CaCO_3$ and BSi varies between 0.5–3.2 $g.m^{-2}yr^{-1}$, 10–30 $g.m^{-2}yr^{-1}$ and 1.20–7.13 $g.m^{-2}yr^{-1}$ respectively. During LGM, both OC and $CaCO_3$ show high accumulation rates despite moderate sediment accumulation rate suggesting high productivity. But during early Holocene, high accumulation rates of OC and $CaCO_3$ suggests high terrestrial input as evident by high sediment accumulation rate (Fig 2.2). The BSi flux does not show much variation till 11 ka similar to its concentration. Post 11 ka, an increase in flux is observed. The OC and $CaCO_3$ in marine sediments serve as potential surface productivity indicators (Kessarkar et al., 2010). The high values of OC in the sediment core during the past is either due to high surface productivity linked to strong monsoonal winds (Schulte et al., 1999; von Rad et al., 1999; Thamban et al., 2001; Kessarkar et al., 2010; Punyu et al., 2014) or is a function of better preservation of OC under anoxic conditions at sediment-water interface (Sarkar et al., 1993; Pattan et al., 2003; Rao et al., 2010).

The present core retrieved from the water depth of 3400 m falls well within the oxygenated water depth. As OC is prone to degradation and $CaCO_3$ is prone to dissolution, the proxies associated with productivity such as Ca, Ni, Cu, Sr, Ba when normalized with Ti provides clues to the surface productivity variations. Both, enhanced values of OC with Ni/Ti and Cu/Ti ratios and high values of $CaCO_3$ along with Ca/Ti and Sr/Ti ratios observed in this study during LGM indicates high surface productivity (Fig 3.3 & 3.4). The geochemical study of the sediment core from the SE Arabian Sea suggested strong winter monsoon winds, which resulted in enhanced convective mixing that triggered improved overhead productivity during glacial period (Thamban et al., 2001; Kessarkar et al., 2010; Rao et al., 2010).

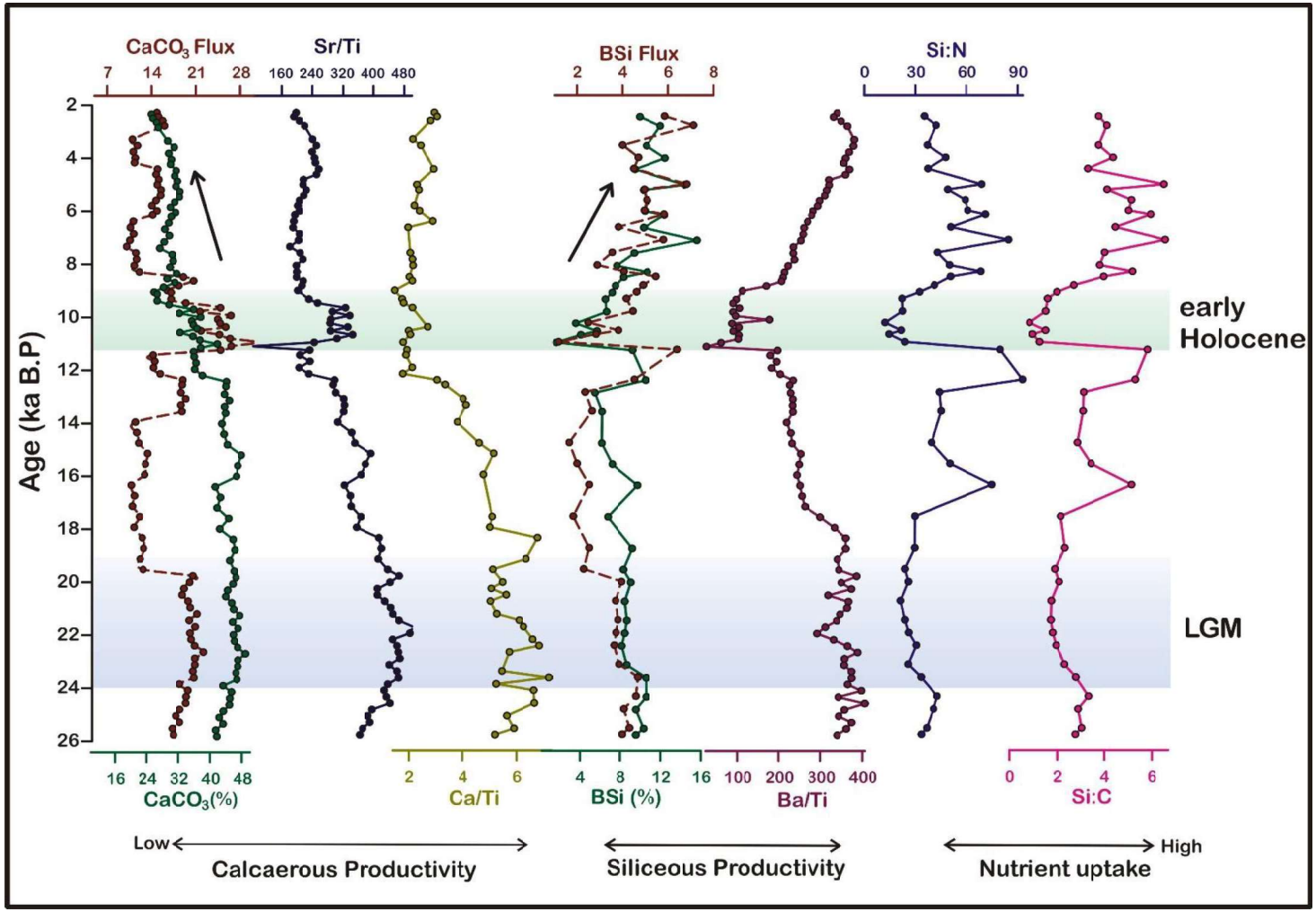

Figure 3.4: Comparative plot for Calcareous and Siliceous productivity along with nutrient uptake for the core SK-304A/05.

Contrarily, pollen and foraminiferal based study from the western Arabian Sea indicated high productivity during interglacial periods as result of strong coastal upwelling (Prell and Campo, 1986). These are mostly confined to the regions significantly influenced by the coastal upwelling and similar processes cannot be expected for productivity outside these regions (Luther et al., 1990; Pailler et al., 2002). In the present study, high productivity observed during LGM corroborates well with the globally known low summer insolation in the Northern Hemisphere. The present observation is comparable with the high productivity from a nearby equatorial Indian Ocean core located towards Arabian Sea during the LGM (Pailler et al., 2002). Thus, apart from changing solar insolation, some other mechanism has played a crucial role in controlling the productivity variations. The latitudinal migration of ITCZ in response to the alteration in solar insolation has been demonstrated based on $\delta^{18}O$ records of speleothem from different caves (Wang et al., 2001; Sinha et al., 2005; Fleitmann et al., 2007). Such high productivity during LGM can only be explained on the basis of southward migration of ITCZ due to low solar insolation (Fig 3.5) thereby leading to weakening of SW monsoon winds and intensification of NE monsoon winds (trade winds) (Böll et al., 2015) (Saher et al., 2007). These strong NE trade winds or monsoon winds caused divergence of the surface waters near the southwest coast of Sri Lanka resulting in upwelling of nutrient rich deep waters (nitrate and phosphate). This enhanced supply of nutrients to surface water triggered high surface productivity in this region. Strengthened NE monsoon winds during LGM also led to increased dust supply to the region bringing in high concentrations of trace elements (such as iron) which supports primary productivity (Mahowald et al., 1999). Moreover, the low C/N values and enriched $\delta^{13}C$ of the organic matter suggests marine origin of the organic matter.

In 2014, de Vos et al using satellite imaginary and numerical simulations with the help of Regional Ocean Modelling System (ROMS) near Sri Lanka suggested that presently during NE monsoon, the flow of wind is along eastern coast of Sri Lanka and shifting the upwelling center from east to west which enhances productivity along the southwestern coast. But, during SW monsoon, the flow of the wind is along western coast of Sri Lanka and the upwelling center

shifts from west to east (discussed in chapter 1). With the possibility of such scenario existing during LGM, when NE monsoon winds strengthened, it can be suggested that the combined effect of strong NE monsoon winds and increased dust influx triggered local upwelling that improved overhead productivity during glacial period (Fig 3.3 & 3.4). This is in agreement with previous studies from the equatorial Indian Ocean based on organic geochemical studies which suggested high productivity in the region during glacial period as a result of intensified NE monsoon (Rostek et al., 1993; Punyu et al., 2014).

During LGM, the region experienced low siliceous productivity and high calcareous and organic productivity (Fig 3.4). The region experienced low Si:N and Si:C values when calcareous plankton inputs were high in the total biogenic flux export. This suggests that both nutrient replete waters and dust influx resulted in low Si uptake and consequently reduced opal accumulation to the region. Hence, dominance of calcareous over siliceous productivity can be observed during LGM.

Tropical regions are the locale for intense monsoon systems, an integral component of deglacial climate changes. With the increase in the solar insolation, the onset of deglacial period after 17.5 ka witnessed weakening of NE winds thereby causing decline in productivity till 11 ka. The productivity proxies OC, $CaCO_3$ and Sr/Ti shows an abrupt increase between 11–8 ka associated with increased detrital components Ti, Al and Fe contents (index of terrestrial flux), while BSi, Ni/Ti and Cu/Ti did not show any such increase in values. Enhanced values associated with increase in terrestrial flux compared with high summer solar insolation (Fig 3.4) indicates strengthened SW monsoon after 11 ka (Ramisch et al., 2016) associated with high sediment accumulation rate during 11–9 ka (Fig 2.2), attesting better preservation of productivity proxies. The C/N of the organic matter shows values >12 suggesting terrestrial origin of organic matter during early Holocene due to enhanced lithogenic input. Post 8 ka, all the productivity proxies ($CaCO_3$, Sr/Ti, Ca/Ti, OC, Ni/Ti, Cu/Ti) shows decrease in concentration till present. Whereas, BSi, Ba/Ti, Si:N and Si:C values show an increasing trend and increase in Si uptake, with a shift towards the dominance of siliceous productivity over calcareous productivity with a better preservation

during mid and late Holocene. The C/N ratios <12 with fluctuating $\delta^{13}C$ values at ~ -21 ‰ suggest organic matter primarily of marine origin after 8.5 ka. During Holocene, in response to increase in Northern Hemisphere summer solar insolation, ITCZ shifted northward till 30°N latitude as shown in figure 3.5 (Stager et al., 2011; Chabangborn et al., 2014). This northward shift of ITCZ induced strong SW monsoon and weak NE monsoon winds compared to LGM, inhibiting upwelling and dust influx to the region thereby resulting in decreased surface organic and calcareous productivity during Holocene.

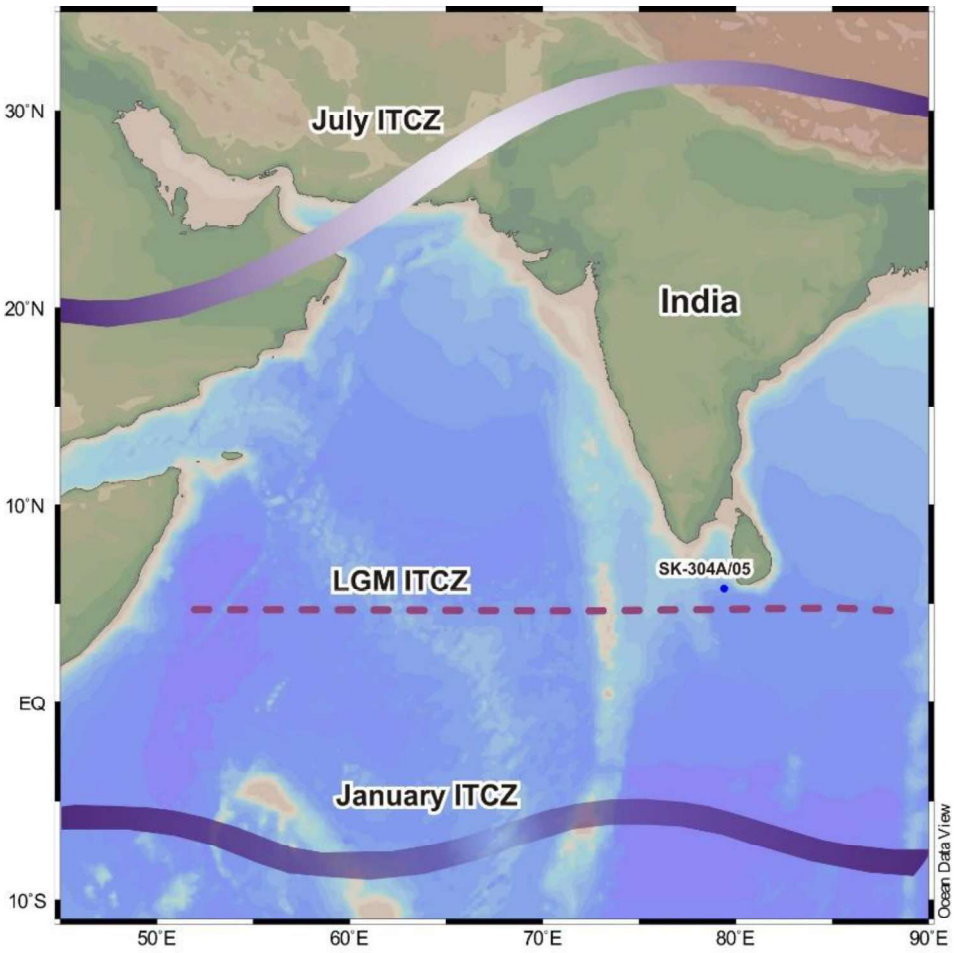

Figure 3.5: Reconstructed northern boundary of ITCZ during LGM and its present-day boundary of ITCZ in January and July (modified after Stager et al., 2011; Chabangborn et al., 2014).

3.3.3 $\delta^{15}N$ variation and its plausible causes

In nature, nitrogen has two stable isotopes ^{14}N and ^{15}N with abundance of 99.64 % and 0.36 % respectively. Physical, chemical and biologically mediated processes discriminate between the two isotopes known as isotopic fractionation leading to measurable difference in the ^{15}N to ^{14}N ratios among various forms of nitrogen present in different marine environments (Sigman et al., 2010).

Nitrogen is the major component of marine biota and act as a major nutrient required for phytoplankton which gets incorporated into the system through photosynthesis. Thus, nitrogen gets stored along with OC in the marine sediments. Similar to $\delta^{13}C$, the isotopic signatures of nitrogen has been widely used to delineate various biogeochemical processes such as OM synthesis, denitrification, nutrient utilisation and OC accumulation in the sediments (Hedges and Keil, 1995).

In the marine realms, the two major sources of N fixing are (a) continental input through river influx and the atmosphere and (b) marine N_2 fixation. Some species of algae (*Trichodesmium)* present in the open ocean fixes atmospheric N directly. The $\delta^{15}N$ of newly fixed N ranges from -1 to +2 ‰ compared to $\delta^{15}N$ of ~0.6 ‰ for dissolved N_2. The photosynthate produced directly from such organisms yield lighter $\delta^{15}N$ close to atmospheric N_2 (~0–2 ‰) (Capone, 1997; Brandes et al., 1998), and such process are mainly confined to oligotrphic low latitude waters. The inventory of marine N isotope budget suggests low contribution of continental nitrogen isotope to the marine system. The anthropogenically fixed N introduced as fertilizer along with the river input to oceans have $\delta^{15}N$ of 0–3 ‰.

Under oxic conditions, the microorganisms fix nitrogen by reducing N_2 to ammonia (NH_3) and ammonium (NH_4^+). Further, the nitrogen fixing bacteria (diazotrophs) converts the NH_3, NH_4^+ to nitrate (NO_3^-) or nitrite (NO_2^-) through a process known as nitrification. In suboxic/anoxic conditions, the bacterially mediated organic matter degradation utilises nitrate as electron acceptor, leading to denitrification. During the process, the bacteria preferentially take lighter $^{14}NO_3^-$, sequential reduction of NO_3^- to N_2O and N_2 that are lost into the

atmosphere. Residual nitrate in the oxygen deficient subsurface waters gets enriched in $^{15}NO_3^-$ than the mean deep water (Farrell et al., 1995).

The global average mean isotopic values of $\delta^{15}N$ in oxic waters is ~5±1 ‰ (Sigman et al., 1999), but under oxygen deficient conditions, the isotopic fractionation related to denitrification can lead to enriched nitrate in the subsurface waters as high as +18 ‰ (Cline and Kaplan, 1975). Globally, the water column denitrification has been primarily observed in three major areas: the Arabian Sea, eastern tropical North Pacific and eastern tropical South Pacific, and witness nearly zero oxygen concentrations. These regions are supplied by isotopically heavy nitrate to the surface by upwelling and are utilized by biota leading to $\delta^{15}N$ enriched organic matter that gets preserved in sediments (Saino and Hattori, 1987). Thus, enriched $\delta^{15}N$ can be used as one of the signatures of denitrification, which can be linked with climate induced productivity changes (Ganeshram et al., 1995).

The climatic perturbation during glacial-interglacial cycles influences the nutrient availability in the surface ocean which in turn plays an important role in monitoring the overhead primary productivity. Changes in productivity and nutrient levels in the water column versus nitrate uptake by phytoplanktons has revealed changes in $\delta^{15}N$ (Altabet and Francois, 1994; Ostrom et al., 1997; Freudenthal et al., 2001). Studies from north Atlantic, the Southern Ocean, eastern equatorial Pacific and Angola Basin, Africa (Altabet et al., 1992; Altabet and Francois, 1994; Farrell et al., 1995; Holmes et al., 1997) have demonstrated a linear relationship between nitrate depletion in the water column and an increase in underlying sedimentary $\delta^{15}N$. Besides nitrate utilisation, the sedimentary $\delta^{15}N$ is also governed by the isotopic signature of nitrate being utilised by phytoplankton. Deep water nitrate is the principal source of nitrogen to the surface ocean. According to First order Rayleigh fractionation kinetics, once the nitrate reaches the photic zone, preferential uptake of $^{14}NO_3^-$ over $^{15}NO_3^-$ by phytoplankton takes place, giving rise to isotopically depleted $\delta^{15}N$ photosynthate and a progressively enriched dissolved nitrate pool. This observation has led to an inverse relationship between sedimentary $\delta^{15}N$ and nitrate utilisation which gets reflected in the $\delta^{15}N$ of sedimentary organic matter (Mariotti et al., 1981; Kienast,

2000). Thus, the sedimentary $\delta^{15}N$ isotopic values can be used to elucidate the source and fate of the organic matter in the sediments (Peters et al., 1978; Thornton and McManus, 1994; Gordon and Goni, 2003; Wu et al., 2007; Zhang et al., 2007; Ramaswamy et al., 2008) and to reconstruct past nitrate utilisation changes in the region (Altabet and Francois, 1994; Farrell et al., 1995; Holmes et al., 1997).

The $\delta^{15}N$ varies in the studied core varies from 2 ‰ to 12 ‰, with depleted values during LGM and enriched values during mid-late Holocene. Enhanced overhead productivity as a result of ITCZ migration has been deciphered during LGM based on OC and $CaCO_3$ related proxies (as discussed in section 3.3.3). Additionally, the organic fraction of the sediments is predominantly of marine origin as evident by $\delta^{13}C$ and C/N<12 eliminates the terrestrial contribution during LGM (Fig 3.4 & 3.6). Depleted $\delta^{15}N$ (~6 ‰) observed during LGM cannot be attained by terrestrial contribution only. Unlike LGM, dominance of terrestrially derived organic matter during early Holocene has been suggested with high OC, C/N > 12 and depleted $\delta^{13}C$. Gradual enrichment of $\delta^{15}N$ post early Holocene period has been observed in spite of low overhead productivity and high terrestrial flux. Thus, the nitrogen isotopic composition in the study area has been controlled by following mechanisms, which are discussed in detail.

(a) Denitrification

Various studies from the Arabian Sea and Eastern Tropical North Pacific (ETNP) regions have reported change in $\delta^{15}N$ values as a result of denitrification in the water column (Altabet et al., 1995; Ganeshram et al., 1995). On the contrary, the present study area doesn't witness oxygen concentrations below 0.2 ml L^{-1} and hence cannot trigger nitrate reduction. Generally, denitrification in the water column is associated with high rates of biological productivity where the supply of oxygen exceeds demand for respiration and degradation of the OM, and NO_3^- is used as alternate electron acceptor.

Thus, if denitrification was the triggering mechanism for the observed changes in downcore variations of $\delta^{15}N$, then high $\delta^{15}N$ values would resemble

high OC content. On the contrary, an inverse relation between OC and $\delta^{15}N$ in the core (Fig 3.6) suggests that denitrification is not the responsible mechanism in controlling the sedimentary $\delta^{15}N$ values. Based on the above discussion and considering the present oceanographic conditions, it can be suggested that denitrification has definitely not played role in governing the overhead productivity during glacial-interglacial period.

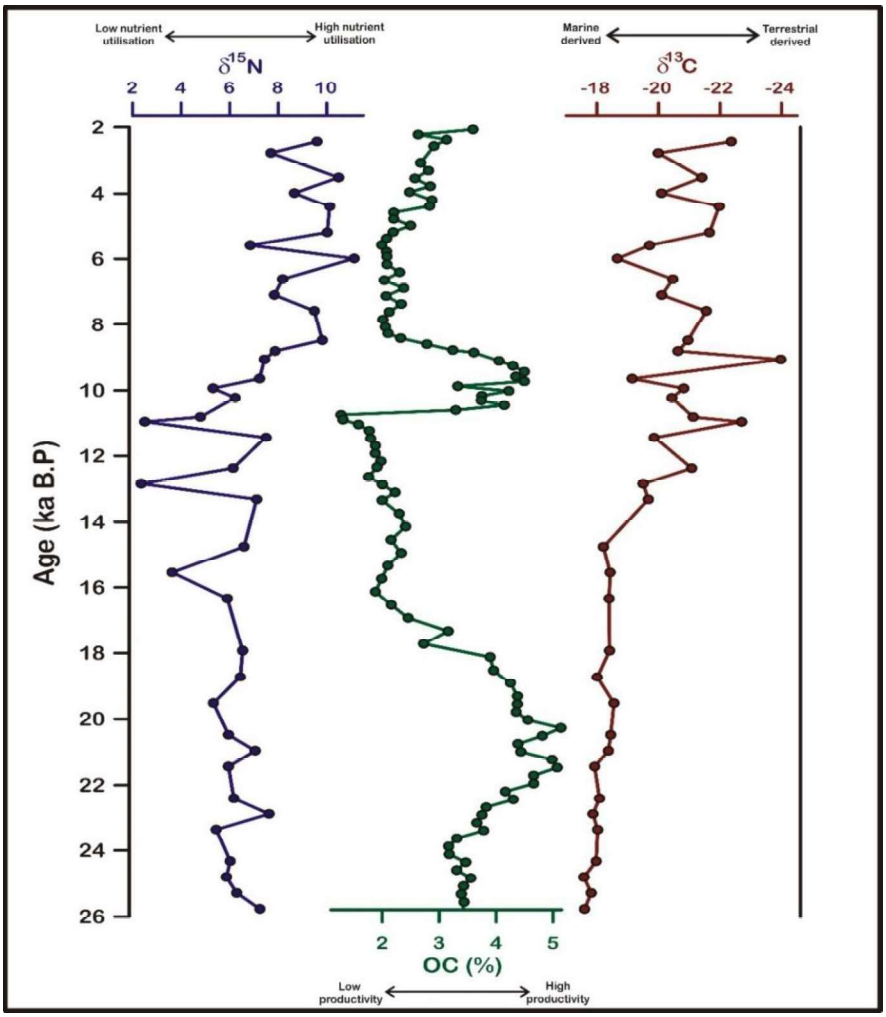

Figure 3.6 : The downcore variation of OC and stable isotopes ($\delta^{15}N$ & $\delta^{13}C$); where high productivity and low nutrient utilisation is observed during LGM

(b) Terrestrial influence and Nitrogen fixation

Mixing of terrestrial organic matter (~2 ‰) with marine organic matter can produce isotopically lighter $\delta^{15}N$ values of the sedimentary organic matter

(Sweeney and Kaplan. I. R., 1980). Any possible input of terrestrial organic matter that can affect the $\delta^{15}N$ values in the core can be assessed by the C/N and $\delta^{13}C$ of the organic matter. Therefore, the influence of terrestrial organic matter to region must be evaluated based on C/N and $\delta^{13}C$ of the organic matter. The $\delta^{13}C$ values of terrestrially and marine derived organic matter exhibit values of about -26 ‰ to -28 ‰, and -18 ‰ to -22 ‰ respectively. In the present study, even though the depleted $\delta^{15}N$ (~6 ‰) has been observed during LGM, but enriched $\delta^{13}C$ (~-18 ‰) and C/N<12 implies marine origin of organic matter. In addition, the Ti concentrations were also low implying reduced terrestrial influence in the region. On the contrary, during early Holocene both $\delta^{13}C$ and C/N showed terrestrially derived organic matter supported by enhanced Ti concentration but $\delta^{15}N$ showed enriched values. Therefore, it can be suggested that terrestrial contribution of $\delta^{15}N$ didn't affect the persistence of depleted and enriched $\delta^{15}N$ during LGM and early Holocene respectively.

The presence of nitrogen fixing cyanobacteria *Trichodesmium* can also result in depleted sedimentary $\delta^{15}N$. *Trichodesmium* comprises marine planktonic blue-green algae that survive in nutrient depleted oligotrophic waters and produce photosynthate directly fixing atmospheric N_2 rather than NH_3 or NH_4^+ (Tiwari, 2010). The organic matter produced by such organisms by fixing directly atmospheric N_2 are lighter in $\delta^{15}N$ values and has $\delta^{15}N$ values of about 0-2 ‰ (Capone, 1997). In the present study, strengthening of NE monsoonal winds triggered regional upwelling causing improved productivity as a result of high nutrient supply from the subsurface waters. As a matter of fact, *Trichodesmium* can only sustain in nutrient deplete waters which rules out the presence of *Trichodesmium* as a cause of $\delta^{15}N$ depleted values during LGM (Fig 3.6).

(c) Nutrient utilization

The nitrate uptake follows Rayleigh fractionation kinetics, wherein preferentially lighter $^{14}NO_3^-$ is consumed by the phytoplankton, giving rise to a lighter photosynthate and an enriched NO_3^- residual (Farrell et al., 1995). When the nutrient supply is abundant, and incomplete use of the nutrients leads to isotopically lighter sedimentary organic matter (relative low nitrate utilisation).

Contrarily, nutrient depleted surface waters lead to isotopically enriched sedimentary organic matter (relative high nitrate utilisation). Thus, other plausible cause of changing sedimentary $\delta^{15}N$ values is the incomplete nutrient utilisation in near surface waters (Farrell et al., 1995; Francois et al., 1997; Holmes et al., 1997; Ganeshram et al., 2000; Müller and Opdyke, 2000). In addition to nutrient availability and productivity, the degree of nutrient utilisation thus plays a significant role in controlling the $\delta^{15}N$ of the sedimentary organic matter. During LGM, the concomitant occurrence of low $\delta^{15}N$ and high productivity as evident by high OC and $CaCO_3$, reflects a decrease in relative nitrate utilisation. This underpins that though productivity was higher, nutrients utilisation was lower. In contrast, higher relative nitrate utilisation during late Holocene persisted as suggested by higher $\delta^{15}N$ with concurrent occurrence of low productivity. As discussed in previous section (section no. 3.3.3), during LGM high nutrient levels appeared as a result of regional upwelling caused by NE monsoonal winds. The upwelled waters provided large pool of available nutrient for photosynthesis, leading to phytoplankton with depleted $\delta^{15}N$ values (Altabet and Francois, 1994). Similar results of high productivity and depleted $\delta^{15}N$ caused by low nutrient utilisation have been reported from the sediments of Mediterranean (Calvert et al., 1992), equatorial Pacific (Farrell et al., 1995), eastern Angola basin (Holmes et al., 1997), and eastern Indian Ocean (Müller and Opdyke, 2000).

Presently, the south-eastern side of Sri Lanka witnesses intense upwelling during SW monsoon, while, during NE monsoon the study area experiences upwelling (discussed in Chapter-1). In view of this, during Holocene, though the study region witnessed high detrital flux due to strengthen SW monsoon but remained deprived of upwelling and thereby productivity due to limited supply of nutrients. Thus, the absence of upwelling during Holocene led to low nutrient concentrations and inhibited the productivity resulting in heavier $\delta^{15}N$ values of the organic matter due to high nutrient utilisation.

3.3.4 Regional climatic evolution

The regional climatic conditions of the central equatorial Indian Ocean (off Sri Lanka) were investigated based on the comparison of the paleo

productivity variation of the present study with that of the reconstructed productivity records from the Arabian Sea.

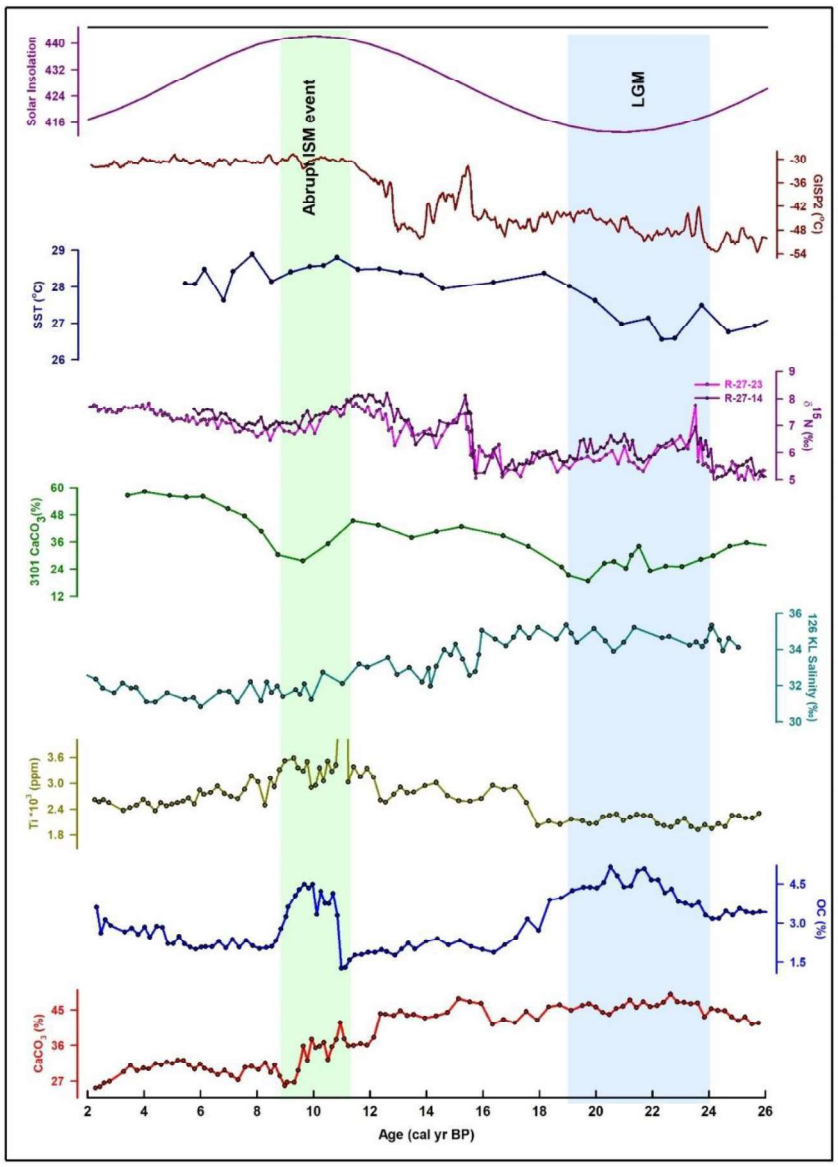

Figure 3.7: Comparison of Reconstructed high resolution paleomonsoon records from the northern Indian Ocean with present study for the last glacial-interglacial transition. GISP2 temperature records (Alley, 2004); SST (Saraswat et al., 2005); RC27-14, RC27-23 $\delta^{15}N$ (Altabet et al., 2002); 3101 (Agnihotri et al., 2003); 126KL Salinity (Kudrass et al., 2001); Ti, OC and $CaCO_3$ record of present studied core SK-304A/05.

In addition to this, the detrital proxy of the present study which varied as a function of SW monsoon changes was compared with temperature records from high latitude climate reconstructed from GISP2 ice record, solar insolation, reconstructed salinity from the Bay of Bengal and SST from the equatorial Indian Ocean (Fig 3.7). Low Ti content during LGM observed in the present study location has been attributed to weakening of SW monsoon which corroborated well with the low solar insolation (Berger and Loutre, 1991) and high salinity recorded from northern Bay of Bengal (Kudrass et al., 2001). Conspicuously high productivity during the same period has been recorded from the present study which differs from the observations made by Agnihotri et al., (2003) and Altabet et al., (2002) from the Arabian Sea.

Generally, the productivity and denitrification in the Arabian Sea has been significantly controlled by SW monsoon intensities. Thus, weakening of SW monsoon wind during LGM resulted in reduced surface productivity and denitrification as indicated by low $CaCO_3$ (SS 3101 G) (Agnihotri et al., 2003) and depleted $\delta^{15}N$ (RC-27-23; RC-27-14) (Altabet et al., 2002). Thus, suggesting that the present study area must have been influence by some other local mechanism that triggered the local upwelling resulting in enhanced surface productivity. Based on the present-day observations along the Sri Lanka coast, strong NE monsoon winds caused enhance upwelling along the SW coast of Sri Lanka towards the core site thus triggering high productivity. Hence, intensification of NE monsoonal winds resulted in strong upwelling causing high productivity during LGM.

An improved SW monsoon during deglacial and Holocene period (Post ~17.5 ka) has been suggested based on high detrital flux from the present study which corroborated well with improved productivity (Agnihotri et al., 2003) and denitrification (Altabet et al., 2002) from Arabian sea, increase in SST from northern Indian Ocean (Saraswat et al., 2005) and high solar insolation (Berger and Loutre, 1991). Such comparison and observation suggested that unlike Arabian Sea or Bay of Bengal, the present study area in spite of being influenced by solar insolation; it experiences high detrital contribution instead of high productivity during SW monsoon intensification. Whereas, the NE monsoonal

winds during glacial period triggers the upwelling in the study region resulting in improved productivity.

On the basis of such observation and comparisons it can be suggested that even though the study area witnesses SW monsoon and NE monsoon similar to the two distinct basins of the northern Indian Ocean but the regional circulation pattern near the central equatorial Indian Ocean plays a crucial role in controlling the productivity and detrital contribution. Moreover, it implies that both strengthening/weakening of NE monsoon winds and weakening/strengthening of SW monsoon winds are governed by changing solar insolation.

3.4 Inferences

The multiproxy approach on a radiocarbon dated sediment core from the central equatorial Indian Ocean off Sri Lanka investigated for deciphering productivity variations and nutrient utilisation during the past 25 ka provides the following understanding:

1. The central equatorial Indian Ocean off Sri Lanka experiences high productivity during glacial periods and low during interglacial periods. This is result of the combined effect of regional upwelling along the SW Sri Lanka and dust influx to the region due to the strong NE winds, relating to the southward shift of ITCZ associated with low solar insolation during glacial period. And productivity is found to be in anti-phase with the solar insolation in the Northern Hemisphere. This phenomenon is conspicuously absent both in the Arabian Sea or the Bay of Bengal.
2. Initiation of the deglacial period can be marked at 17.5 ka based on this study indicated by strengthening of the SW monsoon.
3. The region experienced high sedimentation rate with enhanced preservation of organic carbon during early Holocene period (11-9 ka), which can be attributed to high summer solar insolation after 11 ka with a northward shift of ITCZ.

4. Downcore variations in terrestrial records compared with TSI suggests early Holocene intensification of SW monsoon till 8.5 ka which weakened gradually.
5. The weakening of monsoon for narrow windows between 8.5-7.5 ka and 6.5-5 ka with a short spell of wet interval ~6.5 ka has been observed. After 3.5 ka, a gradual increase in terrestrial values is seen as a result of increase in monsoon intensity during late Holocene.
6. Increase in BSi and decrease in $CaCO_3$ suggests dominance of siliceous productivity over calcareous productivity during Holocene signifies enhanced nutrient utilisation.
7. Concomitant occurrence of low $\delta^{15}N$ and high OC indicates relative low nutrient utilization with high productivity during LGM, and inverse relation during Holocene.

CHAPTER 4

EVIDENCES OF POOR BOTTOM WATER VENTILATION DURING LGM

4.1 Introduction

The depositional conditions in the marine environment can be oxic, suboxic and anoxic based on the presence or absence of oxygen at the sediment-water interface. Redox sensitive elements have demonstrated their potential in deciphering the past bottom water anoxic condition in the oceanic basin. The elemental concentrations in marine sediments are mainly controlled by various processes such as terrestrial influx, biological processes, in-situ precipitation and/or by hydrothermal activity (Pattan and Pearce, 2009). The oxygen concentration in bottom water plays an important role in altering oxygen gradients in the sedimentary column and this in turn depends upon change in deep water circulation during the past glacial-interglacial period (Bareille et al., 1998; Ahmad et al., 2008; Pattan and Pearce, 2009).

Based on the dissolved oxygen (O_2) and/or hydrogen sulfide (H_2S) concentrations, the sedimentary environment has been categorized as oxic (>2.0 ml O_2 L^{-1}), suboxic/dysoxic (2.0–0.2 ml O_2 L^{-1}) and anoxic/euxinic (0.2–0 ml O_2 L^{-1}) (Tyson and Pearson, 1991). In addition to oxygen concentration, the labile organic matter (OM) also controls the redox element cycling in the bottom water. Under oxic conditions, aerobic bacteria utilises dissolved oxygen for OM degradation, while with decrease in dissolved O_2, the degradation continues using secondary oxidant sources leading to oxygen deficient conditions in the water column. Redox sensitive elements are often portrayed as classic tool to reconstruct the past depositional conditions in the bottom water (Brumsack, 1980; 2006; Calvert and Pedersen, 1993; Dean et al., 1999; Algeo and Tribovillard, 2009). The redox elements such as Mo, V, Cr, Mn have different solubilities in marine water depending on the redox conditions and has been commonly used to trace anoxic conditions near the sediment-water interface (Agnihotri et al., 2003; Rimmer, 2004; Algeo and Lyons, 2006; Tribovillard et al., 2006; Banerji et al., 2016). In oxic waters, Mn gets precipitated as Mn-oxides into the sediments, while V as vanadate oxyanions (HVO_4^{2-} and H_2VO^{4-}), Mo as molybdate (MoO_4^{2-}) Cr as chromate anions (CrO_4^{2-}) are present in dissolved form. Unlike Mn, all other redox sensitive elements are conservative in oxygenated waters with a constant

concentration, but under anoxic conditions they are highly enriched in sediments especially where bottom water oxygen is zero (Calvert and Pedersen, 1993; 1996; Algeo and Lyons, 2006; Tribovillard et al., 2006; Pattan and Pearce, 2009).

The Indian Ocean is situated in mid-way of global conveyor belt, between the Atlantic deep water formation and return of surface water from the Pacific, deep waters in the Indian Ocean are ventilated only from south (Piotrowski et al., 2009). Presently, in the northern Indian Ocean (NIO), intermediate depths comprises high salinity water masses such as Red Sea and Persian Gulf Waters and contribution from Pacific Ocean through Indonesian Archipelago at depths of 500 to 1500 m (Kallel et al., 1988). The Indian Ocean deep water is mainly North Atlantic Deep Water (NADW) between ~2000–4000 m relatively rich in dissolved oxygen compared to Antarctic Bottom Water (AABW) found below ~4000 m (Sarkar et al., 1993). Various studies have shown that during last glacial period, the formation rate of the NADW was reduced, while the AABW remained unchanged or probably enhanced (Duplessy et al., 1988; Ahmad et al., 2008).

High resolution paleoclimatic records from late-Quaternary sediments has become increasingly useful tool for deciphering variability in sedimentary paleoproductivity and paleo redox conditions (Ivanochko and Pedersen, 2004; Hendy and Pedersen, 2005; Dean et al., 2006; Cartapanis et al., 2011). A study based on organic carbon (OC) and Mn concentrations from the Arabian Sea, suggested deposition of sediments under oxic conditions during deglacial period as result of lower productivity and high Mn concentration (Shetye et al., 2014). The prevalence of near anoxic bottom water conditions during glacial cycle has been demonstrated based on U and OC content in marine sediment from the SE Arabian Sea (Sarkar et al., 1993). Study based on Mo and V concentrations near the SE Arabian Sea suggested prevalence of suboxic conditions during LGM (Pattan and Pearce, 2009). During LGM, reduced proportion of NADW and increased proportion of AABW near the equatorial Indian Ocean has been inferred on the basis of Nd-isotopic composition of ferromagnese oxides and $\delta^{13}C$ of foraminifera implying a major trigger in the development of oxygen deficient bottom conditions (Piotrowski et al., 2009). There have been substantial studies indicating the development and persistence of oxygen deficient conditions in the

northern Indian Ocean that are related to either productivity or change in bottom water conditions (Naqvi, 1987; Pailler et al., 2002; Rao et al., 2010). However, there remains unaddressed issues on the simultaneous signatures of productivity and bottom water anoxia on redox sensitive elements. Thus, to address the role of productivity and thermohaline ventilation during glacial-interglacial periods, a sediment core (SK-304A/05) from the intermixing zone of two distinct basins of NIO near the equatorial region was geochemically investigated. This study attempts to substantiate the influence of both productivity and the bottom water ventilation during glacial-interglacial period near the equatorial region of NIO. The objectives of the present study are (i) to reconstruct the redox conditions during glacial-interglacial periods and (ii) to identify the variations in the bottom water oxygen conditions with its causative mechanism during the last 25 ka.

4.2 Results and Discussion

4.2.1 Geochemical Proxies

Globally, the late quaternary period has been divided in Last Glacial Maxima (LGM: 22.5-17.5 ka), Deglacial Period (DP: 17.5-11 ka) and Holocene Period (HP: 11-Present) (Rao et al., 2010). The downcore geochemical signatures were studied to reconstruct the paleoproductivity and paleoredox conditions prevailed during sediment deposition during the last 25 ka. Generally, Al and Ti are considered as extremely resistant to weathering and conservative elements as they remain unaffected under changes in redox conditions (Nesbitt and Markovics, 1997; Wei et al., 2003) and has been extensively used to estimate the terrigenous material in the sedimentary environment (Murray and Leinen, 1993; 1996; Schroeder et al., 1997; Klump et al., 2000). Under certain circumstances, Al can form as the result of authigenic clay mineral formation (Timothy and Calvert, 1998) or it may get scavenged as hydroxides coating over biogenic particles (Murray and Leinen, 1996). Similar to Al, Si is also associated with biogenic opal and this limits its use as terrestrial tag. In the present study, the elements have been normalized by Ti rather than Al and Si. The Ti concentration in the studied sediment core varies between 1923–3585 ppm (Fig 4.1). Sedimentary OC and $CaCO_3$ are important constituents of the biogenic fraction of the marine

sediments, and thus can be used as a proxy for paleoproductivity. Although, OC and $CaCO_3$ constitute only a fraction of total biological productivity in the surface oceanic water due to its biological degradation during its passage through the water column (Tribovillard et al., 2006). The OC and $CaCO_3$ concentration ranges from 1.28–5.14 wt% and 25.30–48.92 wt% respectively (Fig 4.3 & 4.4). High OC concentration results in enhanced bacterial degradation causing oxygen deficient conditions (suboxic, anoxic and euxinic) in the water column and at sediment-water interface. Under such oxygen deficient conditions at the sediment-water interface, the behavioral pattern of redox sensitive elements is generally used to comprehend the paleoredox conditions persisted at the time of sediment deposition. The elemental concentration of V, Mn, Cr, Mo, Ni, Co that has been used to access the paleoredox conditions ranges from 45–110 ppm, 204–380 ppm, 45–91 ppm, 0.6–2.8 ppm, 35–90 ppm and 7–15 ppm respectively (Fig 4.1 & 4.3).

The organic matter (Shetye et al., 2014) and Fe- and Mn- oxyhydroxides (Tribovillard et al., 2006) are the major sources for the transportation of the trace elements from water column to the sediments. In oxic and anoxic environments, the trace elements behave differently based on their oxidation states which is influenced by the redox conditions (Shetye et al., 2014).

4.2.2 Biogenic productivity during glacial interglacial periods

Consistently high values for the $CaCO_3$ (Fig 4.3) were observed during LGM with gradually declining trend during the early Holocene and subsequently marginal increase during the late Holocene. Such consistently high values suggest high calcareous productivity during LGM. Two conspicuous peaks of OC (Fig 4.4) during ~21 ka and at early Holocene (11–8 ka) has been observed. The early Holocene OC peak corroborates well with the abrupt increase in the sedimentation rate ~13.5 $cm.ka^{-1}$ primarily suggesting preservation of OC with efficient burial and not due to abrupt high overhead productivity. The OC peak at ~21 ka, however, corresponding to LGM period resulted due to high productivity and better OC preservation. High OC and $CaCO_3$ observed during LGM can be due to high productivity because of strong NE monsoonal winds that enhanced nutrient levels in the photic zone (Rostek et al., 1997; Punyu et al., 2014). With the

commencement of deglacial period, weakening of NE monsoonal winds led to decrease in productivity during the Holocene period. Thus, high productivity could be one of the factors responsible for triggering reducing conditions at the sediment-water interface (Tribovillard et al., 2006).

4.2.3 Redox proxy with detrital affect

Generally, Cr is present as Cr (VI) as mobile chromate anion in oxygenated waters, while under anoxic conditions it gets reduced to Cr (III) which is very unstable and forms complex cations with humic and fulvic acids. It also gets adsorbed with Fe-Mn oxyhydroxides and transported to the sediments (Calvert and Pedersen, 1993; Tribovillard et al., 2006). Cr also gets transported to the sediments along with the detrital fraction due to its presence in chromite and ferromanganese minerals (Dill et al., 1988; Francois, 1988; Hild and Brumsack, 1998). The average Cr concentration in the studied sediment core is ~69 ppm, much higher than the average crustal value of 35 ppm (Taylor and McLennan, 1995). Synchronised variation in vertical profiles of detrital proxies Ti and C/N along with Cr has been observed in this study (Fig 4.1). Consistent low values of Ti and Cr till 18 ka with C/N<12 suggests reduced terrestrial contribution at the core location due to weakening of summer monsoon (Naidu and Malmgren, 1996; Rashid et al., 2007; Anand et al., 2008). Gradual increase in Ti and Cr after 18 ka till 8 ka with C/N ≥12 indicates enhanced land-driven clastic fraction to the region instigated by the summer monsoon intensification (Govil and Naidu, 2011). The Cr concentrations in the studied sediment core is thus a function of changing detrital influx to the region rather than changing redox conditions in the water column and limits its application as redox proxy but can be a potential proxy to decipher terrestrial influence.

Co has been used as potential tool to decipher paleoredox conditions at the sediment-water interface due to its complex formation with fluvic or humic acid under oxic seawaters (Achterberg et al., 2003). Whereas, in oxygen deficient waters it can get incorporated into the solid phase authigenic by sulphide formation as Fe sulphides (Algeo and Maynard, 2004; Tribovillard et al., 2006). Co is prone to be influenced by detrital clastic material. The average Co concentration throughout the

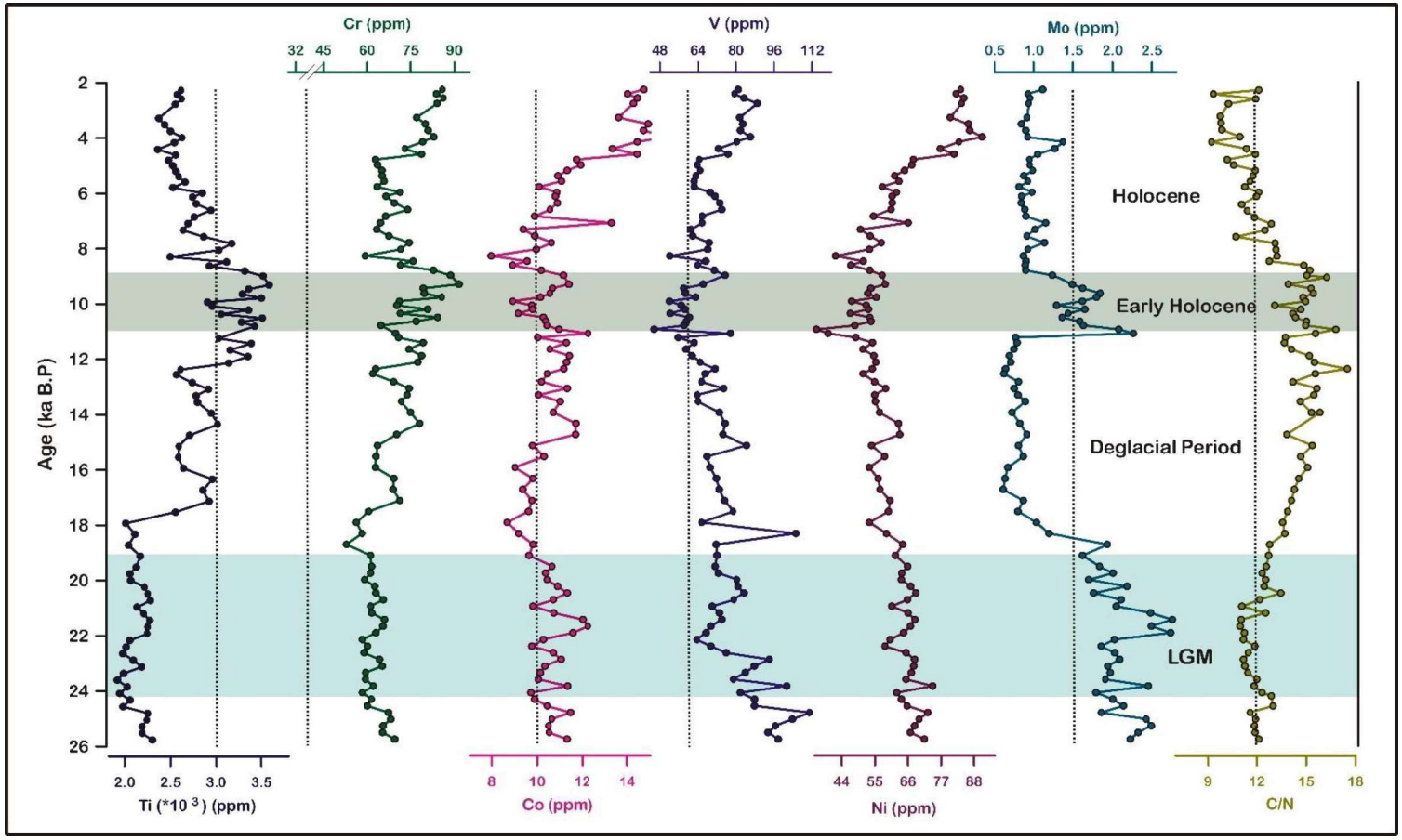

Figure 4.1: Downcore variation of elemental concentration in the sediment core SK-304A /05 indicates low terrestrial flux during LGM with gradual increasing values during Deglacial and Holocene period. The dotted line in each of the plot indicates average crustal values for the respective elements.

sediment core is ~11 ppm similar to the average crustal Co value of 10 ppm (Fig 4.1) (Taylor and McLennan, 1995). Near similar values of Co with crustal values suggest its detrital contribution, but marginal enrichment in Co/Ti during LGM could be indicative of being a reasonable proxy to decipher past redox conditions.

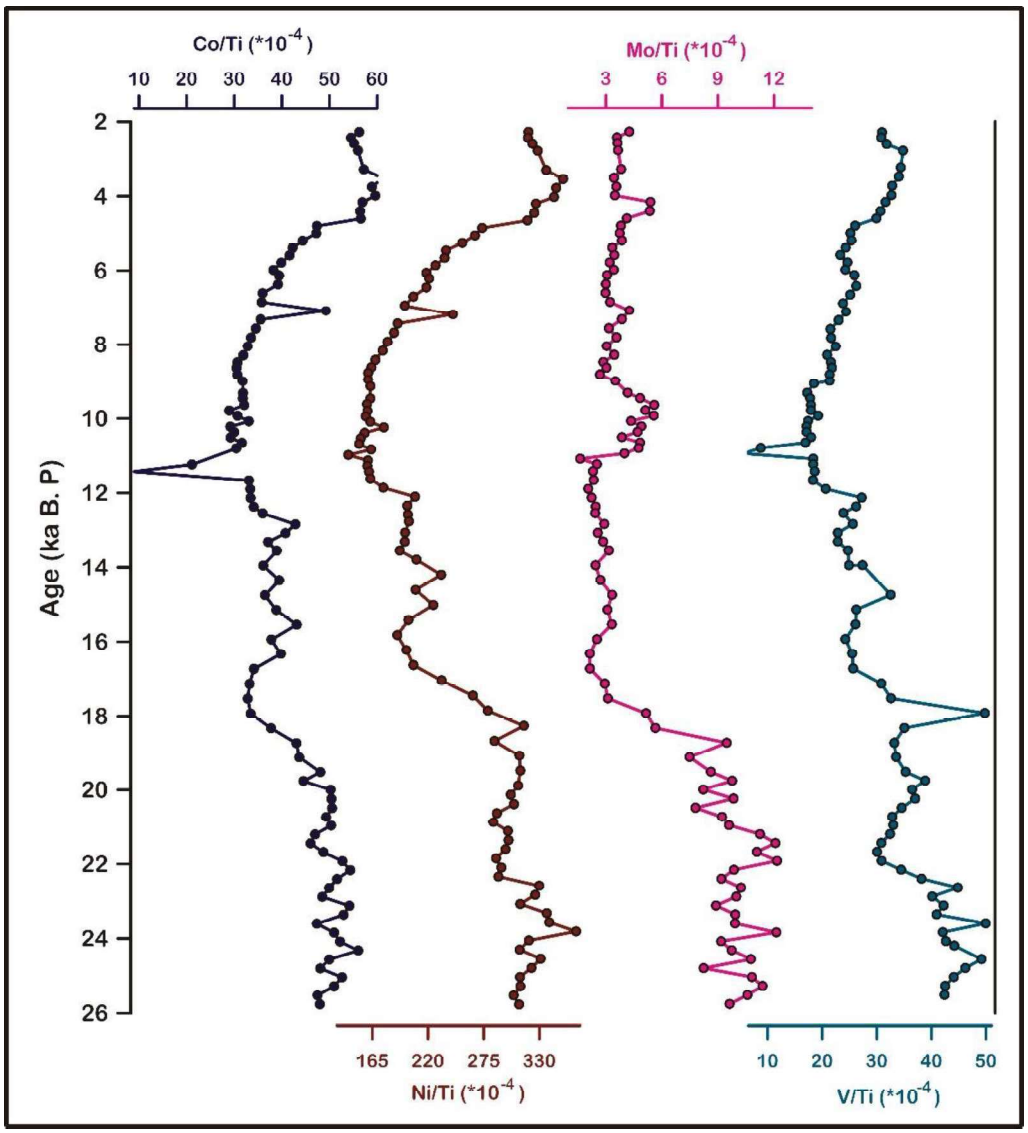

Figure 4.2: Downcore variation of Ti normalised redox sensitive elements (Co, Ni, V, Mo), OC and OC flux. High values of OC and redox sensitive elements observed during LGM

4.2.4 Redox proxy with low detrital affect

Under oxic conditions, vanadium occurs as V(V) as vanadate species getting adsorbed onto Mn-Fe oxyhydroxide (Morford and Emerson, 1999), whereas Mo remains as unreactive dissolved molybdate species (MoO_4^-) (Emerson and Huested, 1991; Calvert and Pedersen, 1993; Tribovillard et al., 2006; Pattan and Pearce, 2009). Under oxygen deficient conditions, both V and Mo are removed from the water column and its enrichment in the sediment serves as potential tool to decipher reducing conditions at sediment-water interface (Calvert and Pedersen, 1993; Tribovillard et al., 2006; Pattan and Pearce, 2009).

The average V and Mo concentrations in the present study, are ~72 ppm and ~1.4 ppm respectively. The co-occurrence of high values for Mo, V, OC, Mo/Ti and V/Ti observed during LGM suggests prevalence of anoxic conditions at the sediment-water interface. Synchronous decline in Mo, V, OC, Mo/Ti and V/Ti during deglacial period indicates resumption of oxic conditions at the sediment-water interface (Fig 4.1 & 4.2). Unlike V and V/Ti, a conspicuous enrichment in OC, Mo and Mo/Ti has been observed during early Holocene between 11–8 ka. This can be corroborated well with the high sedimentation rate of ~ 13.5 $cm.ka^{-1}$ during early Holocene. This underpins better preservation of organic matter as a function of high sedimentation rate, while enhanced Mo and Mo/Ti plausibly resulted due to the formation of Mo-S complexes (Tribovillard et al., 2004). Similar to V/Ti and Mo/Ti, enhanced values of Ni/Ti during LGM indicate its role as a redox sensitive proxy. Generally, Ni acts as a micronutrient and occurs as soluble cation either as Ni^{2+} in soluble nickel carbonate ($NiCO_3$) or $NiCl^+$ in oxic environments (Calvert and Pedersen, 1993; Whitfield, 2001). The average Ni concentration (60 ppm) in the present study is higher than the average crustal abundance of 20 ppm (Taylor and McLennan, 1995). Simultaneous enhancement in Ni/Ti and OC during LGM suggest scavenging of Ni by organic matter in the water column (Piper and Perkins, 2004; Naimo et al., 2005). During organic matter degradation under extreme reducing conditions (sulphate redution), Ni generally precipitates as NiS in sediments. Therefore, high Ni/Ti along with OC during LGM implies deposition of the sediments under anoxic conditions. At the same time, during deglacial period (17.5–10 ka), synchronous decrease in

Ni/Ti ratio and OC suggests oxic conditions in the sediment-water interface (Fig 4.2).

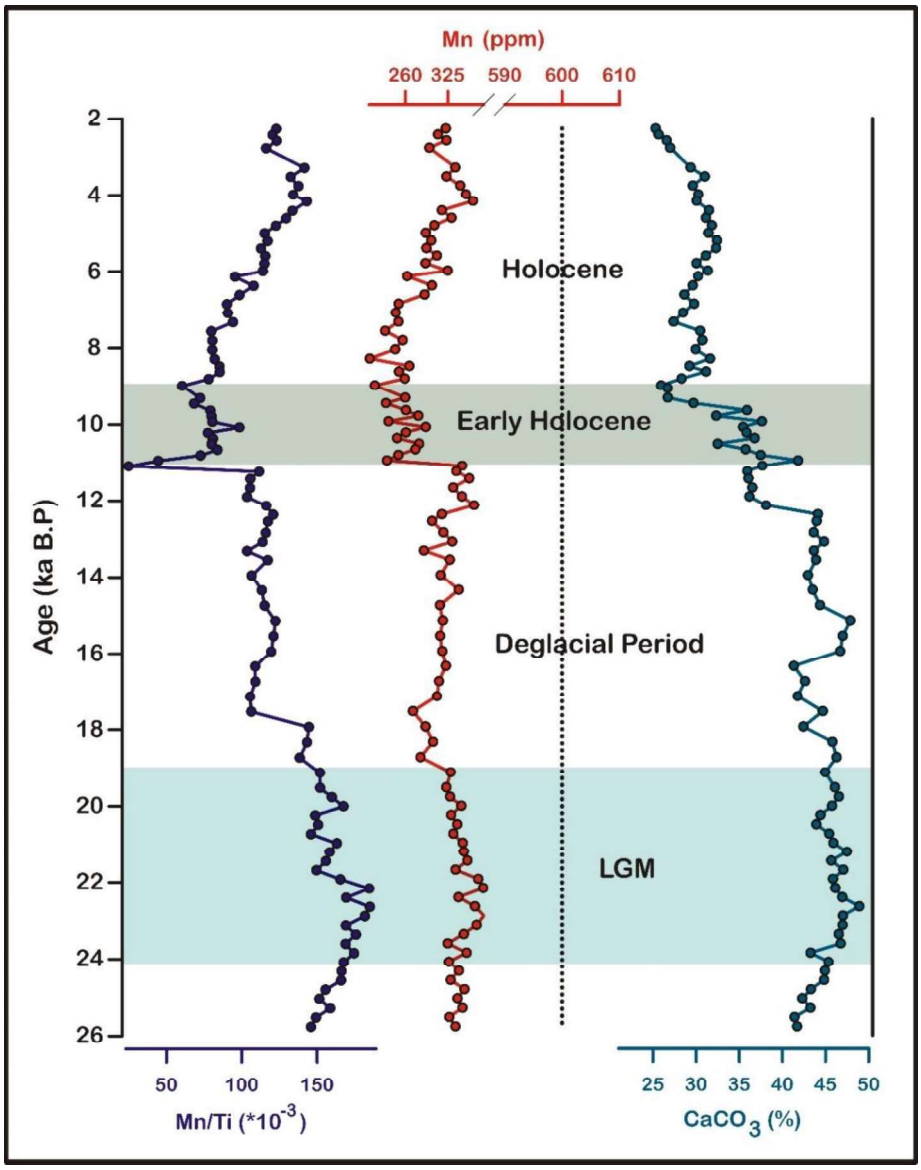

Figure 4.3: Downcore variation of Mn, CaCO3 and Mn/Ti indicates that the Mn has formed authegenic carbonate in presence of CaCO3

In oxygenated waters, the Mn is present as Mn (II) which is highly unstable and gets oxidized to insoluble Mn (IV) (Mn-oxyhydroxides) and is delivered to the sediments (Tribovillard et al., 2006). Manganese thus plays a significant role in transferring trace metals by scavenging them from the water

column to the ocean bottom. However, during anoxic conditions, at the sediment-water interface, the dissolution of oxides and hydroxides releases Mn (II) back to the waters (Rajendran et al., 1992). Identical vertical distribution in V/Ti and Mn/Ti suggests adsorption of vanadate onto Fe- and Mn-oxyhydroxides (Calvert and Piper, 1984).

The co-occurrence of high values of Mo/Ti and V/Ti during LGM suggests anoxic conditions, which results in dissolution of oxides and hydroxides and releasing Mn (II) back to the waters (Rajendran et al., 1992) leading to depletion of Mn concentration in the sediment. Contrarily, the simultaneous enrichment of V/Ti and Mo/Ti with Mn/Ti is observed along with the enhancement of $CaCO_3$ during LGM (Fig 4.2 & 4.3). Such conspicuous behaviour of Mn can be attributed to trapping of Mn in authigenic Mn-carbonates during its export to the sediments (Pedersen and Price, 1982; Morford et al., 2001; Tribovillard et al., 2006).

4.2.5 Sulfur Isotope: a proxy for paleoredox conditions

Sulfur has four stable isotopes ^{32}S, ^{33}S, ^{34}S, and ^{36}S. ^{32}S being more abundant comprises of 95.02 %, followed by ^{34}S (4.22 %), ^{33}S (0.76 %) and ^{36}S being least abundant (0.0136 %) of the total sulfur present on earth (Canfield, 2001). Earth's surface redox conditions associated with distinctive stable isotopic fractionations of sulfur isotopes is mediated by various abiotic and biotic processes (Garrels and Lerman, 1981; Canfield, 2001; Fike et al., 2015; Pasquier et al., 2017). Variations in the sedimentary sulfur isotopic composition are often used to infer the changes in the Earth's environment such as rise of the atmospheric oxygen, ocean oxygenation and mass extinction (Riccardi et al., 2006; Jones and Fike, 2013). The biogeochemical processes in the nearshore sediments are mainly controlled by the organic matter degradation. The degradation of the organic matter involves various reactions such as the reduction of O_2, nitrate, Mn-Fe oxyhydroxides and sulfates. Geologically, the formation of sedimentary pyrite by biologically mediated reduction of seawater sulfate is one of the important process in sulfur geochemical cycle in anoxic marine sediments (Jorgensen, 1983; Henrichs and Reeburgh, 1987; Strauss, 1999). Thus, high sedimentary organic carbon concentration will lead to high reduced sulfur in the

form of pyrite by bacterially stimulated sulfate reduction (Berner, 1970; Raiswell and Berner, 1985). The sequence of reduction is determined by the Gibbs Free Energy yield (Claypool and Kaplan, 1974; Bender and Heggie, 1984). Biologically controlled processes can impose substantial isotopic fractionation between reactant and product, with dissimilatory sulfate reduction resulting in a major kinetic sulfur isotope effect. During kinetic fractionation, the resulted sedimentary pyrite from bacterial sulfate reduction acquires negative $\delta^{34}S$ compared to the coexisting sulfate due to preferential utilisation of ^{32}S over ^{34}S by sulfate reducing bacteria under open system conditions (Harrison and Thode, 1958; Canfield, 2001; Habicht et al., 2002). $\delta^{34}S$ of evaporites or seawater sulfates ranges from +35 ‰ to +5 ‰, while a range between +40 ‰ to -50 ‰ is observed in the sedimentary sulfides (Thode, 1970). Thus, the variation in the $\delta^{34}S$ provides a crucial platform to decipher past redox conditions and acts as a proxy to identify the prevalence of oxygen deficient conditions.

In the studied sediment core SK-304A/05, the Total Sulfur (TS) and its isotopic ratios ($\delta^{34}S$) were estimated. The TS concentrations and $\delta^{34}S$ varied from 0.09–0.78 wt% and -8 ‰ to -40 ‰ respectively (Fig 4.4). The extremely depleted values of $\delta^{34}S$ were observed during LGM (25-18 ka), later a marginal enrichment from -37 ‰ to -28 ‰ was observed for $\delta^{34}S$ till the onset of early Holocene (~11.5 ka). During early Holocene (11-9 ka), $\delta^{34}S$ depletion from -31 ‰ was followed by significant enrichment to -27 ‰ to -8 ‰ during mid-late Holocene. Unlike $\delta^{34}S$, TS does not show much variation throughout the core, except during early Holocene wherein a conspicuous enhancement in the TS values was observed. As mentioned earlier (Chapter 3), the $\delta^{13}C$ shows enriched values during glacial period till 11 ka, after that a fluctuating pattern tending towards depleted values is observed during Holocene. In case of C/N ratio, low values (<12) are observed during glacial period and mid-late Holocene, while values slightly higher (>12) were noticed between 18-8 ka.

During glacial period, the depleted $\delta^{34}S$ has been found to be associated with high OC, low C/N ratio and enriched $\delta^{13}C$, often attributed to marine origin of organic matter. During interglacial period or the Holocene, enriched $\delta^{34}S$ is

associated with high C/N ratio, depleted $\delta^{13}C$ and reduced OC, attributing to terrestrially mediated organic matter. There could be two possible mechanism responsible for such conditions (i) change in microbial activity or (ii) change in sedimentation in the overlying water column. Changing microbial activity can be an outcome of sulfate reduction, which results in dominant isotopic fractionation leading to depletion of $\delta^{34}S$. Generally, sulfate reduction rate increases in anoxic to euxinic conditions, when the organic matter is mainly decomposed by sulfate reducing bacteria (Canfield, 1989). As discussed in the previous section, the study region witnessed anoxic conditions as apparent from high Mo/Ti, Ni/Ti and V/Ti. The occurrence of such anoxic conditions activated degradation of organic matter by sulfate reducing bacteria at sediment-water interface leads to depleted $\delta^{34}S$ values of the organic matter. Additionally, the sediment accumulation rate being comparatively high during LGM than during deglacial period (Fig 2.2), which ensures availability of more labile organic matter as a function of enhanced preservation for sulfate reduction at the sediment-water interface. During deglacial period, low sediment accumulation rate reduces preservation of organic matter at sediment-water interface, that results in less sulfate reduction of organic matter leading to enriched $\delta^{34}S$. During early Holocene, with the intensification of SW monsoon, abrupt increase in sediment accumulation rate resulted in better preservation of OC and would lead to depleted $\delta^{34}S$ of the organic matter (Fig 4.4). In addition, sudden increase in TS during early Holocene observed along with high Mo suggest possibility of formation of Mo-S complexes (Tribovillard et al., 2004). During mid-late Holocene, reduction in OC content and redox sensitive elements led to enrichment in $\delta^{34}S$.

During LGM, high OC and $CaCO_3$ values observed in the sediment core has been attributed to enhanced productivity, whereas abrupt enhancement of OC during early Holocene (11–8 ka) to better preservation with high sedimentation rate. Similarly, high OC during LGM associated with enhanced redox sensitive elements (Mo/Ti, V/Ti, Ni/Ti) and depleted $\delta^{34}S$ suggests anoxic conditions triggered by high bacterial degradation (sulfate reduction) of OC at the sediment-water interface. At ~21 ka, unlike $CaCO_3$ and redox sensitive elements, marginal enrichment in the OC is observed which later declined, however, $CaCO_3$ and

redox sensitive elements showed consistently high values with declining pattern until 11 ka. The OC values are nearly similar at LGM and the early Holocene. Thus, anoxic conditions persisted as demonstrated by redox sensitive elements during LGM, while, no decipherable reducing conditions could be observed during the early Holocene (11–8 ka). An observation in SE Arabian Sea similar to the present study suggests high productivity induced low oxygenated bottom water conditions during LGM (Rao et al., 2010). It has been reported that the sediments from the equatorial Arabian Sea (Pailler et al., 2002) and SE Arabian Sea (Pattan and Pearce, 2009) never experienced complete anoxic conditions in the water column during LGM, instead it fluctuated between oxic and suboxic conditions. Contrarily, another study from the SE Arabian Sea suggests near-anoxic conditions probably enhanced the preservation of OC and removal of U from seawater during LGM (Sarkar et al., 1993).

Therefore, based on anomalous high OC values and changing behavior of redox sensitive elements, it can be inferred that it is not only the high sedimentation rate or organic matter degradation which influenced the redox elements, but some other mechanism is responsible for initiating the oxygen deficient conditions at the sediment-water interface during LGM.

4.2.6 Evidence of anoxic bottom waters during LGM

The redox conditions at the sediment-water interface is mainly controlled by (i) bottom water oxic conditions influenced by deep water circulation and (ii) increased oxygen demand for enhanced OC supply and its degradation (Pattan and Pearce, 2009; Pattan et al., 2013). Enhanced overhead productivity leads to greater organic matter export to the sediments. The tracer C/N ratio has been extensively used to decipher the provenance of organic matter, i.e. values of C/N≤ 12 and C/N≥ 12 suggests provenance of marine and terrestrial origin of OC respectively (Hedges and Parker, 1976; Emerson and Hedges, 1988; Meyers, 1997; Bhushan et al., 2001; Pattan et al., 2013). The C/N ratio in the present study varies from 9 to 17 with an average of 12. The C/N ratio followed pattern similar to Ti with low values during LGM with gradual increasing trend during the early Holocene followed by marginal decrease till present (Fig. 6). Low C/N (~ 10) and high OC

(~ 5 wt%) during LGM suggests reduced contribution of terrestrial OC primarily derived from overhead productivity. Marine OC being more labile is prone to microbial activity leading to oxygen deficient conditions, both in water column and sediment-water interface. In the present study, if the enhanced OC peak is due to high overhead productivity, similar pattern is expected for the redox sensitive elements during ~ 21 ka. In the present scenario, however, the OC peak at ~ 21 ka probably demonstrates better preservation of OC (Fig 4.4).

Due to its geographical setup, the deep waters of the Indian Ocean is ventilated solely from south (Piotrowski et al., 2009). Previous studies on $\delta^{13}C$ and $\delta^{18}O$ isotopic composition of benthic and planktonic foraminifera suggest significant changes during the glacial-interglacial period in the characteristics of surface and deep water masses (Duplessy, 1982; Naqvi et al., 1994; Schmiedl and Leuschner, 2005; Ahmad et al., 2008). NADW is the main source for deep water ventilation in the northern Indian Ocean and changes in deep water circulation alters the bottom water oxygen conditions. Previous studies have reported that during LGM, the export of deep water from north Atlantic was reduced, which further compensated increased formation of Southern Ocean deep water (Kallel et al., 1988; Ahmad et al., 2008) and allowed replacement of NADW with AABW penetrating further northward (Curry et al., 1988; Curry and Oppo, 2005).

The present study is based on a sediment core raised from a water depth of 3400 m from the equatorial Indian Ocean. Based on behavior of redox sensitive elements and $\delta^{34}S$ as discussed in previous section, it can be inferred that anoxic conditions prevailed during LGM in the equatorial Indian Ocean. This anoxic condition was established due to enhanced productivity with OC degradation with weak ventilation (poor in O_2 and rich CO_2) of Southern Ocean deep waters due to changes in deep-water circulation. This further augmented oxygen deficient conditions causing enhanced preservation of OC. High OC peak at ~ 21 ka can be attributed to post depositional preservation of organic matter at the sediment-water interface due to the bottom water anoxic conditions (Fig 4.4). The present observations of anoxic bottom water due to poor ventilation is further supported by Ahmad et al., 2008 and Piotrowski et al., 2009 from the equatorial Indian Ocean. They suggested weak ventilation of deep-waters in northern Indian Ocean

due to reduced proportion of NADW (poor in CO_2 and rich in O_2) and increased AABW (rich in CO_2 and poor in O_2) during LGM. During early Holocene (11–8 ka), enhanced OC with C/N >12 (~ 16) suggests terrestrial origin of organic carbon (Fig 4.1 & 4.4). The Holocene period experienced better OC preservation without significant variation in redox sensitive elements, which can mainly be attributed to high sedimentation rate with deposition under well ventilated bottom water conditions.

4.3 Inferences on ventilation of equatorial Indian Ocean

The behavior of redox sensitive elements and Sulphur isotopes has been extensively used to decipher paleo redox conditions at the sediment-water interface. On the basis of investigation of redox sensitive elements and OC content in a sediment core from the equatorial Indian Ocean, the present study demonstrates prevalence of anoxic conditions during LGM. The anoxic condition in the water column at the sediment-water interface at ~ 21 ka is due to organic matter degradation under enhanced overhead productivity conditions further supported by poorly ventilated bottom water. Enhanced OC during LGM is function of the post depositional preservation of OC and bottom water redox conditions. Increased OC during the early Holocene (11–8 ka) has been attributed to high sedimentation rate supported by high overhead OC flux without significant variation in the redox sensitive elements. The present study provides a valuable signature of poor bottom water ventilation at the equatorial Indian Ocean during LGM and its role in better OC preservation with concurrent occurrence of high surface productivity.

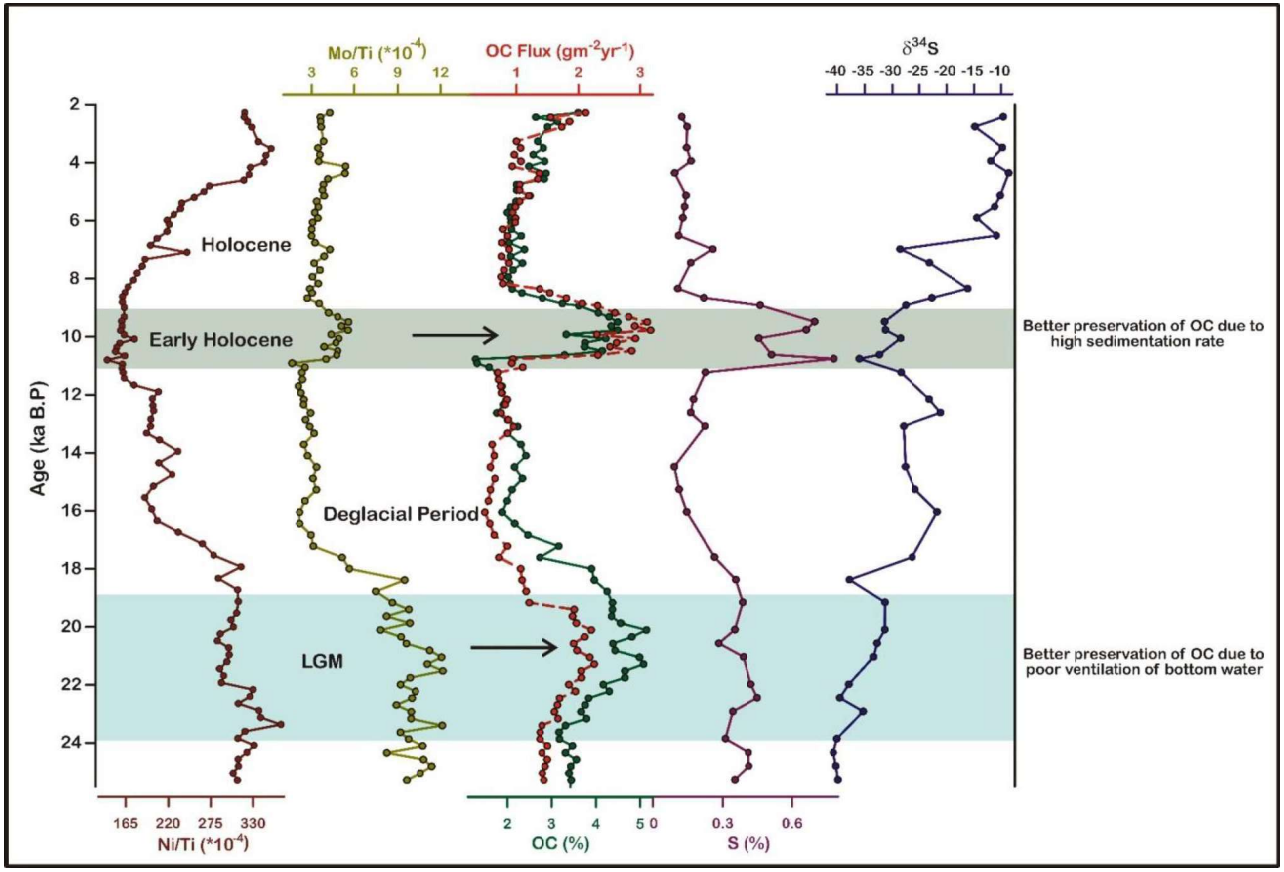

Figure 4.4: Comparative plot for detrital and redox proxies with OC suggesting preservation of OC during LGM and early Holocene Period.

CHAPTER 5

SOLAR FORCING

5.1 Sun-climate relation

The Sun is a variable star and the prime source of energy for the earth's climate system (Steinhilber and Jürg, 2011). Throughout the geological timescale, solar activity has played crucial role in controlling the earth's climate (Agnihotri et al., 2002). Various internal or external factors such as ocean-atmosphere oscillations, volcanic eruptions, incoming solar radiation variability caused by either sun-earth geometry (changes in Milankovitch forcing) or due to changes in the solar activity itself (Rind, 2002) has been identified that can lead to climate change. Extensive studies has demonstrated the interlink between climate and solar activity but the concept was first introduced by Eddy (1976) who suggested low solar activity can potentially cause colder climate. A positive correlation between sunspots and globally averaged sea surface temperature has been observed (Reid, 1987). In the later part of 19^{th} century, the sun-climate relationship was established based on the association between the sunspot cycles, occurrence of aurora, geomagnetic storms and weather patterns (Hoyt and Schatten, 1993). Studies have suggested that a small variation in solar activity on multi decadal time scales can be coupled with various feedback mechanism such as ice cover, vegetation extent, changes in atmospheric greenhouse gas concentration, water vapor and low altitude clouds etc. that can cumulatively effect the regional climate changes (Mehta and Lau, 1997; Beer et al., 2000).

The solar energy received at the top of the earth's atmosphere defined as *Solar Constant* was thought to be constant prior to the satellite era, and any small variation in it was difficult to detect due to the presence of atmosphere. Since 1978, the existence of the variations in the incoming solar radiation was revealed by the radiometers sent in space. *Total Solar Irradiance* (TSI) is the solar energy flux over the entire electromagnetic spectrum passing through a unit area at the top of the earth's atmosphere at a distance of 1 AU (Astronomical unit) and is represented as watts per square unit (W/m^2) (Beer et al., 2000; Mendoza, 2005). The average value of TSI at the earth's atmosphere is solar constant, about 1367 W/m^2. The average solar energy reaching the earth's surface depends on the latitude and the angle of incidence and has been termed as incoming solar

radiation or the *Insolation* (Tiwari and Ramesh, 2007). The processes responsible for the changes in solar insolation include changes in solar diameter, amount of magnetic flux of the sun (Lean et al., 1998; Sofia and Li, 2001). The solar radiation reaching the top of the earth's atmosphere comprises many wavelengths and the radiation is mainly limited to wavelengths less than 500 nm and is more for the shorter wavelength.

5.2 Paleo records of solar forcing and the embedded solar periodicities

Numerous natural archives viz. ice cores, terrestrial and marine sediments have underscored the prevalence of climate oscillations during the glacial-interglacial cycle (Sirocko et al., 1996; Chondrogianni et al., 2004; Rodrigo-Gámiz et al., 2014). Periodicities in the earth's climate system on longer timescales have been linked with changing orbital cycles (Rodrigo-Gámiz et al., 2014). At longer timescales, the forcing mechanism on climate change is poorly understood. Possible causes may entail linear (Berger et al., 2006) and non-linear (van Geel et al., 1999; Bond, 2001) responses to orbital cycles. In the North Atlantic regions, the cyclic patterns during late Pleistocene-Holocene are predicted as sub-Milankovitch timescales corresponding to Dansgaard-Oeschger (D-O) oscillations and Bond cycles (Rodrigo-Gámiz et al., 2014). Additionally, the influence of solar activity on surface hydrography may have elicited the North Atlantic Deep Water production and thereby causing cold climate in Europe recorded at an average of 1470±500 yr (Bond, 1997; 2001). A teleconnection between North Atlantic climate and Indian Ocean summer monsoon has been established based on the $\delta^{13}C$ records of peat from the Tibet Plateau, suggesting simultaneous occurrence of ice-rafted debris events in North Atlantic and weakening of summer monsoon strength (Hong et al., 2003). Similarly, speleothems and tree rings have proved to be a potential proxy for climate reconstruction. A comparison between $\delta^{18}O$ GRIP ice core with $\delta^{18}O$ of speleothems from Oman and Dongge cave and $\Delta^{14}C$ of tree rings (which is dependent on cosmic ray fluxes) indicates solar variability to be the major factor responsible for the Holocene monsoon intensity (Neff et al., 2001; Wang et al., 2001; 2005; Fleitmann, 2003).

The sun shows variability on time scales from less than a minute to more than billions of years (Beer et al., 2000). The energy generated in the core of the Sun can be calculated for any time in the past over millions of years through direct or indirect measurements. The direct measurements are available only for the past ~300 years, beyond this indirect measurements were made based on cosmogenic radionuclide production (^{10}Be, ^{14}C, ^{36}Cl), as their atmospheric production rate depends on cosmic flux modulated by solar wind (Masarik and Beer, 1999; Bard et al., 2000; Beer et al., 2000). In order to reconstruct the past solar variability, the measurements of ^{10}Be, ^{14}C, ^{36}Cl in natural archives (ice cores and tree rings) has been used (Stuiver and Braziunas, 1993). Similarly, the solar insolation values for the climate for the last 10 Ma was calculated based on numerical and analytical solutions for the astronomical parameters of the Earth's orbit and rotation (Berger and Loutre, 1991). On the basis of direct and indirect measurements, the periodicities of solar variability have been estimated.

The first detected periodicity in solar activity is the 11-year solar cycle called Schwabe cycle, discovered in the year 1844 based on the changing sunspot number. The magnetic polarity of the sun reverses in a 22-year cycle called as Hale cycle (by George Hale in 12th century). The periodicities longer than these has been identified based on cosmogenic nuclides (Stuiver and Braziunas, 1993) and the records reveal longer cyclic patterns in the solar activity such as Gleissberg cycle of 88-year (Engels and van Geel, 2012), Suess cycle of 208-year and Hallstatt cycle of ~2300-year (Mayewski et al., 1997). The proxy records also show periods of low solar activity such as Oort minimum (980-1120 AD), Wolf minimum (1282-1342 AD), Sporer minimum (1416-1534 AD), Maunder minimum (1645-1715 AD) and Dalton minimum (1790-1820 AD) (Agnihotri et al., 2002; Tiwari and Ramesh, 2007).

Study based on spectral density of stable isotope δ^{18}O in speleothems and combining radionuclide production rates with a new model geomagnetic dipole moment exhibits ~210 yr periodicity (Knudsen et al., 2009; 2011). Likewise, a ~200 yr periodicity has been reported from the sediment core of Tibetan lake which corroborates well with the Suess solar cycle of ~208 yr. A high-resolution speleothem study from southern China showed periodicities of 558, 206, 159 and

24 years in Asian monsoon which corresponded well with $\Delta^{14}C$ record (Wang et al., 2005). Ji et al., (2005) reported 200 yr periodicity in a sediment core from a Tibetan lake. Thus, studies pertaining to periodicities in various archives suggest a well-defined control of solar activity over Asian monsoon

Lack of continuity and preservation are the major limitation in terrestrial archives. Unlike terrestrial records, marine archives are generally undisturbed and can preserve a long term climate records. Based on the oxygen isotopic data of foraminifera from the eastern Arabian Sea sediment core, it has been demonstrated that the modulation of monsoon by the Atlantic deep water formation followed periodicities of 390, 500, 620 yrs and the 500 yr (Kessarkar et al., 2013).

5.3 Influence of solar forcing on the equatorial Indian Ocean

The tropical regions are significantly influenced by changing incoming solar radiation. The equatorial regions receive almost double insolation the maximum insolation received in tropical latitude over the course of the year. And has been found to have 11 kyr and 5.5 kyr periodicities corresponding to earth's precession (Berger et al., 2006). Thus, equatorial region are potential zones to decipher the impact of changing solar insolation (as a result of changing solar cycles and earth's precession) over monsoon system and on climate. In view of this, a multi proxy approach has been undertaken to reconstruct the climate as a function of changing monsoon caused by solar insolation during last 25 ka and to establish prominent periodicities governing these changes.

Enhanced solar insolation leads to improved monsoon intensity, which results in warm and wet climate accompanied by increased in-situ productivity and detrital influx (Kessarkar et al., 2013, Saraswat et al., 2013). The sediment core from the central equatorial Indian Ocean, off Sri Lanka provides a climatic history for the last 25 ka. The sample resolution of the present core is ~120 years. The study area is directly exposed to SW monsoon winds (Malmgren et al., 2003) marked with high freshwater influx during SW monsoon. To establish a link between SW monsoon and solar forcing, a comparison between detrital, productivity and redox proxies of the present study has been made with the

northern hemisphere solar insolation maximum. Variability in solar insolation results in alteration of monsoonal strength, which in turn affects the detrital and productivity flux to the study area. Thus, significant variation in any proxy is reflected as a function of the monsoonal variation.

Based on the geochemical multiproxy approach, the present study demonstrated low detrital influx with enhanced productivity resulting in oxygen deficient conditions due to SW monsoon weakening during LGM. With the onset of deglacial period, warm and wet conditions persisted causing increased in detrital contribution and reduced productivity triggered by SW monsoon strengthening (detailed discussing is done in Chapter 3).

On comparing the geochemical proxies with Northern Hemisphere solar insolation maximum, in-phase lowering of detrital influx and solar insolation during LGM is observed (23–19 ka) (Fig. 5–1). As the region receives maximum detrital inputs during SW monsoon, lowering of detrital contribution indicates SW monsoon weakening triggered by lowering of solar insolation during LGM. The present observation corroborates well with the investigation based on geochemical proxies from equatorial Indian Ocean (Pailler et al., 2002). They found that the region is dominated by precessional forcing and high productivity in phase with low summer insolation in the northern hemisphere. The study area witnessed high detrital contribution during deglacial period (17.5–11.5 ka) suggesting SW monsoon strengthening with simultaneous increase in solar insolation. After 12 ka, abrupt increase in detrital concentrations and productivity fluxes till 8.2 ka indicates increased continued rainfall as a result of strengthen ISM corresponding to the post 11 ka northern hemisphere solar insolation maximum (Ramisch et al., 2016). After 7 ka, detrital proxies remained constant with slight decrease in trend coinciding with descending phase of solar insolation, while productivity proxies show slightly increasing trend (Fig. 5–1).

A paleoproductivity reconstruction for the last millennia using the Arabian Sea core suggests significant role of solar forcing in monitoring the overhead productivity and detrital influx to the region (Agnihotri et al., 2002). Based on the synchronous trend being followed by the detrital proxies and the solar insolation,

it can be deduced that solar insolation played a significant role in monitoring the monsoon intensity.

A reverse trend for in-situ productivity with solar insolation during LGM suggests that low solar irradiance triggered the southward migration of ITCZ resulting in prominent influence of NE monsoon winds in the region (discussed in chapter- 3).

5.4 Spectral Analysis

Despite sampling resolution of the core being constant (1 cm), varying sedimentation rates results in uneven sampling time interval. To determine periodic signals from an unevenly spaced time series data in frequency domain, spectral analysis was carried out to decipher the link between the solar forcing and the paleoclimatic process.

The periodicities for the productivity, redox and terrestrial proxies in the core SK-304A/05 was obtained using the spectral analysis package called SPECTRUM (Schulz and Stattegger, 1997), which is based on the Lomb-Scarlge Fourier transform algorithm designed for unevenly spaced time series data. The dominant periodicities can be determined by this algorithm in the time series. Analysis of our study is mainly focussed on cycles recorded in the frequency band with higher possibilities for primary cycles, and thus to interpret only significant peaks (primary) by avoiding secondary cycles, the cycles corresponding to periodicities between 600 yr and 5000 yr have been considered.

The spectral powers of high periodicities mask the smaller periodicities and thus the higher periodic components in the output power spectra are removed using FFT filtering method and the time domain is reconstructed using Table Curve 2D v5. These reconstructed time series are again subjected to spectral analyses. By following this method, the suppressed smaller periodicities can be unmasked from the higher periodic components in the power spectra.

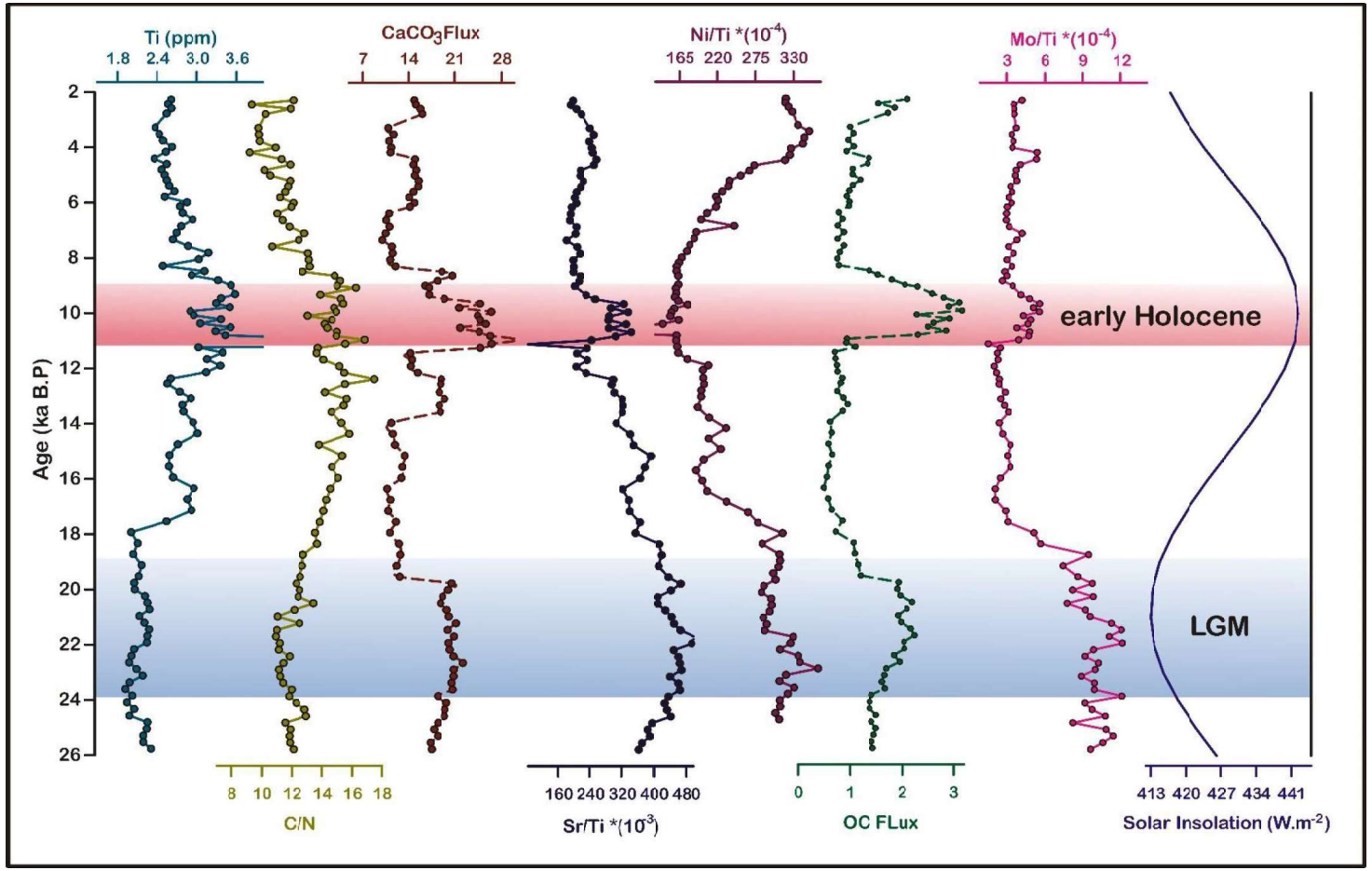

Figure 5.1: Comparison of various geochemical proxies studied in the core SK-304A/05 with the solar insolation.

The spectral analysis of various geochemical proxies viz. detrital, productivity and redox proxies has been conducted. All groups show distinct cyclic pattern in their spectrum as summarized in Table 1. Before interpreting the cycles recorded at different periodicities, it is necessary to differentiate between primary cycles and secondary harmonics.

(a) ***Spectral Analysis of Detrital Proxies***

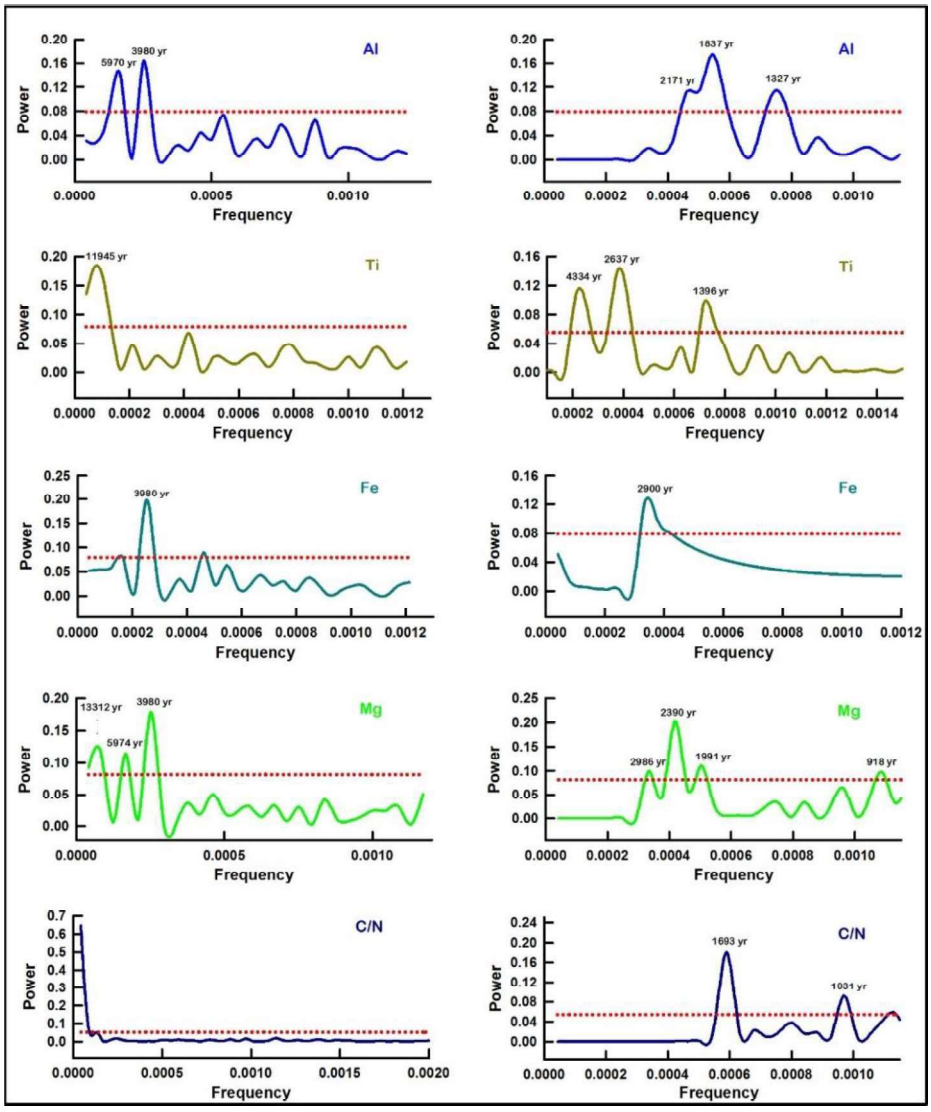

Figure 5.2: Power spectral analysis for the detrital elements. Spectral peaks registered with non-detrended are shown on the left; spectral peaks obtained after detrending are shown on the right. Dotted line represents 95% confidence.

The spectral analyses of detrital proxies for the present studied core showed periodicities only beyond ~4000 yr, while the other periodicities were not significant due to masking. For estimation of lower periodicities, detrending of the data was done with the help of Table Curve software for masking higher periodicities.

After detrending, the detrital group displays periodicities ranging from 918 to ~4000 yr. The highest frequency at 918 yr was shown by Mg corresponding to 1150 yr cycle. The periodicities 1375 yr and 1327 yr obtained for Ti and Al are synchronous to ~1300 yr periodicity (Fig 5.2). The 1837 yr, 1991 yr, 2171 yr periodicities can be linked with ~2000 yr periodicity, while 2637 yr and 2390 yr periodicities observed in Mg and Al are linked with ~2600 yr. The 2900 yr and 2986 yr periodicities are related to 3000 yr cycle (Fig 5.2). The lowest frequency cycle at 4300 yr is only demonstrated by Ti.

(b) ***Spectral Analysis of Productivity proxies***

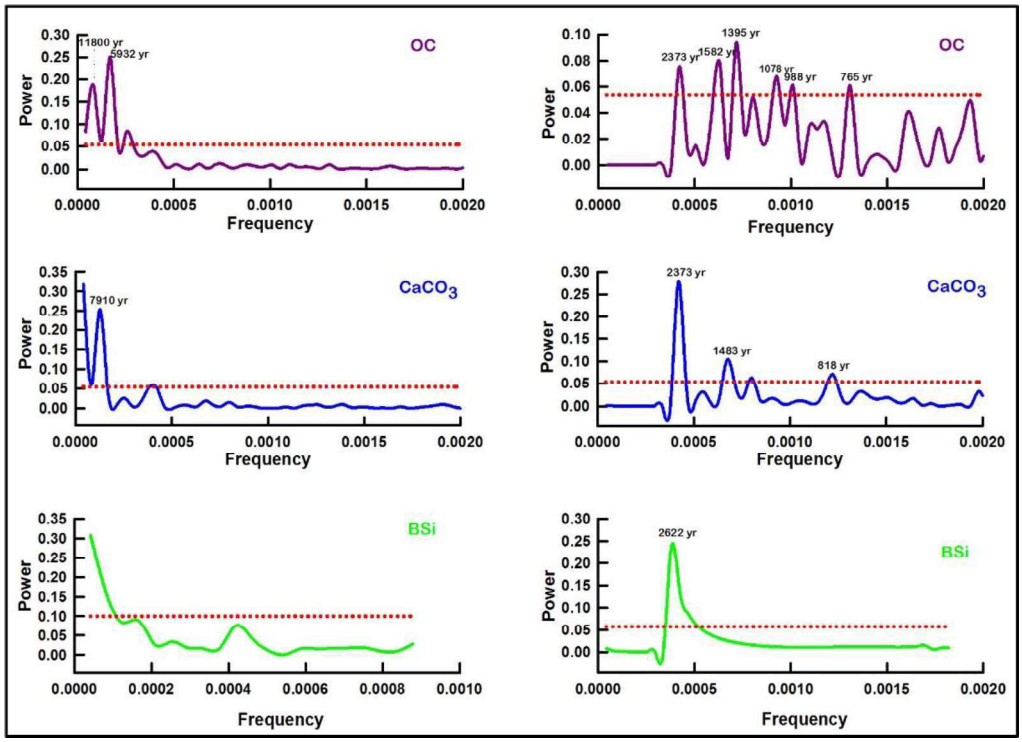

Figure 5.3a

.

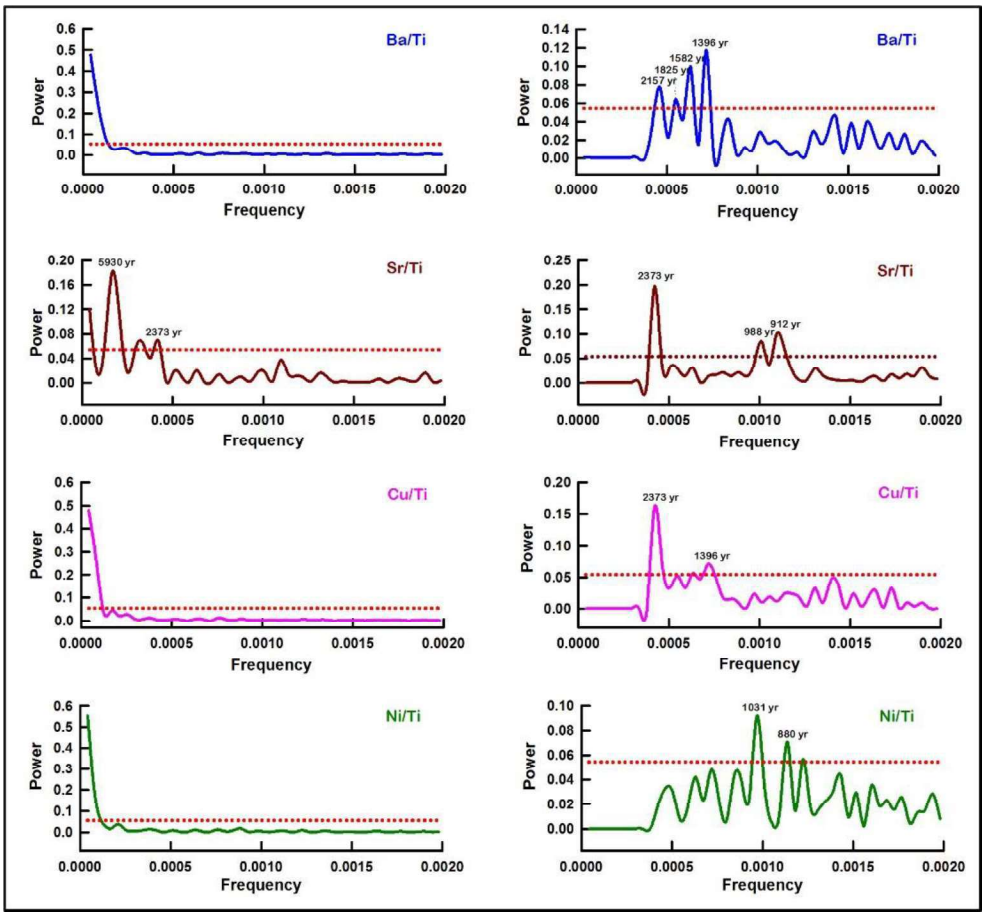

Figure 5.3a,b: Power spectral analysis for the productivity proxies. Spectral peaks with non-detrended are shown on the left; significant spectral peaks obtained after detrending are shown on the right. Dotted line represents 95% confidence level.

The spectral analyses of the non-detrended data for the productivity proxies didn't show any significant periodicities. To obtain lower frequency cyclicities, data was detrended. After detrending, the periodicities observed were 765, 988, 1396, 1582, 2350, 2373 and 2622 yr in all the proxies (Fig 5.3 a, b). These periodicities corroborate well with known periodicities such as 1047, 1300, 1500 and 2300 yr.

(c) *Spectral analysis of Redox sensitive elements*

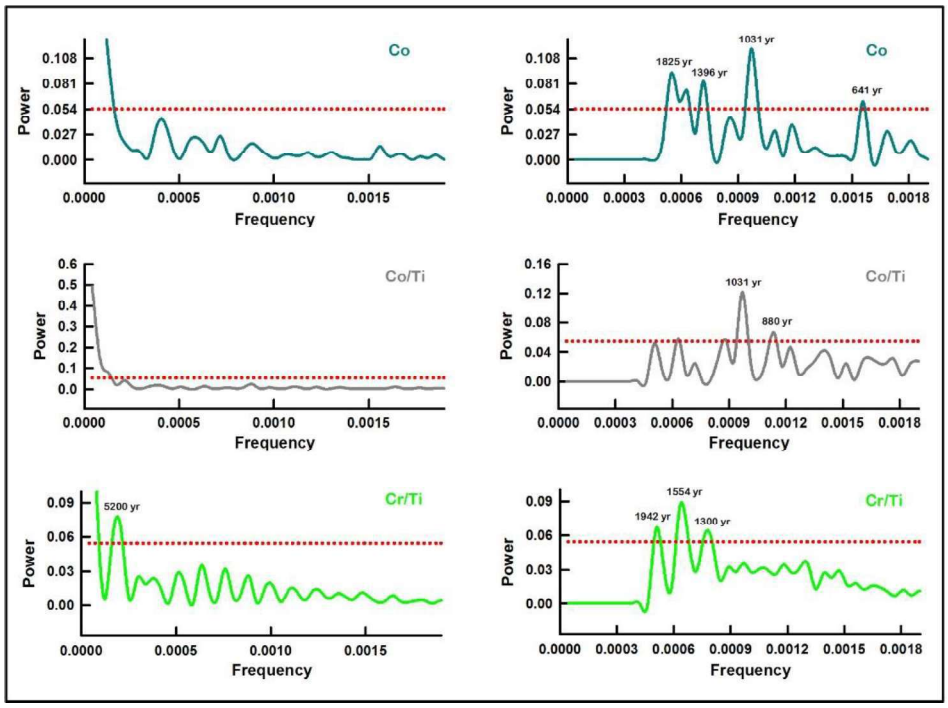

Figure 5.4a

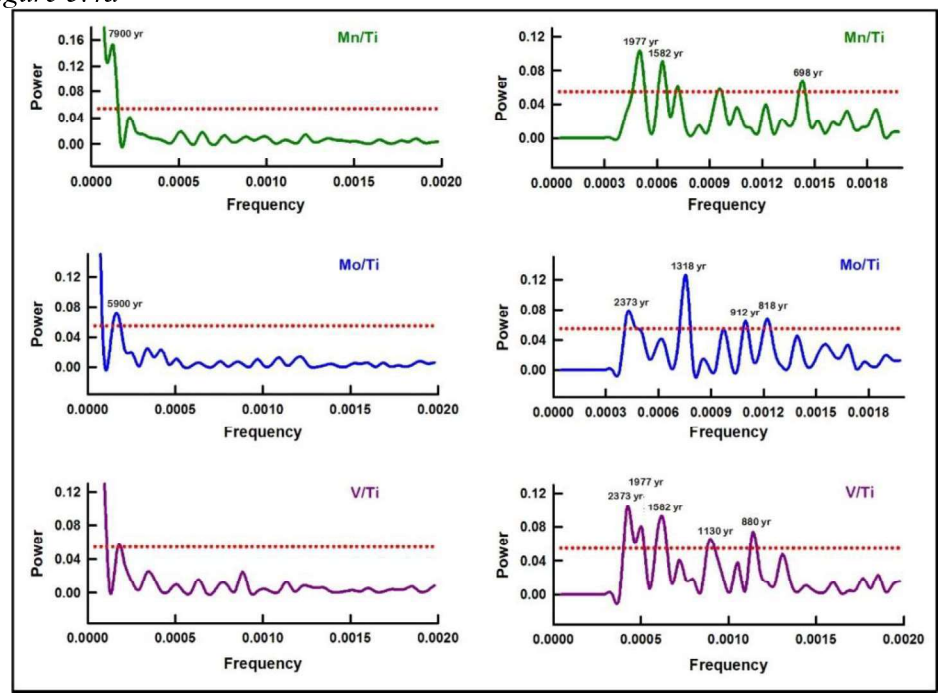

Figure 5.4a,b: Power spectral analysis for the redox sensitive elements. Spectral peaks with non-detrended are shown on the left; spectral peaks obtained after detrending are shown on the right. Dotted line represents 95% confidence level.

The spectral analyses of the non-detrended data of redox group shows cycles above 5000 yr only. After detrending, the redox proxies showed significant periodicities similar to that observed for productivity proxies at 880 yr, 1031 yr, 1396 yr, 1582 yr, 1977 yr and 2373 yr. Mn/Ti and Co show high frequency cycles ~700 yr periodicity (Fig 5.4 a,b).

5.5 Classification of cycles

(a) *The 1500 yr cycle*

The 1500 yr cycle is analogous to a cooling event detected in the ice rafted debris of the North Atlantic with a periodicity of 1470±500 yr as described by Bond et al., (1997, 2001), where a solar forcing mechanism underlies at the Holocene segment and may have affected the North Atlantic Deep Water production. Similar cycles have been reported during the last glacial cycle and the Holocene in the Arabian Sea (Sirocko et al., 1996; Leuschner and Sirocko, 2003). Grootes and Stuiver (1997) have shown that Dansgaard-Oeschger events in the Greenland ice core showed 1470 yr cycle, implying a common link between low latitude monsoon variation and north Atlantic climate. Additionally, a primary cycle of 1300 yr is not evident in most of the climatic records, which is associated with North Atlantic ice rafted debris events during Holocene (Bond, 1997; 2001; Bu¨tikofer, 2007; Wanner et al., 2008). Gasse (2000) proposed such cycles prevailed as a result of changes between solar insolation and oceanic and atmospheric circulation. The wavelet analysis of the paleo records from Atlantic, Pacific spanning the Holocene described 1500 yr cycle being associated not only with any external solar forcing but also with oceanic internal forcing that resulted in changing thermohaline circulation (Debret et al., 2007; 2009; Fletcher et al., 2013; Rodrigo-Gámiz et al., 2014). The paleoproductivity and redox proxies underpins this cycle (1500 yr) with a high degree of significance and suggests the productivity variations could be associated with a greater supply of nutrients through upwelling and its preservation under anoxic bottom water conditions as indicated by redox proxies. The primary cycle of 1500 yr and its corresponding secondary cycle at 3000 yr has been clearly obtained in most of the geochemical proxies (Table 5.1). Absence of 1500 yr cycle related to terrigenous material

implies that the phenomenon behind the paleoproductivity significance of this cycle is related to nutrient enhancement with oceanographic variations. While aeolian proxy (Fe) records, secondary peak (~2900 yr) indicates enhanced aridification and low weathering triggered by the southerly shifting of the ITCZ.

(b) ***The 2000 yr cycle***

Cycles between 1600-2000 yr recorded in the Arabian Sea are linked to monsoonal activities which corroborate extremely well with the northern hemisphere solar insolation maximum (Sirocko et al., 1996; Leuschner and Sirocko, 2003). The other cycles at 1600 yr and 1000 yr recorded in North Atlantic and other locations are explained by variation in solar activity based on ^{10}Be and ^{14}C isotopic records (Debret et al., 2009). The 2300 yr cycle known as Hallstatt cycle is recorded in SST and season intensity of the Siberian High (Rohling et al., 2002) and in upwelling indices of marine sediment core from the Arabian Sea (Pestiaux et al., 1988; Naidu and Malmgren, 1996). The 2300 yr cycle suggests non-linear response of the monsoonal system to solar forcing at sub-Milankovitch cycles previously documented in the atmospheric ^{14}C record induced by solar modulation. A similar cycle linked to changes in monsoonal activity has been recorded at ~1100 yr from Iceland (Bianchi and Mccave, 1999) and from the western Arabian Sea (Sirocko et al., 1996). This has secondary peaks at ~650, ~700, ~765 and ~818 corresponding to periodicity of short SST cooling event at 730±40 yr (Cacho et al., 2001) and solar excursion at 820 yr cycle (Hong et al., 2000) respectively. The 2000 yr cycle and its secondary cycle at 1047 yr is obtained in all the geochemical proxies. The significant cycles obtained in detrital proxies can be interpreted as prevailing wet conditions. The 2000 yr cycle appears not to be influenced only by solar forcing but also by the subsequent monsoonal intensification.

(c) ***The 5000 yr cycle***

The climate models have shown that the changes in the earth's orbital parameters increased the amplitude of the seasonal cycle of solar radiation in the Northern Hemisphere, enhancing the land-ocean thermal contrast and strengthening the SW monsoon (Kutzbach et al., 1996). The monsoon affected areas have shown pronounced variations at periodicity of 10000 yr and 5000 yr

related to runoff variations in response to precessional forcing (Berger et al., 2006; Tuenter et al., 2007). Therefore, the 5000 yr cycle displayed by detrital proxy is strongly related to orbital forcing.

5.6 Evidences of forcing mechanisms from the equatorial Indian Ocean

The global temperature and climate is monitored by the sun demonstrating strong correlation between monsoon and incoming solar radiation (Hong et al., 2000; Gupta et al., 2005; Kessarkar et al., 2013; Rodrigo-Gámiz et al., 2014). The present study is thus an attempt to understand the response of equatorial ocean to the variation in solar radiation.

Table 5.1: List of periodicities obtained for various geochemical proxies and their corresponding globally known periodicities.

Proxies	Variable	Periodicities (yr)	Corresponding cycles (yr)
Detrital	*Ti*	1375, 2637, 4334	1300, 2500, 4600
	Al	1327, 1837, 2171	1300, 2000
	Mg	918, 1991, 2390, 2986	1047, 2000, 2300, 3000
	Fe	2900	3000
	C/N	1031, 1693	1047, 1600
Productivity	*OC*	765, 988, 1078, 1396, 1582, 2373	730, 1047, 1300, 1500, 2300
	$CaCO_3$	818, 1249, 1483, 2373	820, 1047, 1300, 1500, 2300
	BSi	2622	2300
	Ba/Ti	1396, 1582, 1825, 2157	1300, 1500, 2000
	Sr/Ti	912, 988, 2373	1047, 2300
	Ni/Ti	880, 1031	1047
	Cu/Ti	1396, 2350	1300, 2300
Redox Sensitive	*Co*	641, 1031, 1396, 1600, 1825	730, 1047, 1300, 1600, 1800
	Cr/Ti	1300, 1554, 1942	1300, 1500, 2000
	Mn/Ti	698, 1396, 1582, 1977	730, 1047, 1300, 1500, 2000
	Mo/Ti	818, 912, 1318, 2373	820, 1047, 1300, 2300
	V/Ti	880, 1130, 1582, 1977, 2373	820, 1047, 1500, 2000, 2300

The climatic history for the last 25 ka of the equatorial Indian Ocean has shown that the productivity, detrital and redox changes in the region has responded harmonically with the changing solar insolation. High productivity, high redox and low detrital influx conditions during LGM in the region are dominated by precessional forcing and are in phase with low solar insolation. However, early Holocene period witnessed enhanced detrital influx resulted due to high Northern Hemisphere solar insolation maximum which triggered the SW monsoon intensity

The spectral analysis of the sediment core provided prominent solar periodicities of 730 yr, 820 yr, 1047 yr, 1300 yr, 1500 yr, 2000 yr, 2300 yr. Periodicities of 820 yr and 1047 yr can be related to solar excursions, 1300 yr and 1500 yr cycles are associated with oceanic internal forcing that causes changes in thermohaline circulation (Debret et al., 2007; 2009; Fletcher et al., 2013; Rodrigo-Gámiz et al., 2014). The cycles 1600-2000 yr and 2300 yr appears to be caused not only by solar forcing but also by subsequent monsoonal intensification. The equatorial Indian Ocean thus has responded well towards the changing solar irradiation

CHAPTER 6

SUMMARY AND CONCLUSION

6.1 Summary and Conclusion

This study aims to address processes responsible for variation in monsoon, productivity and behavior of redox sensitive elements as a function of surface ocean processes for the late Quaternary period (~25000 to 2000 yr BP) on millennial timescale using multi-proxy approach of high-resolution radiocarbon dated sediment core from central equatorial Indian Ocean, off Sri Lanka. Additionally, an attempt is made to decipher nutrient utilisation as a function of changing monsoonal variation. To accomplish these goals, various geochemical and isotopic parameters have been investigated to decode the signatures of the past events. Major and trace elemental concentrations in the sediments were used to infer the changing SW monsoonal variation along the SW coast of Sri Lanka. Whereas, the organic carbon, calcium carbonate and biogenic silica along with various trace elements and carbon isotopes were used to obtain temporal variation in productivity. Various redox sensitive elements and sulphur isotopes were studied to decipher the causative mechanism for the prevalence of paleo-redox conditions at sediment-water interface. In addition, nitrogen isotopes were analysed to reconstruct past nutrient utilisation for the region devoid of denitrification zone. To assess solar forcing on Indian monsoon, various paleoclimatic proxies from the present core were subjected to spectral analysis. Some of the major observations and conclusions as part of this study.

6.1.1 Paleomonsoonal reconstruction for the central equatorial Indian Ocean using geochemical proxies

(a) *Influence of monsoon on detrital proxy*

The southwestern part of Sri Lanka receives high precipitation during SW monsoon and there is high freshwater discharge and high detrital contribution to the study area. The change in detrital proxies can be used to delineate the change in SW monsoon variation. The detrital flux to the study area deciphered from Ti, Al, Fe, $\delta^{13}C$ and C/N shows a synchronous behavior with the mid-summer low latitude solar insolation and monsoon index. Beginning from ~25 ka BP, low values of detrital proxies and low monsoon index indicates low terrestrial influx, suggests decreasing trend of SW monsoon with minimum precipitation at LGM

(24 to 18 ka). While, enriched $\delta^{13}C$ and low C/N ratio suggests marine origin of the organic matter, further indicating weakening of SW Monsoon. The transition period from glacial to Holocene known as deglacial period is marked with several fluctuations in the SW monsoon intensity. In the present study, a sudden increase in detrital contribution associated with increase in solar insolation after ~17.5 ka can be prominently marked as initiation of the deglacial period. This period has witnessed higher precipitation during warm periods (Bolling-Allerod) and weakened precipitation during cooler times (Younger Dryas and Heinrich event). Early Holocene (after ~11 ka BP) shows sudden increase in detrital values with shift in C/N and $\delta^{13}C$ towards terrestrial values following the maximum summer solar insolation indicates strengthening of SW monsoon intensity. Onset of Holocene is known for monsoon intensification as a result of maximum solar insolation in the Northern Hemisphere, which played significant role in improved SW monsoon intensity. Mid-late Holocene witnessed several fluctuations in SW monsoon intensity with a prominent decline at ~8.2 ka BP and ~4.1 ka BP.

(b) ***Biogenic proxies, $\delta^{15}N$ variation and evidences of ITCZ migration***

The oceanic productivity and biogeochemical cycle of carbon plays a crucial role in regulating global climate change, which has reinforced extensive studies on the reconstruction of paleoproductivity variations. The bulk biogenic fraction of sediment encompasses mainly sedimentary organic matter, calcium carbonate and opal (biogenic silica) collectively used to infer ocean surface productivity. High OC and the $CaCO_3$ concentration were observed during LGM and early Holocene. Enhanced values during early Holocene accompanied with high terrestrial flux with high summer solar insolation indicates strengthened SW monsoon associated with high sediment accumulation rate during 11-9 ka BP, attesting better preservation of productivity proxies.

Presently, the SW coast of Sri Lanka experiences upwelling during NE monsoon, while during SW monsoon the upwelling center shifts towards the SE coast of Sri Lanka. Thus, it can be suggested that during LGM, strong NE monsoon winds prevailed. The high productivity observed during LGM corroborated well with the globally known low summer insolation in the Northern Hemisphere. During LGM, the ITCZ migrated southward in association with low

solar insolation leading to strengthening of NE monsoonal winds. These strong NE monsoon winds augmented upwelling along the SW Sri Lanka resulting in enhanced productivity. The northward migration of ITCZ associated with increase in solar insolation lead to decline in the NE monsoon intensity during deglacial and Holocene periods and the region experienced decline in upwelling intensity and hence low productivity. The biogenic silica representing siliceous productivity shows inverse relation with calcium carbonate corresponding to calcareous productivity. The study showed low BSi and high values of $CaCO_3$ during glacial period, while, higher values of BSi and low $CaCO_3$ were observed during Holocene. This suggests shift in productivity from calcareous to siliceous productivity during glacial to Holocene. The productivity in central equatorial Indian Ocean has been in anti-phase with the solar insolation in the Northern Hemisphere. This phenomenon is conspicuously absent both in the Arabian Sea or the Bay of Bengal.

The sedimentary $\delta^{15}N$ isotopic values can be used to elucidate past nitrate utilisation in the region. According to First order Rayleigh fractionation kinetics, preferential uptake of $^{14}NO_3^-$ over $^{15}NO_3^-$ by phytoplankton takes place, giving rise to isotopically depleted $\delta^{15}N$ photosynthate and a progressively enriched dissolved nitrate pool. During abundant (low) nutrient supply, incomplete use of nutrients leads to depleted (enriched) $\delta^{15}N$ values of the sedimentary organic matter. In the present study during LGM, the concomitant occurrence of low $\delta^{15}N$ and high productivity as evident by high OC and CaCO3, reflected decrease in relative nitrate utilisation. As the region experienced intense upwelling caused by strong NE monsoon winds resulting in excess supply of nutrients. Under abundant supply of nutrients, the region experienced incomplete nutrient utilisation leading to isotopically depleted sedimentary organic matter. During Holocene, shifting of upwelling center led to decrease in nutrient supply inhibiting productivity resulting in enriched $\delta^{15}N$ of sedimentary organic matter and thus indicating complete nutrient utilisation.

6.1.2 Evidence of poor bottom water ventilation during LGM

The depositional conditions in the marine environment can be oxic, suboxic and anoxic based on the presence or absence of oxygen at the sediment-

water interface. Redox sensitive elements (Mo, V, Cr, Mn) have varying mobilities depending on their oxidation state influenced by the redox conditions at sediment water interface. Sulfur isotopes demonstrate large variation in sediments from anoxic to oxic conditions and variations in the sedimentary sulfur isotopic composition along with redox sensitive elements are often used to infer the changes in the Earth's environment. In the present study, based on high OC, high redox sensitive elements and depleted $\delta^{34}S$, two phases of anoxic conditions could be identified: one during LGM and other at early Holocene. Enhanced OC during early Holocene has been attributed to its better preservation due to high sedimentation rate, thereby causing anoxic conditions triggered by high bacterial degradation of OC. NADW is the main source for deep water ventilation in the northern Indian Ocean and changes in deep water circulation alters the bottom water oxygen conditions. During glacial times, change in deep water circulation caused weak ventilation of deep-waters by reduced proportion of NADW and increased AABW in northern Indian Ocean. Thus, during LGM (~21 ka BP), prevalence of anoxic conditions has been attributed both to high organic matter degradation as a result of high productivity and poorly ventilated bottom water conditions.

6.1.3 Solar forcing of Indian Monsoon

To understand the Sun-Climate relation between solar and SW monsoon intensity, the paleoclimatic proxies were compared with solar insolation and Total Solar Irradiance (TSI). Broadly, the region showed reduction in SW monsoon precipitation during the period of low TSI and low solar insolation, whereas periods of high TSI and solar insolation show increased SW monsoon precipitation.

Spectral analysis of various proxies indicates that the precessional cycle of the earth's orbit induces the insolation variations which mainly governs the monsoonal variation in the region. The sediment core exhibited prominent solar periodicities of 730 yr, 820 yr, 1047 yr, 1300 yr, 1500 yr, 2000 yr, 2300 yr. The occurrence of these solar periodicities in various time series proxy records suggest solar forcing of SW monsoon and high latitude climatic changes that cause change in thermohaline circulation on millennial timescales.

6.2 Future work

The detailed multi-proxy study from the marine sediments of the SW coast of Sri Lanka described in the thesis has provided significant information on the processes involved in distribution of various geochemical and isotopic proxies in the sediments. Additionally, the study raises few questions that needs further understanding.

Sri Lanka experiences both the SW and NE monsoon. The work in thesis has demonstrated that the total productivity along SW coast varied as a function of changing monsoon winds and shifting of upwelling center. To attest these conclusions, more high-resolution cores from both SW and SE coast of Sri Lanka employing multi-proxy technique should be investigated.

One of the major addition to the present study would be to assess the past fluctuation in sea surface temperature, salinity and precipitation. For this purpose, the $\delta^{18}O$ and elemental ratios of foraminiferal calcite shells should be analysed.

The downcore variation Sr and Nd isotopic ratios in sediments are used for provenance studies. As the study area is at the intermixing zone of the two contrasting basins, the Sr-Nd isotopic ratios can help in identifying the inter-basin exchange of the waters between the Bay of Bengal and Arabian Sea.

REFERENCES

References

Abbey, S., 1983. Studies in "Standard Samples" of Silicate Rocks and Minerals 1969-1982. Canadian Geological Survey Paper 114, 83–15.

Abram, N.J., McGregor, H. V., Gagan, M.K., Hantoro, W.S., Suwargadi, B.W., 2009. Oscillations in the southern extent of the Indo-Pacific Warm Pool during the mid-Holocene. Quaternary Science Reviews 28, 2794–2803. doi:10.1016/j.quascirev.2009.07.006

Achterberg, E.P., Berg, C.M.G. Van Den, Colombo, C., 2003. High resolution monitoring of dissolved Cu and Co in coastal surface waters of the western North Sea. Continental Shelf Research 23, 611–623. doi:10.1016/S0278-4343(03)00003-7

Agnihotri, R., 2001. Chemical and Isotopic studies of sediment from the Arabian Sea and Bay of Bengal.

Agnihotri, R., Dutta, K., Bhushan, R., Somayajulu, B.L.K., 2002. Evidence for solar forcing on the Indian monsoon during the last millennium. Earth and Planetary Science Letters 198, 521–527. doi:10.1016/S0012-821X(02)00530-7

Agnihotri, R., Sarin, M.M., Somayajulu, B.L.K., Jull, A.J.T., Burr, G.S., 2003. Late-Quaternary biogenic productivity and organic carbon deposition in the eastern Arabian Sea. Palaeogeography, Palaeoclimatology, Palaeoecology 197, 43–60. doi:10.1016/S0031-0182(03)00385-7

Agnihotri, R., Kumar, R., Prasad, M., Sharma, C., Bhatia, S., Arya, B., 2015. Experimental Setup and Standardization of a Continuous Flow Stable Isotope Mass Spectrometer for Measuring Stable Isotopes of Carbon, Nitrogen and Sulfur in Environmental Samples. Mapan 29, 195–205.

Agnihotri, R., Kurian, S., Fernandes, M., Reshma, K., D'Souza, W., Naqvi, S.W. a., 2008. Variability of subsurface denitrification and surface productivity in the coastal eastern Arabian Sea over the past seven centuries. The Holocene 18, 755–764. doi:10.1177/0959683608091795

Ahmad, S.M., Patil, D.J., Rao, P.S., Nath, B.N., Rao, B.R., Rajagopalan, G., 2000.

Glacial-interglacial changes in the surface water characteristics of the Andaman Sea: Evidence from stable isotopic ratios of planktonic foraminifera. J Earth Syst Sci 1, 153–156.

Ahmad, S.M., Anil Babu, G., Padmakumari, V.M., Dayal, A.M., Sukhija, B.S., Nagabhushanam, P., 2005. Sr, Nd isotopic evidence of terrigenous flux variations in the Bay of Bengal: Implications of monsoons during the last ~34,000 years. Geophysical Research Letters 32, 1–4. doi:10.1029/2005GL024519

Ahmad, S.M., Babu, G.A., Padmakumari, V.M., Raza, W., 2008. Surface and deep water changes in the northeast Indian Ocean during the last 60 ka inferred from carbon and oxygen isotopes of planktonic and benthic foraminifera. Palaeogeography, Palaeoclimatology, Palaeoecology 262, 182–188. doi:10.1016/j.palaeo.2008.03.007

Ahmad, S.M., Padmakumari, V.M., Raza, W., Venkatesham, K., Suseela, G., Sagar, N., Chamoli, A., Rajan, R.S., 2011. High-resolution carbon and oxygen isotope records from a scleractinian (Porites) coral of Lakshadweep Archipelago. Quaternary International 238, 107–114. doi:10.1016/j.quaint.2009.11.020

Ahmad, S.M., Patil, D.J., Rao, P.S., Nath, B.N., Rao, B.R., Rajagopalan, G., 2000. Glacial-interglacial changes in the surface water characteristics of the Andaman Sea: Evidence from stable isotopic ratios of planktonic foraminifera. J Earth Syst Sci 1, 153–156.

Algeo, T.J., Lyons, T.W., 2006. Mo-total organic carbon covariation in modern anoxic marine environments: Implications for analysis of paleoredox and paleohydrographic conditions. Paleoceanography 21, 1–23. doi:10.1029/2004PA001112

Algeo, T.J., Maynard, J.B., 2004. Trace-element behavior and redox facies in core shales of Upper Pennsylvanian Kansas-type cyclothems. Chemical Geology 206, 289–318. doi:10.1016/j.chemgeo.2003.12.009

Algeo, T.J., Tribovillard, N., 2009. Environmental analysis of paleoceanographic systems based on molybdenum-uranium covariation. Chemical Geology 268, 211–225. doi:10.1016/j.chemgeo.2009.09.001

Alley, R.B., 2004. GISP2 ice core temperature and accumulation data. IGBP PAGES/World Data Center for Paleoclimatology Data Contribution Series 13.

Altabet, M.A., Francois, F., 1994. Sedimentary nitrogen isotopic ratio as a recorder for surface ocean ntirate utilization. Biogeochemical cycles 8, 103–116. doi:10.1029/93GB03396

Altabet, M.A., Francois, R., Murray, D.W., Prell, W.L., 1995. Climate-related variations in denitrification in the Arabian Sea from sediment $^{15}N/^{14}N$ ratios. Nature. doi:10.1038/373506a0

Altabet, M.A., Higginson, M.J., Murray, D.W., 2002. The effect of millennial-scale changes in Arabian Sea denitrification on atmospheric CO_2. Nature 415, 159–162. doi:10.1038/415159a

Amin, B., Likhite, S., Radhakrishnamurty, C., Somayajulu, B., 1972. Susceptibility stratigraphy and paleomagnetism of some deep Pacific Ocean cores. Deep Sea Research and Oceanographic 19, 249–252.

Anand, P., Kroon, D., Singh, A.D., Ganeshram, R.S., Ganssen, G., Elderfield, H., 2008. Coupled sea surface temperature-seawater $\delta^{18}O$ reconstructions in the Arabian Sea at the millennial scale for the last 35 ka. Paleoceanography 23, 1–8. doi:10.1029/2007PA001564

Banerji, U.S., Bhushan, R., Jull, A.J.T., 2017. Mid–late Holocene monsoonal records from the partially active mudflat of Diu Island, southern Saurashtra, Gujarat, western India. Quaternary International 443, 200–210. doi:10.1016/j.quaint.2016.09.060

Banerji, U.S., Bhushan, R., Mauraya, D. M., 2016. Sedimentary Records of Paleoredox Conditions at Relict Mudflat of Vasoj , Southern Saurashtra Sedimentary Records of Paleoredox Conditions at Relict Mudflat. Earth Science India 9 (II), 114–125.

Bard, E., Raisbeck, G., Yiou, F., Jouzel, J., 2000. Solar irradiance during the last 1200 yr based on cosmogenic nuclides. Tellus 52B, 985–992. doi:10.1034/j.1600-0889.2000.d01-7.x

Bareille, G., Labracherie, M., Bertrand, P., Labeyrie, L., Lavaux, G., Dignan, M., 1998. Glacial-interglacial changes in the accumulation rates of major biogenic components in Southern Indian Ocean sediments. Journal of Marine Systems 17, 527–539. doi:10.1016/S0924-7963(98)00062-1

Bender, M.L., Heggie, D.T., 1984. Fate of organic carbon reaching the sea floor: a status report. Geochim. Cosmochim. Acta 48, 977–986.

Beer, J., Mende, W., Stellmacher, R., 2000. The role of the sun in climate forcing. Quaternary Science Reviews 19, 403–415. doi:10.1016/S0277-3791(99)00072-4

Berger, A., Loutre, M.F., 1991. Insolation values for the climate of the last 10 million years. Quaternary Science Reviews 10, 297–317. doi:10.1016/0277-3791(91)90033-Q

Berger, A., Loutre, M.F., Mélice, J.L., 2006. Equatorial insolation: from precession harmonics to eccentricity frequencies. Climate of the Past Discussions 2, 519–533. doi:10.5194/cpd-2-519-2006

Berner, R.A., 1970. Sedimentary pyrite formation. American Journal of Science, 268, 1–23.

Bhushan, R., Dutta, K., Somayajulu, B.L.K., 2001. Concentrations and burial fluxes of organic and inorganic carbon on the eastern margins of the Arabian Sea. Marine Geology 178, 95–113. doi:10.1016/S0025-3227(01)00179-7

Bianchi, G.G., Mccave, I.N., 1999. Holocene periodicity in North Atlantic climate and deep- ocean flow south of Iceland. Arctic 35, 515–517. doi:10.1038/17362

Blackburn, T.H., 1983. The Microbial Nitrogen Cycle. Microbial Geochemistry, Krumbein,. ed. Blackwell Scientific, Oxford.

Böll, A., Schulz, H., Munz, P., Rixen, T., Gaye, B., Emeis, K.C., 2015. Contrasting sea surface temperature of summer and winter monsoon variability in the northern Arabian Sea over the last 25 ka. Palaeogeography, Palaeoclimatology, Palaeoecology 426, 10–21. doi:10.1016/j.palaeo.2015.02.036

Bond, G., 1997. A Pervasive Millennial-Scale Cycle in North Atlantic Holocene and Glacial Climates. Science 278, 1257–1266. doi:10.1126/science.278.5341.1257

Bond, G., 2001. Persistent Solar Influence on North Atlantic Climate During the Holocene. Science 294, 2130–2136. doi:10.1126/science.1065680

Böttcher, M.E., Oelschläger, B., Höpner, T., Brumsack, H.-J., Rullkötter, J., 1998. Sulfate reduction related to the early diagenetic degradation of organic matter and "black spot" formation in tidal sandflats of the German Wadden Sea (southern North Sea): stable isotope (^{13}C, ^{34}S, ^{18}O) and other geochemical results. Organic Geochemistry 29, 1517–1530. doi:https://doi.org/10.1016/S0146-6380(98)00124-7

Bottrell, S.H., Newton, R.J., 2006. Reconstruction of changes in global sulfur cycling from marine sulfate isotopes. Earth-Science Reviews 75, 59–83.

Bouquillon, A., France-Lanord, C., Michard, A., Tiercelin, J.J., 1990. Isotopic chemistry and sedimentology of the Bengal fan sediments: The denudation of the Himalaya. Chemical Geology 84, 368–370. doi:10.1016/0009-2541(90)90269-D

Bradtmiller, L.I., Anderson, R.F., Fleisher, M.Q., Burckle, L.H., 2006. Diatom productivity in the equatorial Pacific Ocean from the last glacial period to the present: A test of the silicic acid leakage hypothesis. Paleoceanography 21, 1–12. doi:10.1029/2006PA001282

Bradtmiller, L.I., Anderson, R.F., Fleisher, M.Q., Burckle, L.H., 2007. Opal burial in the equatorial Atlantic Ocean over the last 30 ka: Implications for glacial-interglacial changes in the ocean silicon cycle. Paleoceanography 22, 1–15. doi:10.1029/2007PA001443

Brandes, J.A., Devol, A.H., Yoshinari, T., Jayakumar, D.A., Naqvi, S.W.A., 1998. Isotopic composition of nitrate in the central Arabian Sea and eastern tropical North Pacific: A tracer for mixing and nitrogen cycles. Limnology and Oceanography 43, 1680–1689. doi:10.4319/lo.1998.43.7.1680

Broccoli, A.J., Dahl, K.A., Stouffer, R.J., 2006. Response of the ITCZ to Northern Hemisphere cooling. Geophysical Research Letters 33, 1–4. doi:10.1029/2005GL024546

Brumsack, H.J., 1980. Geochemistry of Cretaceous black shales from the Atlantic Pcean (DSDP Legs 11, 14, 36 and 41). Chemical Geology 31, 1–25. doi:10.1016/0009-2541(80)90064-9

Brumsack, H.J., 2006. The trace metal content of recent organic carbon-rich sediments: Implications for Cretaceous black shale formation. Palaeogeography, Palaeoclimatology, Palaeoecology 232, 344–361. doi:10.1016/j.palaeo.2005.05.011

Bu¨tikofer, J., 2007. Millennial scale climate variability during the last 6000 years – tracking down the Bond cycles., Diploma thesis. University of Bern-doi:(http://www. giub.unibe.ch/klimet/docs/diplom_jbuetikofer.pdf)

Cacho, I., Grimalt, J.O., Canals, M., Sbaffi, L., Shackleton, N.J., Schonfeld, J., Zahn, R., 2001. Variability of the western Mediterranean Sea surface temperature during the last 25,000 years and its connection with the Northern Hemisphere climatic changes. Paleoceanography 16, 40–52.

Calvert, S.E., Nielsen, B., Fontugne, M.R., 1992. Evidence from nitrogen isotope ratios for enhanced productivity during formation of eastern Mediterranean sapropels. Nature 359, 223–225. doi:10.1038/359223a0

Calvert, S.E., Pedersen, T.F., 1993. Geochemistry of Recent oxic and anoxic marine sediments: Implications for the geological record. Marine Geology 113, 67–88. doi:10.1016/0025-3227(93)90150-T

Calvert, S.E., Pedersen, T.F., 1996. Sedimentary geochemistry of manganese: Implications for the environment of formation of manganiferous black shales. Economic Geology 91, 36–47. doi:10.2113/gsecongeo.91.1.36

Calvert, S.E., Piper, D.Z., 1984. Geochemistry of ferromanganese nodules from DOMES site a, Northern Equatorial Pacific: Multiple diagenetic metal sources in the deep sea. Geochimica et Cosmochimica Acta 48, 1913–1928. doi:10.1016/0016-7037(84)90374-0

Capone, D.G., 1997. Trichodesmium, a Globally Significant Marine Cyanobacterium. Science 276, 1221–1229. doi:10.1126/science.276.5316.1221

Canfield, D.E., Habicht, K.S., Thamdrup, B., 2000. The Archean Sulfur Cycle and the Early History of Atmospheric Oxygen 288, 658–662.

Canfield, D.E., 1989. Sulfate reduction and oxic respiration in marine sediments: implications for organic carbon preservation in euxinic environments. Deep-Sea Research 36, 121–138.

Canfield, D.E., 2001. Biogeochemistry of Sulfur Isotopes. Reviews in Mineralogy and Geochemistry 43, 607–636. doi:10.2138/gsrmg.43.1.607

Cartapanis, O., Tachikawa, K., Bard, E., 2011. Northeastern Pacific oxygen minimum zone variability over the past 70 kyr: Impact of biological production and oceanic ventilation. Paleoceanography 26, 1–17. doi:10.1029/2011PA002126

Carter, S.J., Colman, S.M., 1994. Biogenic Silica in Lake Baikal Sediments: Results From 1990-1992 American Cores.

Chabangborn, A., Brandefelt, J., Wohlfarth, B., 2014. Asian monsoon climate during the Last Glacial Maximum: Palaeo-data-model comparisons. Boreas 43, 220–242. doi:10.1111/bor.12032

Chandana, K.R., Bhushan, R., Jull, A.J.T., 2017. Evidence of Poor Bottom Water Ventilation during LGM in the Equatorial Indian Ocean. Frontiers in Earth Science 5, 1–10. doi:10.3389/feart.2017.00084

Chao, W.C., Chen, B., 2001. The Origin of Monsoons. Journal of the Atmospheric Sciences 58, 3497–3507. doi:10.1175/1520-0469(2001)058<3497:TOOM>2.0.CO;2

Chauhan, O. S., Vogelsang, E., 2006. Climate induced changes in the circulation and dispersal patterns of the fluvial sources during late Quaternary in the middle Bengal Fan. Journal of earth system science 115, 379–386.

Chester, R., 2003. Marine Geochemistry, 2nd ed. ed. Blackwell publishing.

Chondrogianni, C., Ariztegui, D., Rolph, T., Juggins, S., Shemesh, A., Rietti-Shati, M., Niessen, F., Guilizzoni, P., Lami, A., McKenzie, J.A., Oldfield, F.,

2004. Millennial to interannual climate variability in the Mediterranean during the Last Glacial Maximum. Quaternary International 122, 31–41. doi:https://doi.org/10.1016/j.quaint.2004.01.029

Claypool, G.E., Kaplan, I.R., 1974. The origin and distribution of methane in marine sediments. In: Kaplan, I.R. (Ed.), Natural Gases in Marine Sediments. Plenum Press, London, p. 99– 139.

Clemens, S.C., Prell, W.L., Howard, W.R., 1987. Retrospective dry bulk density estimates from southeast Indian Ocean sediments - Comparison of water loss and chloride-ion methods. Marine Geology 76, 57–69. doi:10.1016/0025-3227(87)90017-X

Clemens, S., Wang, P., Prell, W., 2003. Monsoons and global linkages on Milankovitch and sub-Milankovitch time scales. Marine Geology 201, 1–3. doi:10.1016/S0025-3227(03)00195-6

Clift, P.D., Giosan, L., Blusztajn, J., Campbell, I.H., Allen, C., Pringle, M., Tabrez, A.R., Danish, M., Rabbani, M.M., Alizai, A., Carter, A., Lückge, A., 2008. Holocene erosion of the Lesser Himalaya triggered by intensified summer monsoon. Geology 36, 79–82. doi:10.1130/G24315A.1

Cline, J.D., Kaplan, I.R., 1975. Isotopic fractionation of dissolved nitrate during denitrification in the eastern tropical north pacific ocean. Marine Chemistry 3, 271–299. doi:10.1016/0304-4203(75)90009-2

Curry, W.B., Oppo, D.W., 2005. Glacial water mass geometry and the distribution of $\delta^{13}C$ of ΣCO_2 in the western Atlantic Ocean. Paleoceanography 20, 1–12. doi:10.1029/2004PA001021

Curry, W.B., Duplessy, J.C., Labeyrie, L.D., Shackleton, N.J., 1988. Changes in the distribution of $\delta^{13}C$ of deep water ΣCO_2 between the last glaciation and the Holocene. Paleoceanography 3, 317–341. doi:10.1029/PA003i003p00317

Dalai, T.K., Rengarajan, R., Patel, P., 2004. Sediment geochemistry of the Yamuna River System in the Himalaya: Implications to weathering and transport. Geochemical Journal 38, 441–453.

Das, A., Krishnaswami, S., 2007. Elemental geochemistry of river sediments from the Deccan Traps, India: Implications to sources of elements and their mobility during basalt-water interaction. Chemical Geology 242, 232–254. doi:10.1016/j.chemgeo.2007.03.023

Dean, W.E., Piper, D.Z., Peterson, L.C., 1999. Molybdenum Accumulation in Cariaco Basin Sediment Over the Past 24 k.y.: A Record of Water-Column Anoxia and Climate. Geology 27, 507–510.

Dean, W.E., Zheng, Y., Ortiz, J.D., Geen, A. van, 2006. Sediment Cd and Mo accumulation in the oxygen-minimum zone off western Baja California linked to global climate over the past 52 kyr. Paleoceanography 21, 1–13. doi:10.1029/2005PA001239

Debret, M., Bout-Roumazeilles, V., Grousset, F., Desmet, M., McManus, J.F., Massei, N., Sebag, D., Petit, J.-R., Copard, Y., Trentesaux, A., 2007. The origin of the 1500-year climate cycles in Holocene North-Atlantic records. Climate of the Past Discussions 3, 679–692. doi:10.5194/cpd-3-679-2007

Debret, M., Sebag, D., Crosta, X., Massei, N., Petit, J.R., Chapron, E., Bout-Roumazeilles, V., 2009. Evidence from wavelet analysis for a mid-Holocene transition in global climate forcing. Quaternary Science Reviews 28, 2675–2688. doi:10.1016/j.quascirev.2009.06.005

Dill, H., Teschner, M., Wehner, H., 1988. Petrography, inorganic and organic geochemistry of Lower Permian carbonaceous fan sequences ("Brandschiefer Series") - Federal Republic of Germany: Constraints to their paleogeography and assessment of their source rock potential. Chemical Geology 67, 307–325. doi:10.1016/0009-2541(88)90136-2

Dixit, Y., Hodell, D.A., Sinha, R., Petrie, C.A., 2014a. Abrupt weakening of the Indian summer monsoon at 8.2 kyr B.P. Earth and Planetary Science Letters 391, 16–23. doi:10.1016/j.epsl.2014.01.026

Dixit, Y., Hodell, D.A., Petrie, C.A., 2014b. Abrupt weakening of the summer monsoon in northwest India ~4100 yr ago. Geology 42, 339–342. doi:10.1130/G35236.1

Doney, S.C., Fabry, V.J., Feely, R.A., Kleypas, J.A., 2009. Ocean Acidification: The Other CO2 Problem. Annual Review of Marine Science 1, 169–192. doi:10.1146/annurev.marine.010908.163834

Duplessy, J.C., 1982. Glacial to interglacial contrasts in the northern Indian Ocean. Nature 295, 494–498. doi:10.1038/295494a0

Duplessy, J.C., Shackleton, N.J., Fairbanks, R.G., Labeyrie, L., Oppo, D., Kallel, N., 1988. Deepwater source variations during the last climatic cycle and their impact on the global deepwater circulation. Paleoceanography 3, 343–360. doi:10.1029/PA003i003p00343

Dutta, K., Bhushan, R., Somayajulu, B.L.K., 2001. ΔR correction values for the northern Indian Ocean. Radiocarbon 43, 483–488. doi:https://doi.org/10.1017/S0033822200038376

Eddy, J.A., 1976. The Maunder Minimum. Science 192.

Elderfield, H., Rickaby, R., 2000. Oceanic Cd/P ratio and nutrient utilization in the glacial Southern Ocean. Nature 405, 305–10. doi:10.1038/35012507

Emerson, S., Hedges, J.I., 1988. Processes controlling the organic carbon content of open ocean sediments. Paleoceanography 3, 621–634. doi:10.1029/PA003i005p00621

Emerson, S.R., Huested, S.S., 1991. Ocean anoxia and the concentrations of molybdenum and vanadium in seawater. Marine Chemistry 34, 177–196. doi:10.1016/0304-4203(91)90002-E

Engels, S., Geel, B. van, 2012. The effects of changing solar activity on climate contributions from palaeoclimatology. Journal of Space Weather and Space Climate 2, A09. doi:10.1051/swsc/2012009

Farrell, J., Pederson, T., Calvert, S., Nielsen, B., 1995. Glacial-interglacial changes in nutrient utilization in the equatorial Pacific Ocean. Nature.

Fike, D.A., Bradley, A.S., Rose, C.V., 2015. Rethinking the ancient sulfur cycle. Annual Review of Earth Planet Science 43, 593–622.

Fleitmann, D., 2003. Holocene Forcing of the Indian Monsoon Recorded in a Stalagmite from Southern Oman. Science 300, 1737–1739. doi:10.1126/science.1083130

Fleitmann, D., Burns, S.J., Mangini, A., Mudelsee, M., Kramers, J., Villa, I., Neff, U., Al-Subbary, A.A., Buettner, A., Hippler, D., Matter, A., 2007. Holocene ITCZ and Indian monsoon dynamics recorded in stalagmites from Oman and Yemen (Socotra). Quaternary Science Reviews 26, 170–188. doi:10.1016/j.quascirev.2006.04.012

Fletcher, W.J., Debret, M., Goñi, M.F.S., 2013. Mid-Holocene emergence of a low-frequency millennial oscillation in western Mediterranean climate: Implications for past dynamics of the North Atlantic atmospheric westerlies. The Holocene 23, 153–166. doi:10.1177/0959683612460783

Fontugne, M.R., Duplessy, J.-C., 1986. Variations of the monsoon regime during the upper Quaternary: evidence from carbon isotopic record of organic matter in North Indian Ocean sediment cores. Palaeogeography, Palaeoclimatology, Palaeoecology 56, 69–88.

France-Lanord, C., 1993. Evolution of the Himalaya since Miocene time: isotopic and sedimentological evidence from the Bengal Fan. Society, London, Special 603–621. doi:10.1144/GSL.SP.1993.074.01.40

Francois, R., 1988. A study on the regulation of the concentrations of some trace metals (Rb, Sr, Zn, Pb, Cu, V, Cr, Ni, Mn and Mo) in Saanich Inlet Sediments, British Columbia, Canada. Marine Geology 83, 285–308. doi:10.1016/0025-3227(88)90063-1

Francois, R., Altabet, M.A., Yu, E.-F., Sigman, D.M., Bacon, M.P., Frank, M., Bohrmann, G., Bareille, G., Labeyrie, L.D., 1997. Contribution of the Southern Ocean surface water stratification to low atmospheric CO_2 concentrations during the last glacial period. Nature 389, 929–935.

Freudenthal, T., Wagner, T., Wenzhffer, F., Zabel, M., Wefer, G., 2001. Early diagenesis of OM from sediments of the eastern subtropical Atlantic: evidence

from stable nitrogen and carbon isotopes. Geochim. Cosmochim. Acta 65, 1795–1808.

Gadgil, S., 2003. The Indian Monsoon and its Variability. Annual Review of Earth Planet Science 31, 429–67. doi:doi: 10.1146/annurev.earth.31.100901.141251

Ganeshram, R.S., Pedersen, T.F., Calvert, S.E., Murray, J.W., 1995. Large changes in oceanic nutrient inventories from glacial to interglacial periods. Nature 376, 755–758.

Ganeshram, S., Pedersen, F., Calvert, E., Mcneill, W., Fontugne, M.R., 2000. Glacial-interglacial variability in denitrification in the world's oceans: Causes and consequences. Paleoceanography 15, 361–376.

Garrels, R.M., Lerman, A., 1981. Phanerozoic cycles of sedimentary carbon and sulfur. Proceedings of the National Academy of Sciences USA 78, 4652–4656.

Gasse, F., 2000. Hydrological changes in the African tropics since the Last Glacial Maximum. Quaternary Science Reviews 19, 189–211. doi:10.1016/S0277-3791(99)00061-X

Gearing, G.N., Gearing, P.L., Rudnick, D.T., Requejo, A.G., Hutchins, M.J., 1984. Isotope variability of organic carbon in a phytoplankton based temperate estuary. Geochim. Cosmochim. Acta 48, 1089–1098.

Geel, B. van, Raspopov, O.M., Renssen, H., Plicht, J. van der, Dergachev, V.A., Meijer, H.A.J., 1999. The role of solar forcing upon climate change. Quaternary Science Reviews 18, 331–338. doi:http://dx.doi.org/10.1016/S0277-3791(98)00088-2

Gladney, E.S., Roelandts, I., 1987. Compilation of Elemental Concentration Data for USGSBHVO-1, MAG-1, QLO-1, RGM-1, SCo-1, SDC-1, SGR-1, and STM-1. Geostandards Newsletter 12, 253–362.

Gordon, E.S., Goni, M.A., 2003. Sources and distribution of terrigenous organic matter delivered by the Atchafalaya river to sediments in the northern gulf of Mexico. Geochim. Cosmochim. Acta 67, 2359–2375.

Govil, P., Naidu, P.D., 2010. Evaporation-precipitation changes in the eastern Arabian Sea for the last 68 ka: Implications on monsoon variability. Paleoceanography 25, 1–11. doi:10.1029/2008PA001687

Govil, P., Naidu, P.D., 2011. Variations of Indian monsoon precipitation during the last 32 kyr reflected in the surface hydrography of the Western Bay of Bengal. Quaternary Science Reviews 30, 3871–3879. doi:10.1016/j.quascirev.2011.10.004

Govindaraju, K., 1994. 1994 Compilation of Working Values and Descriptions for 383Geostandards. Geostandards Newsletter 18, 1–158.

Grootes, P.M., Stuiver, M., 1997. Oxygen 18/16 variability in Greenland snow and ice with 10^{-3}- to 10^{5}-year time resolution. Journal of Geophysical Research: Oceans 102, 26455–26470. doi:10.1029/97JC00880

Gupta, A.K., Anderson, D.M., Overpeck, J.T., 2003. Abrupt changes in the Asian southwest monsoon during the Holocene and their links to the North Atlantic Ocean. Nature 421, 354–357. doi:10.1038/nature01340

Gupta, A.K., Das, M., Anderson, D.M., 2005. Solar influence on the Indian summer monsson during the Holocene. Geophysical Research Letters 32, 1–4. doi:10.1029/2005GL022685

Habicht, K.S., Gade, M., Thamdrup, B., Berg, P., Canfield, D.E., 2002. Calibration of sulfate levels in the Archean Ocean. science 298, 2372–2374.

Harrison, A.G., Thode, H.G., 1958. Mechanism of the bacterial reduction of sulfate from isotope fractionation studies. Faraday Soc. Trans. 54, 84–92.

Hedges, J.I., Keil, R.G., 1995. Sedimentary organic matter preservation: an assessment and speculative synthesis. Marine Chemistry 49, 81–115. doi:https://doi.org/10.1016/0304-4203(95)00008-F

Hedges, J.I., Parker, P.L., 1976. Land-derived organic matter in surface sediments from the Gulf of Mexico. Geochimica et Cosmochimica Acta 40, 1019–1029. doi:10.1016/0016-7037(76)90044-2

Hendy, I.L., Pedersen, T.F., 2005. Is pore water oxygen content decoupled from productivity on the California Margin? Trace element results from Ocean Drilling

Program Hole 1017E, San Lucia slope, California. Paleoceanography 20, 1–12. doi:10.1029/2004PA001123

Heinrichs, S.M., 1992. Early diagenesis of organic matter in marine sediments: progress and perplexity. Marine Chemistry 39, 119–149.

Henrichs, S.M., Reeburgh, W.S., 1987. Anaerobic mineralization of marine sediment organic matter: rates and the role of anaerobic processes in the oceanic carbon economy. Geomicrobiology Journal 5, 191–237.

Higginson, M.J., Altabet, M.A., Wincze, L., Herbert, T.D., Murray, D.W., 2004. A solar (irradiance) trigger for millennial-scale abrupt changes in the southwest monsoon? Paleoceanography 19. doi:10.1029/2004PA001031

Hild, E., Brumsack, H.J., 1998. Major and minor element geochemistry of Lower Aptian sediments from the NW German Basin (core Hohenegglesen KB 40). Cretaceous Research 19, 615–633. doi:10.1006/cres.1998.0122

Holmes, M.E., Schneider, R.R., Muller, P.J., Segl, M., Wefer, G., 1997. Reconstruction of past nutrient utilization in the eastern Angola Basin based an sedimentary $^{15}N/^{14}N$ ratios. Paleoceanography 12, 604–614. doi:Doi 10.1029/97pa00819

Hong, Y.T., Jiang, H.B., Liu, T.S., Qin, X.G., Zhou, L.P., Beer, J., Li, H.D., Leng, X.T., 2000. Response of climate to solar forcing recorded in a 6000-year $\delta^{18}O$ time-series of Chinese peat cellulose. The Holocene 10, 1–7. doi:10.1191/095968300669856361

Hong, Y.T., Hong, B., Lin, Q.H., Zhu, Y.X., Shibata, Y., Hirota, M., Uchida, M., Leng, X.T., Jiang, H.B., Xu, H., Wang, H., Yi, L., 2003. Correlation between Indian Ocean summer monsoon and North Atlantic climate during the Holocene. Earth and Planetary Science Letters 211, 371–380. doi:10.1016/S0012-821X(03)00207-3

Hoyt, D. V., Schatten, K.H., 1993. A discussion of plausible solar irradiance variations, 1700-1992. Journal of Geophysical Research: Space Physics 98, 18895–18906. doi:10.1029/93JA01944

Ishfaq, A.M., Pattan, J.N., Matta, V.M., Banakar, V.K., 2013. Variation of paleo-productivity and terrigenous input in the Eastern Arabian Sea during the past 100 ka. Journal of the Geological Society of India 81, 647–654. doi:10.1007/s12594-013-0086-7

Ittekkot, V., Nair, R.R., Honjo, S., Ramaswamy, V., Bartsch, M., Manganini, S., Desai, B.N., 1991. Enhanced particle fluxes in Bay of Bengal induced by injection of fresh water. Nature 351, 385.

Ivanova, E., Schiebel, R., Singh, A.D., Schmiedl, G., Niebler, H.S., Hemleben, C., 2003. Primary production in the Arabian Sea during the last 135 000 years. Palaeogeography, Palaeoclimatology, Palaeoecology 197, 61–82. doi:10.1016/S0031-0182(03)00386-9

Ivanochko, T.S., Pedersen, T.F., 2004. Determining the influences of Late Quaternary ventilation and productivity variations on Santa Barbara Basin sedimentary oxygenation: a multi-proxy approach. Quaternary Science Reviews 23, 467–480. doi:http://dx.doi.org/10.1016/j.quascirev.2003.06.006

Ji, J., Shen, J., Balsam, W., Chen, J., Liu, L., Liu, X., 2005. Asian monsoon oscillations in the northeastern Qinghai-Tibet Plateau since the late glacial as interpreted from visible reflectance of Qinghai Lake sediments. Earth and Planetary Science Letters 233, 61–70. doi:10.1016/j.epsl.2005.02.025

Jones, D.S., Fike, D.A., 2013. Dynamic sulfur and carbon cycling through the end-Ordovician extinction revealed by paired sulfate-pyrite δ34S. Earth and Planetary Science Letters 363, 144–155. doi:10.1016/j.epsl.2012.12.015

Jorgensen, B.B., 1983. Processes at the sediment-water interface. In: BOLIN, B., COOK, R.B. (Eds.), The Major Biogeochemical Cycles and Their Interactions, Scope 21. Wily, New York, p. 477–509.

Jull, A.J.T., Donahue, D.J., Linick, T.W., 1989. Carbon-14 activities in recently fallen meteorites and Antarctic meteorites. Geochimica et Cosmochimica Acta 53, 2095–2100. doi:10.1016/0016-7037(89)90327-X

Juyal, N., Pant, R.K., Basavaiah, N., Bhushan, R., Jain, M., Saini, N.K., Yadava, M.G., Singhvi, A.K., 2009. Reconstruction of Last Glacial to early Holocene

monsoon variability from relict lake sediments of the Higher Central Himalaya, Uttrakhand, India. Journal of Asian Earth Sciences 34, 437–449. doi:10.1016/j.jseaes.2008.07.007

Kallel, N., Labeyrie, L.D., Juillet-Leclerc, a., Duplessy, J.C., 1988. A deep hydrological front between intermediate and deep-water masses in the glacial Indian Ocean. Nature. doi:10.1038/333651a0

Kessarkar, P.M., Purnachadra Rao, V., Naqvi, S.W.A., Karapurkar, S.G., 2013. Variation in the Indian summer monsoon intensity during the bolling-allerod and holocene. Paleoceanography 28, 413–425. doi:10.1002/palo.20040

Kessarkar, P.M., Rao, V.P., Naqvi, S.W.A., Chivas, A.R., Saino, T., 2010. Fluctuations in productivity and denitrification in the southeastern Arabian Sea during the Late Quaternary. Current Science 99, 485–491.

Kienast, M., 2000. Unchanged nitrogen isotopic composition of OM in the South China Sea during the last climatic cycle: global implications. Paleooceanogria 15, 244– 253.

Klump, J., Hebbeln, D., Wefer, G., 2000. The impact of sediment provenance on barium-based productivity estimates. Marine Geology 169, 259–271. doi:https://doi.org/10.1016/S0025-3227(00)00092-X

Knudsen, M.F., Riisager, P., Jacobsen, B.H., Muscheler, R., Snowball, I., Seidenkrantz, M.S., 2009. Taking the pulse of the Sun during the Holocene by joint analysis of ^{14}C and ^{10}Be. Geophysical Research Letters 36, 3–7. doi:10.1029/2009GL039439

Knudsen, M.F., Seidenkrantz, M.S., Jacobsen, B.H., Kuijpers, A., 2011. Tracking the Atlantic Multidecadal Oscillation through the last 8,000 years. Nature Communications 2, 178. doi:10.1038/ncomms1186

Kudrass, H.R., Hofmann, A., Doose, H., Emeis, K., Erlenkeuser, H., 2001. Modulation and amplification of climatic changes in the Northern Hemisphere by the Indian summer monsoon during the past 80 k.y. Geology 29, 63–66. doi:10.1130/0091-7613(2001)029<0063:MAAOCC>2.0.CO;2

Kumar, M.D., 2006. Biogeochemistry of the North Indian Ocean.

Kutzbach, J., Bonan, G., Foley, J., Harrison, S.P., 1996. Vegetation and soil feedbacks on the response of the African monsoon to orbital forcing in the early to middle Holocene. Nature 384, 623–626. doi:10.1038/384623a0

Lamb, A.L., Wilson, G.P., Leng, M.J., 2006. A review of coastal palaeoclimate and relative sea-level reconstructions using δ13C and C/N ratios in organic material. Earth-Science Reviews 75, 29–57. doi:10.1016/j.earscirev.2005.10.003

Lange, G.J. de, Os, B. van, Pruysers, P.A., Middelburg, J.J., Castradori, D., Santvoort, P. van, Mqller, P.J., Eggenkamp, H., Prahl, F.G., 1994. Possible early diagenetic alteration of palaeo proxies. In: Zahn, R., et al. (Ed.), Carbon Cycling in the Glacial Ocean: Constrains on the Ocean's Role in Global Changes, NATO ASI Series. Springer, pp. 225–258.

Laskar, J., Robutel, P., Joutel, F., Gastineau, M., Correia, a. C.M., Levrard, B., 2004. A long-term numerical solution for the insolation quantities of the Earth. Astronomy and Astrophysics 428, 261–285. doi:10.1051/0004-6361:20041335

Lean, J.L., Cook, J., Marquette, W., Johannesson, a., 1998. Magnetic Sources of the Solar Irradiance Cycle. The Astrophysical Journal 492, 390–401. doi:10.1086/305015

Leuschner, D.C., Sirocko, F., 2003. Orbital insolation forcing of the Indian Monsoon - A motor for global climate changes? Palaeogeography, Palaeoclimatology, Palaeoecology 197, 83–95. doi:10.1016/S0031-0182(03)00387-0

Libby, W.F., 1955. Radiocarbon dating, University of Chicago publications in the physical sciences. University of Chicago Press.

Linick, T.W., Jull, A.J.T., Toolin, L.J., Donahue, D.J., 1986. Operation of the NSF-Arizona Accelerator Facility for Radioisotope Analysis and Results From Selected Collaborative Research Projects. Radiocarbon 28, 522–533.

Luther, M.E., O'Brien, J.J., Prell, W.L., 1990. Variability in upwelling fields in the northwestern Indian Ocean. Model experiments for the past 18000 years. Paleoceanography 5, 447–457. doi:10.1029/PA005i003p00447

Mackenzie, T., 1980. Global Carbon Cycle: Some minor sinks for CO2. Reports of a workshop. In: Flux of Organic Carbon by Rivers to the Oceans. September 21-25, Massachusetts, Woods Hole.

Madhupratap, M., Kumar, S.P., Bhattathiri, P.M.A., Kumar, M.D., Raghukumar, S., Nair, K.K.C., Ramaiah, N., 1996. Mechanism of the biological response to winter cooling in the northeastern Arabian Sea. Nature 384, 549–552. doi:10.1038/384549a0

Mahesh, B.S., Banakar, V.K., 2014. Change in the intensity of low-salinity water inflow from the Bay of Bengal into the Eastern Arabian Sea from the Last Glacial Maximum to the Holocene: Implications for monsoon variations. Palaeogeography, Palaeoclimatology, Palaeoecology 397, 31–37. doi:10.1016/j.palaeo.2013.05.024

Mahowald, N., Kohfeld, K., Hansson, M., Balkanski, Y., Harrison, S.P., Prentice, I.C., Schulz, M., Rodhe, H., 1999. Dust sources and deposition during the last glacial maximum and current climate: A comparison of model results with paleodata from ice cores and marine sediments. Journal of Geophysical Research 104, 15895. doi:10.1029/1999JD900084

Maity, R., Kumar, N.D., 2006. Bayesian dynamic modeling for monthly Indian summer monsoon rainfall using El Niño–Southern Oscillation (ENSO) and Equatorial Indian Ocean Oscillation (EQUINOO). Journal of Geophysical Research 111, D07104. doi:10.1029/2005JD006539

Malmgren, B.A., Hulugalla, R., Hayashi, Y., Mikami, T., 2003. Precipitatioon trends in Sri Lanka since the 1870s and relationships to El Niño-southern oscillation. International Journal of Climatology 23, 1235–1252. doi:10.1002/joc.921

Mariotti, A., Germon, J.C., Hubert, P., Kaiser, P., Letolie, R., Tardieux, A., Tardieux, P.., 1981. Experimental determination of nitrogen kinetic isotope fractionation: Some principles; illustration for the denitrification and nitrification process. Plant Soil 62, 413–430.

Masarik, J., Beer, J., 1999. Simulation of particle fluxes and cosmogenic nuclide production in the Earth's atmosphere. Journal of Geophysical Research 104, 12099–12111. doi:10.1029/2008JD010557

Mayewski, P. a, Meeker, L.D., Twickler, M.S., Lyons, W.B., Prentice, M., 1997. Major features and forcing of high latitude northern hemisphere atmospheric circulation using a 110,000 year long glaciochemical series. Journal of Geophysical Research 102, 26,345-26,366.

Mehta, V.M., Lau, M., 1997. Influence of solar irradiance on the Indian monsoon-ENSO relationship at decadal-multidecadal time scales. Geophysical Research Letters 24, 159–162.

Mendoza, B., 2005. Total solar irradiance and climate. Advances in Space Research 35, 882–890. doi:10.1016/j.asr.2004.10.011

Menzel, P., Gaye, B., Mishra, P.K., Anoop, A., Basavaiah, N., Marwan, N., Plessen, B., Prasad, S., Riedel, N., Stebich, M., 2014. Linking Holocene drying trends from Lonar Lake in monsoonal central India to North Atlantic cooling events. Palaeogeography Palaeoclimatology Palaeoecology 410, 164–178.

Meyers, P.A., 1994. Preservation of elemental and isotopic source identification of sediemntary organic matter. Chem. Geology 114, 289–302. doi:10.1016/0009-2541(94)90059-0

Meyers, P.A., 1997. Organic geochemical proxies of paleoceanographic, plaeolimnologic, and plaeoclimatic processes. Organic Geochemistry 27, 213–250.

Molnar, P., England, P., Martinod, J., 1993. Mantle dynamics, uplift of the Tibetan Plateau, and the Indian Monsoon. Reviews of Geophysics 31, 357–396. doi:10.1029/93RG02030

Morford, J.L., Emerson, S., 1999. The geochemistry of redox sensitive trace metals in sediments. Geochimica et Cosmochimica Acta 63, 1735–1750. doi:10.1016/S0016-7037(99)00126-X

Morford, J.L., Russell, A.D., Emerson, S., 2001. Trace metal evidence for changes in the redox environment associated with the transition from terrigenous

clay to diatomaceous sediment, Saanich Inlet, BC. Marine Geology 174, 355–369. doi:10.1016/S0025-3227(00)00160-2

Müller, A., Opdyke, B.N., 2000. Glacial-interglacial changes in nutrient utilization and paleoproductivity in the Indonesian Throughflow sensitive Timor Trough, easternmost Indian Ocean. Paleoceanography 15, 85. doi:10.1029/1999PA900046

Müller, P.J., Suess, E., 1979. Productivity, sedimentation rate, and sedimentary organic matter in the oceans-I. Organic carbon preservation. Deep Sea Research Part A, Oceanographic Research Papers 26, 1347–1362. doi:10.1016/0198-0149(79)90003-7

Murray, R.W., Leinen, M., 1993. Chemical transport to the seafloor of the equatorial Pacific Ocean across a latitudinal transect at 135°W: Tracking sedimentary major, trace, and rare earth element fluxes at the Equator and the Intertropical Convergence Zone. Geochimica et Cosmochimica Acta 57, 4141–4163. doi:10.1016/0016-7037(93)90312-K

Murray, R.W., Leinen, M., 1996. Scavenged excess aluminum and its relationship to bulk titanium in biogenic sediment from the central equatorial Pacific Ocean. Geochimica et Cosmochimica Acta 60, 3869–3878. doi:http://dx.doi.org/10.1016/0016-7037(96)00236-0

Naidu, P.D., Malmgren, B.A., 1996. A high-resolution record of late Quaternary upwelling along the Oman Margin, Arabian Sea based on planktonic foraminifera. Paleoceanography 11, 129–140.

Naidu, P.D., Singh, A.D., Ganeshram, R., Bharti, S.K., 2014. Abrupt climate-induced changes in carbonate burial in the Arabian. Geochemistry, Geophysics, Geosystems 1398–1406. doi:10.1002/2013GC005065

Naik, S.S., Godad, S.P., Naidu, P.D., Tiwari, M., Paropkari, a. L., 2014. Early- to late-Holocene contrast in productivity, OMZ intensity and calcite dissolution in the eastern Arabian Sea. The Holocene 24, 749–755. doi:10.1177/0959683614526936

Naimo, D., Adamo, P., Imperato, M., Stanzione, D., 2005. Mineralogy and geochemistry of a marine sequence, Gulf of Salerno, Italy. Quaternary International 140–141, 53–63. doi:10.1016/j.quaint.2005.05.004

Nair, R.R., Ittekkot, V., Manganini, S.J., Ramaswamy, V., Haake, B., Degens, E.T., Desai, B.N., Honjo, S., 1989. Increased particle flux to the deep ocean related to monsoons. Nature 338, 749–751.

Naqvi, S.W.A., 1987. Some aspects of the oxygen-deficient conditions and denitrification in the Arabian Sea. Journal of Marine Research 45, 1049–1072. doi:10.1357/002224087788327118

Naqvi, W.A., Charles, C.D., Fairbanks, R.G., 1994. Carbon and oxygen isotopic records of benthic foraminifera from the Northeast Indian Ocean: implications on glacial-interglacial atmospheric CO_2 changes. Earth and Planetary Science Letters 121, 99–10.

Naqvi, S.W.A., Jayakumar, D.A., Narvekar, P. V., Naik, H., Sarma, V.V.S.S., D'Souza, W., Joseph, T., George, M.D., 2000. Increased marine production of N_2O due to intensifying anoxia on the Indian continental shelf. Nature 408, 346–349.

Nath, B.N., 2001. Geochemistry of sediments. Oxford \& IBH New Delhi (India).

Nath, B.N., 1999. Geochemical proxies for understanding Paleoceanography 143–151.

Neff, U., Burns, S.J., Mangini, A., Mudelsee, M., Fleitmann, D., Matter, A., 2001. Strong coherence between solar variability and the monsoon in Oman between 9 and 6 kyr ago. Nature 411, 290–293. doi:10.1038/35077048

Nesbitt, H.W., Markovics, G., 1997. Weathering of granodioritic crust, long-term storage of elements in weathering profiles, and petrogenesis of siliciclastic sediments. Geochimica et Cosmochimica Acta 61, 1653–1670.

Nigam, R., Khare, N., 1995. Significance of correspondence between river discharge and proloculus size of benthic Foraminifera in paleomonsoonal studies. Geo-Marine Letters 15, 45–50. doi:10.1007/BF01204497

Nigam, R., Khare, N., 1999. Spatial and Temporal Distribution of Foraminifera in Sediments off the Central West Coast of India and Use of Their Test Morphologies for the Reconstruction of Paleomonsoonal Precipitation. Micropaleontology 45, 285–303.

Niitsuma, N., Naidu, P.D., 2001. History of monsoons. In: Encyclopedia of Ocean Sciences. London, Academic Press, pp. 1841–1849.

Ogrinc, N., Fontolan, G., Faganeli, J., Covelli, S., 2005. Carbon and nitrogen isotope compositions of organic matter in coastal marine sediments (the Gulf of Trieste, N Adriatic Sea): Indicators of sources and preservation. Marine Chemistry 95, 163–181. doi:10.1016/j.marchem.2004.09.003

Ostrom, N.E., Macko, S.A., Deibel, D., Thompson, R.J., 1997. Geochimica et Cosmochimica Acta Seasonal variation in the stable carbon and nitrogen isotope biogeochemistry of a coastal cold ocean environment. Science 61, 14–15.

Pailler, D., Bard, E., Rostek, F., Zheng, Y., Mortlock, R., Geen, A. Van, 2002. Burial of redox-sensitive metals and organic matter in the equatorial Indian Ocean linked to precession. Geochimica et Cosmochimica Acta 66, 849–865. doi:10.1016/S0016-7037(01)00817-1

Panmei, C., Divakar Naidu, P., Mohtadi, M., 2017. Bay of Bengal Exhibits Warming Trend During the Younger Dryas: Implications of AMOC. Geochemistry, Geophysics, Geosystems 1–9. doi:10.1002/2017GC007075

Parab, S.G., Prabhu Matondkar, S.G., Gomes, H. d R., Goes, J.I., 2006. Monsoon driven changes in phytoplankton populations in the eastern Arabian Sea as revealed by microscopy and HPLC pigment analysis. Continental Shelf Research 26, 2538–2558. doi:10.1016/j.csr.2006.08.004

Pasquier, V., Sansjofre, P., Rabineau, M., Revillon, S., Houghton, J., Fike, D.A., 2017. Pyrite sulfur isotopes reveal glacial–interglacial environmental changes. Proceedings of the National Academy of Sciences 201618245. doi:10.1073/pnas.1618245114

Pattan, J.N., Pearce, N.J.G., 2009. Bottom water oxygenation history in southeastern Arabian Sea during the past 140 ka : Results from redox-sensitive

elements. Palaeogeography, Palaeoclimatology, Palaeoecology 280, 396–405. doi:10.1016/j.palaeo.2009.06.027

Pattan, J.N., Masuzawa, T., Naidu, P.D., Parthiban, G., Yamamoto, M., 2003. Productivity fluctuations in the southeastern Arabian Sea during the last 140 ka. Palaeogeography, Palaeoclimatology, Palaeoecology 193, 575–590. doi:10.1016/S0031-0182(03)00267-0

Pattan, J.N., Mir, I.A., Parthiban, G., Karapurkar, S.G., Matta, V.M., Naidu, P.D., Naqvi, S.W.A., 2013. Coupling between suboxic condition in sediments of the western Bay of Bengal and southwest monsoon intensification: A geochemical study. Chemical Geology 343, 55–66. doi:10.1016/j.chemgeo.2013.02.011

Pausata, F.S.R., Battisti, D.S., Nisancioglu, K.H., Bitz, C.M., 2011. Chinese stalagmite $\delta^{18}O$ controlled by changes in the Indian monsoon during a simulated Heinrich event. Nature Geoscience 4, 474–480. doi:10.1038/ngeo1169

Pedersen, T.F., Price, N.B., 1982. The geochemistry of manganese carbonate in Panama Basin sediments. Geochimica et Cosmochimica Acta 46, 59–68. doi:10.1016/0016-7037(82)90290-3

Pestiaux, P., Mersch, I. Van der, Berger, A., 1988. Paleoclimatic variability at frequencies ranging from 1 cycle per 10000 years to 1 cycle per 100 years: Evidence for nonlinear behaviour of the climate system. Climate Change 12, 9–37.

Peters, K.E., Sweeney, R.E., Kaplan, I.R., 1978. Correlation of carbon and nitrogen stable isotope ratios in sedimentary organic matter. Limnology and Oceanography 23, 598–604.

Piotrowski, A.M., Banakar, V.K., Scrivner, A.E., Elderfield, H., Galy, A., Dennis, A., 2009. Indian Ocean circulation and productivity during the last glacial cycle. Earth and Planetary Science Letters 285, 179–189. doi:10.1016/j.epsl.2009.06.007

Piper, D.Z., Perkins, R.B., 2004. A modern vs. Permian black shale - the hydrography, primary productivity, and water-column chemistry of deposition. Chemical Geology 206, 177–197. doi:10.1016/j.chemgeo.2003.12.006

Prahl, F.G., Lange, G.J. De, Scholten, S., Cowie, G.L., 1997. A case of post-depositional aerobic degradation of terrestrial organic matter in turbidite deposits from the Madeira Abyssal Plain. Organic Geochemistry 27, 141–152. doi:https://doi.org/10.1016/S0146-6380(97)00078-8

Prahl, F.G., Wakeham, S.G., 1987. Calibration of unsaturation patterns in long-chain ketone compositions for palaeotemperature assessment. Nature 330, 367–369. doi:10.1038/330367a0

Prahl, F.G., Dymond, J., Sparrow, M.A., 2000. Annual biomarker record for export production in the central Arabian Sea. Deep Sea Research Part II: Topical Studies in Oceanography 47, 1581–1604. doi:10.1016/S0967-0645(99)00155-1

Prasad, V., Farooqui, A., Sharma, A., Phartiyal, B., Chakraborty, S., Bhandari, S., Raj, R., Singh, A., 2014. Mid-late Holocene monsoonal variations from mainland Gujarat, India: A multi-proxy study for evaluating climate culture relationship. Palaeogeography, Palaeoclimatology, Palaeoecology 397, 38–51. doi:10.1016/j.palaeo.2013.05.025

Prell, W.L., Campo, E. Van, 1986. Coherent response of Arabian Sea upwelling and pollen transport to late Quaternary monsoonal winds. Nature 323, 526--528.

Prell, W.L., Hutson, W.H., Williams, D.F., Bé, A.W.H., Geitzenauer, K., Molfino, B., 1980. Surface circulation of the Indian Ocean during the last glacial maximum, approximately 18,000 yr B.P. Quaternary Research 14, 309–336. doi:10.1016/0033-5894(80)90014-9

Premuzic, E.T., Benkovitz, C.M., Gaffney, J.S., Walsh, J.J., 1982. The nature and distribution of organic matter in the surface sediments of world oceans and seas. Organic Geochemistry 4, 63–77. doi:doi:10.1016/0146-6380(82)90009-2

Punyu, V.R., Banakar, V.K., Garg, A., 2014. Equatorial Indian Ocean productivity during the last 33 kyr and possible linkage to Westerly Jet variability. Marine Geology 348, 44–51. doi:10.1016/j.margeo.2013.11.010

Rad, U. von, Schaaf, M., Michels, K.H., Schulz, H., Berger, W.H., Sirocko, F., 1999. A 5000-yr Record of Climate Change in Varved Sediments from the

Oxygen Minimum Zone off Pakistan, Northeastern Arabian Sea. Quaternary Research 51, 39. doi:10.1006/qres.1998.2016

Rahaman, W., Singh, S.K., Sinha, R., Tandon, S.K., 2009. Climate control on erosion distribution over the Himalaya during the past ~100 ka. Geology 37, 559–562. doi:10.1130/G25425A.1

Raiswell, R., Berner, R.A., 1985. Pyrite formation in euxinic and semi-euxinic sediments. Am. J. Sci. 285, 710–724.

Rajendran, A., Kumar, M.D., Bakker, J.F., 1992. Control of manganese and iron in Skagerrak sediments (norheastern North sea). Chemical Geology 98, 111–129.

Ramaswamy, V., Gaye, B., 2006. Regional variations in the fluxes of foraminifera carbonate, coccolithophorid carbonate and biogenic opal in the northern Indian Ocean. Deep-Sea Research Part I: Oceanographic Research Papers 53, 271–293. doi:10.1016/j.dsr.2005.11.003

Ramaswamy, V., Gaye, B., Shirodka, P.V., Rao, P.S., Chivas, A.R., Wheeler, David, Thwin, S., 2008. Distribution and sources of organic carbon, nitrogen and their isotopic signatures in sediments from the Ayeyarwady (Irrawaddy) continental shelf, northern Andaman Sea. Marine Chemistry 111, 137–150.

Ramisch, A., Lockot, G., Haberzettl, T., Hartmann, K., Kuhn, G., Lehmkuhl, F., Schimpf, S., Schulte, P., Stauch, G., Wang, R., Wunnemann, B., Yan, D., Zhang, Y., Diekmann, B., 2016. A persistent northern boundary of Indian Summer Monsoon precipitation over Central Asia during the Holocene. Scientific Reports 6, 25791. doi:10.1038/srep25791

Ranasinghe, P.N., Ortiz, J.D., Smith, A.J., Griffith, E.M., Siriwardana, C., Silva, S.N. De, Wijesundara, D., 2013. Mid- to late-Holocene Indian winter monsoon variability from a terrestrial record in eastern and southeastern coastal environments of Sri Lanka. Holocene 23, 945–960. doi:10.1177/0959683612475141

Rao, V.P., Kessarkar, P.M., Thamban, M., Patil, S.K., 2010. Paleoclimatic and diagenetic history of the late quaternary sediments in a core from the Southeastern

Arabian Sea: Geochemical and magnetic signals. Journal of Oceanography 66, 133–146. doi:10.1007/s10872-010-0011-2

Rashid, H., Flower, B.P., Poore, R.Z., Quinn, T.M., 2007. A 25 ka Indian Ocean monsoon variability record from the Andaman Sea. Quaternary Science Reviews 26, 2586–2597. doi:10.1016/j.quascirev.2007.07.002

Redfield AC, 1934. On the proportion of organic derivatives in seawater and their relation to the composition of plankton. In: James Johnstone Memorial Volume. , Liverpool: Liverpool University Press, pp. 177–192.

Redfield AC, 1958. The biological controls of chemical factors in the environment. American Journal of Science 46, 205–221.

Reichart, G.J., Dulk, M. Den, Visser, H.J., Weijden, C.H. Van Der, Zachariasse, W.J., 1997. A 225 kyr record of dust supply, paleoproductivity and the oxygen minimum zone from the Murray Ridge (Northern Arabian Sea). Palaeogeography, Palaeoclimatology, Palaeoecology 134, 149–169. doi:10.1016/S0031-0182(97)00071-0

Reid, G.C., 1987. Influence of solar variability on global sea surface temperatures. Nature 329, 219–222.

Reimer, P.J., Baillie, M.G.L., Bard, E., Bayliss, A., Beck, J.W., Blackwell, P.G., Ramsey, C.B., Buck, C.E., Burr, G.S., Edwards, R.L., Friedrich, M., Grootes, P.M., Guilderson, T.P., Hajdas, I., Heaton, T.J., Hogg, A.G., Hughen, K.A., Kaiser, K.F., Kromer, B., McCormac, F.G., Manning, S.W., Reimer, R.W., Richards, D.A., Southon, J.R., Talamo, S., Turney, C.S.M., Plicht, J. van der, Weyhenmeyer, C.E., 2009. IntCal09 and Marine09 Radiocarbon Age Calibration Curves, 0–50,000 Years cal BP. Radiocarbon 51, 1111–1150. doi:10.1017/S0033822200034202

Reimer, P.J., Bard, E., Bayliss, A., Beck, J.W., Blackwell, P.G., Ramsey, C.B., Buck, C.E., Cheng, H., Edwards, R.L., Friedrich, M., Grootes, P.M., Guilderson, T.P., Haflidason, H., Hajdas, I., Hatté, C., Heaton, T.J., Hoffmann, D.L., Hogg, A.G., Hughen, K.A., Kaiser, K.F., Kromer, B., Manning, S.W., Niu, M., Reimer, R.W., Richards, D.A., Scott, E.M., Southon, J.R., Staff, R.A., Turney, C.S.M.,

Plicht, J. van der, 2013. IntCal13 and Marine13 Radiocarbon Age Calibration Curves 0–50,000 Years cal BP. Radiocarbon 55, 1869–1887. doi:10.2458/azu_js_rc.55.16947

Riccardi, A.L., Arthur, M.A., Kump, L.R., 2006. Sulfur isotopic evidence for chemocline upward excursions during the end-Permian mass extinction. Geochimica et Cosmochimica Acta 70, 5740–5752. doi:https://doi.org/10.1016/j.gca.2006.08.005

Rimmer, S.M., 2004. Geochemical paleoredox indicators in Devonian-Mississippian black shales, Central Appalachian Basin (USA). Chemical Geology 206, 373–391. doi:10.1016/j.chemgeo.2003.12.029

Rind, D., 2002. The Sun's Role in Climate Variations. science 296, 673–678. doi:10.1126/science.1069562

Rodrigo-Gámiz, M., Martínez-Ruiz, F., Rodríguez-Tovar, F.J., Jiménez-Espejo, F.J., Pardo-Igúzquiza, E., 2014. Millennial- to centennial-scale climate periodicities and forcing mechanisms in the westernmost Mediterranean for the past 20,000 yr. Quaternary Research 81, 78–93. doi:10.1016/j.yqres.2013.10.009

Rohling, E., Mayewski, P., Abu-Zied, R., Casford, J., Hayes, A., 2002. Holocene atmosphere-ocean interactions: records from Greenland and the Aegean Sea. Climate Dynamics 18, 587–593. doi:10.1007/s00382-001-0194-8

Rostek, F., Ruhland, G., Bassinot, F.C., Muller, P.J., Labeyrie, L.D., Lancelot, Y., Bard, E., 1993. Reconstructing Sea-Surface Temperature and Salinity Using $\delta^{18}O$ and Alkenone Records. Nature 364, 319–321. doi:Doi 10.1038/364319a0

Rostek, F., Bard, E., Beaufort, L., Sonzogni, C., Ganssen, G., 1997. Sea surface temperature and productivity records for the last 240 kyr on the Arabian Sea. Deep-Sea Research Part II: Topical Studies in Oceanography 44, 1461–1480. doi:10.1016/S0967-0645(97)00008-8

Roy, I., Collins, M., 2015. On identifying the role of Sun and the El Nino Southern Oscillation on Indian summer monsoon rainfall. Atmospheric Science Letters 16, 162–169.

Rühland, K., Phadtare, N.R., Pant, R.K., Sangode, S.J., Smol, J.P., 2006. Accelerated melting of Himalayan snow and ice triggers pronounced changes in a valley peatland from northern India. Geophysical Research Letters 33, 1–6. doi:10.1029/2006GL026704

Saher, M.H., Peeters, F.J.C., Kroon, D., 2007. Sea surface temperatures during the SW and NE monsoon seasons in the western Arabian Sea over the past 20,000 years. Palaeogeography, Palaeoclimatology, Palaeoecology 249, 216–228. doi:10.1016/j.palaeo.2007.01.014

Saino, T., Hattori, A., 1987. Geographical variation of the water column distrubution of suspended particulate organic nitrogen and its ^{15}N natural abundance in the Pacific and its marginal seas. Deep Sea Research Part A. Oceanographic Research Papers 34, 807–827. doi:https://doi.org/10.1016/0198-0149(87)90038-0

Saraswat, R., Nigam, R., Weldeab, S., Mackensen, A., Naidu, P.D., 2005. A first look at past sea surface temperatures in the equatorial Indian Ocean from Mg/Ca in foraminifera. Geophysical Research Letters 32, 1–4. doi:10.1029/2005GL024093

Saraswat, R., Nigam, R., Mackensen, A., Weldeab, S., 2012. Linkage between seasonal insolation gradient in the tropical northern hemisphere and the sea surface salinity of the equatorial Indian Ocean during the last glacial period. Acta Geologica Sinica 86, 1265–1275.

Saraswat, R., Lea, D.W., Nigam, R., Mackensen, A., Naik, D.K., 2013. Deglaciation in the tropical Indian Ocean driven by interplay between the regional monsoon and global teleconnections. Earth and Planetary Science Letters 375, 166–175. doi:10.1016/j.epsl.2013.05.022

Sarin, M.M., Borole, D. V, Krishnaswami, S., 1979. Geochemistry and geochronology of sediments from the Bay of Bengal and the equatorial Indian Ocean. Proceedings of the Indian National Science Academy 88, 131–154.

Sarkar, A., Bhattacharya, S.K., Sarin, M.M., 1993. Geochemical evidence for anoxic deep water in the Arabian Sea during the last glaciation. Geochimica et Cosmochimica Acta 57, 1009–1016. doi:10.1016/0016-7037(93)90036-V

Sarkar, A., Ramesh, R., Somayajulu, B.L.K., Agnihotri, R., Jull, A.J.T., Burr, O.S., 2000. High resolution Holocene monsoon record from the eastern Arabian Sea. Earth and Planetary Science Letters 177, 209–218. doi:10.1016/S0012-821X(00)00053-4

Schmiedl, G., Leuschner, D.C., 2005. Oxygenation changes in the deep western Arabian Sea during the last 190,000 years: Productivity versus deepwater circulation. Paleoceanography 20, 1–14. doi:10.1029/2004PA001044

Schnetger, B., Brumsack, H.J., Schale, H., Hinrichs, J., Dittert, L., 2000. Geochemical characteristics of deep-sea sediments from the Arabian Sea: A high-resolution study. Deep-Sea Research Part II: Topical Studies in Oceanography 47, 2735–2768. doi:10.1016/S0967-0645(00)00047-3

Schroeder, J.O., Murray, R.W., Leinen, M., Pflaum, R.C., Janecek, T.R., 1997. Barium in equatorial Pacific carbonate sediment : Terrigenous, oxide, and biogenic associations. Paleoceanography 12, 125–146.

Schott, F., Reppin, J., Fischer, J., Quadfasel, D., 1994. Currents and transports of the Monsoon Current south of Sri Lanka. Journal of Geophysical Research 99, 25127. doi:10.1029/94JC02216

Schott, F.A., McCreary, J.P., 2001. The monsoon circulation of the Indian Ocean. Progress in Oceanography 51, 1–123. doi:10.1016/S0079-6611(01)00083-0

Schott, F.A., Dengler, M., Schoenefeldt, R., 2002. The shallow overturning circulation of the Indian Ocean. Progress in Oceanography 53, 57–103. doi:10.1016/S0079-6611(02)00039-3

Schulte, S., Bard, E., 2003. Past changes in biologically mediated dissolution of calcite above the chemical lysocline recorded in Indian Ocean sediments. Quaternary Science Reviews 22, 1757–1770. doi:10.1016/S0277-3791(03)00172-0

Schulte, S., Rostek, F., Bard, E., Rullkotter, J., Marchal, O., 1999. Variations of oxygen-minimum and primary productivity recorded in sediments of the Arabian Sea. Earth and Planetary Science Letters 173, 205–221. doi:10.1016/S0012-821X(99)00232-0

Schulz, H., Rad, U. van, Erlenkeuser, H., 1998. Correlation between Arabian Sea and Greenland climate oscillations of the past 110,000 years. Nature 393, 54–57. doi:10.1038/31750

Schulz, M., Stattegger, K., 1997. Spectrum: spectral analysis of unevenly spaced paleoclimatic time series. Computers & Geosciences 23, 929–945. doi:10.1016/S0098-3004(97)00087-3

Shankar, D., Vinayachandran, P.N., Unnikrishnan, A.S., 2002. The monsoon currents in the north Indian Ocean. Progress in Oceanography 52, 63–120. doi:http://dx.doi.org/10.1016/S0079-6611(02)00024-1

Shetye, S.S., Sudhakar, M., Mohan, R., Jena, B., 2014. Contrasting productivity and redox potential in Arabian Sea and Bay of Bengal. Journal of Earth Science 25, 366–370. doi:10.1007/s12583-014-0415-9

Sigman, D.M., Altabet, I.M.A., Mccorkle, C., 1999. The isotopic composition of diatom-bound nitrogen in Southern Ocean sediments. Paleoceanography 14, 118–134.

Sigman, D.M., Karsh, K.L., Casciotti, K.L., 2010. Nitrogen Isotopes in the Ocean. Encyclopedia of Ocean Sciences 40–54. doi:10.1016/B978-012374473-9.00632-9

Singh, A.D., Kroon, D., Ganeshram, R.S., 2006. Millennial scale variations in productivity and OMZ intensity in the Eastern Arabian Sea. Journal of the Geological Society of India 68, 369–377.

Sinha, A., Cannariato, K.G., Stott, L.D., Li, H.C., You, C.F., Cheng, H., Edwards, R.L., Singh, I.B., 2005. Variability of Southwest Indian summer monsoon precipitation during the Bolling-Allerod. Geology 33, 813–816. doi:10.1130/G21498.1

Sirocko, F., Garbe-Schonberg, D., Mcintyre, A., Molfino, B., 1996. Teleconnections between the subtropical moonsoons and high-latitude climates

during the last deglaciation. Science 272, 526–529. doi:10.1126/science.272.5261.526

Sirocko, F., Sarnthein, M., Erlenkeuser, H., Lange, H., Arnold, M., Duplessy, J.C., 1993. Century-scale events in monsoonal climate over the past 24,000 years. Nature 364, 322–324. doi:10.1038/364322a0

Sirocko, F., Schonberg, D.G., Devey, C., 2000. Processes controlling trace element geochemistry of Arabian Sea sediments during the last 25,000 years. Global and Planetary Change 26, 217–303.

Sofia, S., Li, L.H., 2001. Solar variability and climate change. Journal of Geophysical Research 76, 12969–12974.

Somayajulu, B.L.K., Bhushan, R., Sarkar, A., Burr, G.S., Jull, A.J.T., 1999. Sediment deposition rates on the continental margins of the eastern Arabian Sea using 210Pb, 137Cs and 14C. Science of The Total Environment 237–238, 429–439. doi:10.1016/S0048-9697(99)00155-2

Sonzogni, C., Bard, E., Rostek, F., 1998. Tropical sea surface temperature during the last glacial period: A view based on alkenones in Indian Ocean sediments. Quaternary Science Reviews 17, 1185–1201.

Southon, J., Kashgarian, M., Fontugne, M., Metivier, B., Yim, W.., 2002. Marine reservoir corrections for the Indian Ocean and Southeast Asia. Radiocarbon 44, 167--180. doi:doi.org/10.1017/S0033822200064778

Stager, J.C., Ryves, D.B., Chase, B.M., Pausata, F.S.R., 2011. Catastrophic drought in the Afro-Asian monsoon region during Heinrich event 1. Science 331, 1299–302. doi:10.1126/science.1198322

Staubwasser, M., Sirocko, F., Grootes, P.M.M., Segl, M., 2003. Climate change at the 4.2 ka BP termination of the Indus valley civilization and Holocene south Asian monsoon variability. Geophysical Research Letters 30, 1425. doi:10.1029/2002GL016822

Steinhilber, F., Beer, J., Fröhlich, C., 2009. Total solar irradiance during the Holocene. Geophysical Research Letters 36, 1–5. doi:10.1029/2009GL040142

Steinhilber, F., Jürg, B., 2011. Solar activity-the past 1200 years. PAGES Newsletter 19, 5–6. doi:10.1029/2009GL040142.Gao

Strauss, H., 1999. Geological evolution from isotope proxy signals — sulfur. Chemical Geology 161, 89–101. doi:10.1016/S0009-2541(99)00082-0

Strauss, H., 2003. Sulphur isotopes and the early Archaean sulphur cycle. Precambrian Research 126, 349–361. doi:https://doi.org/10.1016/S0301-9268(03)00104-9

Stuiver, M., Braziunas, T.F., 1993. Sun, ocean, climate and atmospheric $^{14}CO_2$: an evaluation of causal and spectral relationships. The Holocene 3, 289–305. doi:10.1177/095968369300300401

Stuiver, M., Reimer, P.J., Braziunas, T.F., 1998. High-Precision Radiocarbon Age Calibration for Terrestrial and Marine Samples. Radiocarbon 40, 1127–1151. doi:10.1017/S0033822200019172

Sukumar, R., Ramesh, R., Pant, R.K., Rajgopalan, G., Rajagopalan, G., 1993. A $\delta^{13}C$ record of late Quaternary climate change from tropical peats in southern India. Nature 364, 703–706.

Sweeney, R.E., Kaplan. I. R., 1980. Natural abundances of ^{15}N as a source indicator for nearshore marine sedimentary and dissolved nitrogen. Marine Chemistry 9, 81–94.

Taylor, S.., McLennan, S.., 1995. The geochemical evolution of the continental crust. Reviews of Geophysics 33, 241–265. doi:10.1029/95RG00262

Timothy, D., Calvert, S., 1998. Systematics of variations in excess A1 and A1/Ti in sediments from the central equatorial Pacific. Paleoceanography 13, 127–130.

Thamban, M., Purnachandra Rao, V., Schneider, R.R., Grootes, P.M., 2001. Glacial to Holocene fluctuations in hydrography and productivity along the southwestern continental margin of India. Palaeogeography, Palaeoclimatology, Palaeoecology 165, 113–127. doi:10.1016/S0031-0182(00)00156-5

Thamban, M., Kawahata, H., Rao, V.P., 2007. Indian summer monsoon variability during the holocene as recorded in sediments of the Arabian Sea:

Timing and implications. Journal of Oceanography 63, 1009–1020. doi:10.1007/s10872-007-0084-8

Thode, H., 1970. Sulfur Isotope Geochemistry And Fractionation Between Coexisting Sulfide Minerals Mineral. Soc. Amer. Spec. Pap. 3, 133–144.

Thornton, S.F., McManus, J., 1994. Application of organic carbon and nitrogen stable isotope and C/N ratios as source indicators of organic matter provenance in estuarine systems: evidence from the Tay Estuary, Scotland. Estuar. Coast. Shelf Sci. 38, 219–233.

Timothy, D., Calvert, S., 1998. Systematics of variations in excess A1 and A1/Ti in sediments from the central equatorial Pacific. Paleoceanography 13, 127–130.

Tiwari, M., Ramesh, R., 2007. Solar variability in the past and palaeoclimate data pertaining to the southwest monsoon. Current Science 93, 477–487.

Tiwari, M., Ramesh, R., Somayajulu, B.L.K., Jull, A.J.T., Burr, G.S., 2005. Early deglacial (~19-17 ka) strengthening of the northeast monsoon. Geophysical Research Letters 32, 1–4. doi:10.1029/2005GL024070

Tiwari, M., Ramesh, R., Somayajulu, B.L.K., Jull, A.J.T., Burr, G.S., 2006a. Paleomonsoon precipitation deduced from a sediment core from the equatorial Indian Ocean. Geo-Marine Letters 26, 23–30. doi:10.1007/s00367-005-0012-0

Tiwari, M., Ramesh, R., Bhushan, R., Simayajulu, B.L.K., Jull, a. J.T., Burr, G.S., 2006b. Paleoproductivity Variations in the Equatorial Arabian Sea: Implications for East African and Indian Summer Rainfalls and the El Nino Frequency. Radiocarbon 48, 17–19.

Tiwari, M., Ramesh, R., Bhushan, R., Sheshshayee, M.S., Somayajulu, B.L.K., Jull, A.J.T., Burr, G.S., 2010. Did the Indo-Asian summer monsoon decrease during the Holocene following insolation? Journal of Quaternary Science 25, 1179–1188. doi:10.1002/jqs.1398

Tomczak, M., Godfrey, J.S., 2003. Regional oceanography: An introduction, 2nd ed. Pergamon.

Törnqvist, T.E., Bick, S.J., González, J.L., Borg, K. van der, Jong, A.F.M. de, 2004. Tracking the sea-level signature of the 8.2 ka cooling event: New constraints from the Mississippi Delta. Geophysical Research Letters 31, 1–4. doi:10.1029/2004GL021429

Tribovillard, N., Algeo, T.J., Lyons, T., Riboulleau, A., 2006. Trace metals as paleoredox and paleoproductivity proxies: An update. Chemical Geology 232, 12–32. doi:10.1016/j.chemgeo.2006.02.012

Tribovillard, N., Riboulleau, A., Lyons, T., Baudin, F., 2004. Enhanced trapping of molybdenum by sulfurized marine organic matter of marine origin in Mesozoic limestones and shales. Chemical Geology 213, 385–401.

Tripathy, G.R., Singh, S.K., Bhushan, R., Ramaswamy, V., 2011. Sr – Nd isotope composition of the Bay of Bengal sediments : Geochemical Journal 45, 175–186.

Tripathy, G.R., Singh, S.K., Ramaswamy, V., 2014. Major and trace element geochemistry of Bay of Bengal sediments: Implications to provenances and their controlling factors. Palaeogeography, Palaeoclimatology, Palaeoecology 397, 20–30. doi:10.1016/j.palaeo.2013.04.012

Tuenter, E., Weber, S.L., Hilgen, F.J., Lourens, L.J., 2007. Simulating sub-Milankovitch climate variations associated with vegetation dynamics. Climate of the Past 3, 169–180. doi:10.5194/cp-3-169-2007

Tyson, R. V., Pearson, T.H., 1991. Modern and ancient continental shelf anoxia: an overview. Geological Society, London, Special Publications 58, 1–24. doi:10.1144/GSL.SP.1991.058.01.01

Vidya, P.J., Prasanna Kumar, S., Gauns, M., Verenkar, A., Unger, D., Ramaswamy, V., 2013. Influence of physical and biological processes on the seasonal cycle of biogenic flux in the equatorial Indian Ocean. Biogeosciences 10, 7493–7507. doi:10.5194/bg-10-7493-2013

Vinayachandran, P., Yamagata, T., 1998. Monsoon response of the sea around Sri Lanka: generation of thermal domesand anticyclonic vortices. Journal of Physical Oceanography 28, 1946–1960.

Vinayachandran, P., Chauhan, P., Mohan, M., Nayak, S., 2004. Biological response of the sea around Sri Lanka to summer monsoon. Geophysical Research Letters 31, 4–7. doi:10.1029/2003GL018533

Vinayachandran, P.N., Mathew, S., 2003. Phytoplankton bloom in the Bay of Bengal during the northeast monsoon and its intensification by cyclones. Geophysical Research Letters 30. doi:10.1029/2002GL016717

Vizzini, S., Savona, B., Caruso, M., Savona, A., Mazzola, A., 2005. Analysis of stable carbon and nitrogen isotopes as a tool for assessing the environmental impact of aquaculture: a case study from the western Mediterranean. Aquaculture International 13, 157–165. doi:10.1007/s10499-004-9023-5

Vos, A. de, Pattiaratchi, C., Wijeratne, E., 2014. Surface circulation and upwelling patterns around Sri Lanka. Biogeosciences 11, 5909–5930. doi:10.5194/bg-11-5909-2014

Wakeham, S.G., Peterson, M.L., Hedges, J.I., Lee, C., 2002. Lipid biomarker fluxes in the Arabian Sea, with a comparison to the equatorial Pacific Ocean. Deep Sea Research Part II: Topical Studies in Oceanography 49, 2265–2301. doi:10.1016/S0967-0645(02)00037-1

Wang, Y.J., Cheng, H., Edwards, R.L., An, Z.S., Wu, J.Y., Shen, C.C., Dorale, J.A., 2001. A High-Resolution Absolute-Dated Late Pleistocene Monsoon Record from Hulu Cave , China. Science 294, 2345–2348. doi:10.1126/science.1064618

Wang, Y.J., Cheng, H., Edwards, R.L., He, Y.Q., Kong, X.G., An, Z.S., Wu, J.Y., Kelly, M.J., Dykoski, C.A., Li, X.D., 2005. The Holocene Asian monsoon: Links to solar changes and North Atlantic climate. Science 308, 854–857. doi:DOI 10.1126/science.1106296

Wanner, H., Beer, J., Bütikofer, J., Crowley, T.J., Cubasch, U., Flückiger, J., Goosse, H., Grosjean, M., Joos, F., Kaplan, J.O., Küttel, M., Müller, S.A., Prentice, I.C., Solomina, O., Stocker, T.F., Tarasov, P., Wagner, M., Widmann, M., 2008. Mid- to Late Holocene climate change: an overview. Quaternary Science Reviews 27, 1791–1828. doi:10.1016/j.quascirev.2008.06.013

Warrier, A.K., Shankar, R., 2009. Geochemical evidence for the use of magnetic susceptibility as a paleorainfall proxy in the tropics. Chemical Geology 265, 553–562. doi:10.1016/j.chemgeo.2009.05.023

Webster, P.J., Moore, a M., Loschnigg, J.P., Leben, R.R., 1999. Coupled ocean-atmosphere dynamics in the Indian Ocean during 1997-98. Nature 401, 356–360. doi:10.1038/43848

Wei, G., Liu, Y., Li, X., Shao, L., Liang, X., 2003. Climatic impact on Al, K, Sc and Ti in marine sediments: Evidence from ODP Site 1144, South China Sea. Geochemical Journal 37, 593–602. doi:10.2343/geochemj.37.593

Whitfield, M., 2001. Interactions between phytoplankton and trace metals in the ocean. In: Advances in Marine Biology, Advances in Marine Biology. Academic Press, pp. 1–128. doi:http://dx.doi.org/10.1016/S0065-2881(01)41002-9

Wu, Y., Zhang, J., Liu, S.M., Zhang, Z.F., Yao, Q.Z., Hong, G.H., Cooper, L., 2007. Sources and distribution of carbon within the Yangtze River system. Estuar. Coast. Shelf Sci. 17, 13–25.

Wyrtki, K., 1973. Physical Oceanography of the Indian Ocean. In: Zeitzschel, B., Gerlach, S.A. (Eds.), The Biology of the Indian Ocean. Springer Berlin Heidelberg, Berlin, Heidelberg, pp. 18–36. doi:10.1007/978-3-642-65468-8_3

Yadava, M.G., Ramesh, R., 2005. Monsoon reconstruction from radiocarbon dated tropical Indian speleothems. The Holocene 1, 48–59. doi:10.1191/0959683605h1783rp

Yancheva, G., Nowaczyk, N.R., Mingram, J., Dulski, P., Schettler, G., Negendank, J.F.W., Liu, J., Sigman, D.M., Peterson, L.C., Haug, G.H., 2007. Influence of the intertropical convergence zone on the East Asian monsoon. Nature 445, 74–7. doi:10.1038/nature05431

Zhang, J., Wu, Y., Ittekkot Jennerjahn, V., He, Q., 2007. Distribution of organic matter in the Changjiang (Yangtze River) Estuary and their stable carbon and nitrogen isotopic ratios: implications for source discrimination and sedimentary dynamics. Marine Geology 106, 111–126

List of Publication

Chandana, K. R., Bhushan, R. and Jull, A.J.T. (2017). Evidence of Poor Bottom Water Ventilation during LGM in the Equatorial Indian Ocean. *Frontiers in Earth Science* 5, 1-10.

Abstracts (Conference Proceedings)

Chandana, K. R. and Bhushan, R. (2017). Late Quaternary Productivity Variations in the equatorial Indian Ocean During the last 26 ka. Submitted abstract at conference on 5th National Conference of Ocean Society of India, OSICON-17, held at ESSO-National Centre for Earth Science Studies, Thiruvananthapuram.

Chandana, K. R., Bhushan, R. and Jull, A.J.T. (2016). Productivity fluctuations of the late Quaternary sediments from the Equatorial Indian Ocean. Presented at conference on "Quaternary Climate: Recent Findings and Future Challenges" held at National Institute of Oceanography (NIO), Goa supported by Past Global Changes (PAGES), Oral presentation.

Chandana K. R., Ravi Bhushan, Rajesh Agnihotri, R. Sawlani, and A.J.T. Jull (2016). Surface nutrient utilisation and productivity during glacial-interglacial periods from the Equatorial Indian Ocean. Submitted abstract at American Geophysical Union, Fall Meeting held at San Francisco, USA.

Chandana, K. R., Bhushan, R. and Jull, A.J.T. (2015). Equatorial Upwelling and nutrient utilisation in the northern Indian Ocean during the past 25 ka. Presented at an International conference on Indian Ocean "IO50-Symposium" held at National Institute of Oceanography (NIO), Goa, Poster presentation.